N-Heterocyclic Carbene Complexes of Titanium as a Novel Class of Catalysts for the Copolymerization of Cyclohexene Oxide with CO_2

Coralie C. Quadri

Thesis for the Degree of Philosophiae Doctor (PhD)
University of Bergen, Norway
2018

UNIVERSITY OF BERGEN

N-Heterocyclic Carbene Complexes of Titanium as a Novel Class of Catalysts for the Copolymerization of Cyclohexene Oxide with CO_2

Coralie C. Quadri

Thesis for the Degree of Philosophiae Doctor (PhD)
at the University of Bergen

2018

Date of defence: 27.04.2018

Year: 2018

Title: *N*-Heterocyclic Carbene Complexes of Titanium as a Novel Class of Catalysts for the Copolymerization of Cyclohexene Oxide with CO_2

Name: Coralie C. Quadri

Print: Skipnes Kommunikasjon / University of Bergen

Acknowledgements

First, I would like to thank my supervisor, Associate Professor Erwan Le Roux, for giving me the opportunity to perform this research in his group and for all that I have learned from him.

As well, I would like to thank all the people that are or have been part of my research group. Especially Doctor Lalrempuia Ralte, for all the additional work you had because of me. I imagine you are as happy as me that I got to the end!

A special thanks to Professor Karl Wilhelm Törnroos for his work and expertise in the analysis and resolution of my single crystal X-ray diffraction. Thank you, as well, to my co-supervisor, Professor Pascal D.C. Dietzel, and all the people that have helped me, notably with the different analytical instruments: Doctor Egil Nodland, Inger Johanne Fjellanger, Doctor Bjarte Holmelid, Olav-Audun Bjørkelund, Associate Professor Nils Åge Frøystein, Doctor Christian Totland. I would also like to thank Professor Knut Børve and Associate Professor Kristine Spildo for their accessibility, sympathy and advice.

I am thankful to my colleagues and friends: Markus Baumann, Hjørdis Skår and André Bienfait, for their precious help. As well as Maria Campanyà I Llovet, Mikel Oregui Bengoetxea, Maria del Prado Carrion-Ramirez, Tim Ahnfeldt, Emily MacCready, Wietse Smit, Anna Sobolewska, Karolin Dipper, Konstantinos Christakos, Elvira García de Jalón Viñegra, Jose Carlos Reyes Guerrero. There is not enough place to add all the amazing people I had the chance to meet, for making a good atmosphere at UiB, going through these long rainy months together, and all the coffee, barbecues, diners, cafe opera nights, hikes, trips, etc. You have made Norway an unforgettable journey. A special thought for Matina Karakitsiou for being here and being her.

Almost last but not least, I am grateful to my family: my mum, Isabelle; my dad, Rafael; my twin, Thomas; and all my other family and friends, whom I can always count on, even when I am not easy to deal with (well, this is what you say…). You are my rock! And I know I can achieve anything with you on my side. Guille, I am lucky I have found you on my way. Thanks for helping me out the best you could and for always taking care of me.

Finally, I want to thank the University of Bergen for funding this project, which was also partially supported by the Norwegian Research Council (FRINATEK grant no. 240333).

Abstract

Regarding environmental, economic and political issues, the utilization of CO_2 as C_1 chemical feedstock has received a worldwide interest in the last decade. Indeed CO_2 is considered as a greenhouse gas (submitted to strict regulations), alongside being an optimal raw material (renewable, nontoxic, nonflammable, safe, cheap and naturally abundant). A promising large-scale application is its use as a co-reagent in polymerizations. The copolymerization of CO_2 with epoxides is an attractive alternative for the production of polycarbonates for instance, that are not oil-based and avoiding the use of toxic reagents such as bisphenol A and phosgene.

Since the early ’70s, a range of catalysts based on different metal centers (essentially Zn, Al, Mn, Cr and Co) and bearing a variety of ligands (mostly phenoxide, β-diiminate and salen type) has been reported, showing high activity and selectivity toward the coupling of CO_2 with various epoxides. However, the range of active metal centers and ancillary ligands reported remains surprisingly narrow. Moreover, the development of new greener and competitive catalytic systems for the copolymerization of epoxide with CO_2 is necessary to support a viable sustainable process at reasonable cost. Our focus was to develop complexes based on non-endangered, abundant, inexpensive and nontoxic metal centers, which are active and selective for the production of polymers under mild reaction conditions. The potential of a new family of precursors based on the oxygen-functionalized *N*-heterocyclic carbene (NHC) ligand combined with titanium as catalyst component for the copolymerization of cyclohexene oxide (CHO) with CO_2 was investigated.

Tridentate and bidentate NHC titanium complexes were synthesized and fully characterized. Upon cocatalyst addition, all the tridentate NHC titanium complexes were found to be active and highly selective toward the formation of poly(cyclohexene carbonate), while bidentate NHC titanium showed no activity.

Further, the reactivity of those catalytic systems and the reaction conditions (nature and ratio of cocatalyst and coligand, catalyst loading, use of additional solvent, CO_2 pressure and temperature) were investigated. These studies allowed to improve the understanding of the active species, optimize the reaction conditions and design new and/or modified systems, tridentate NHC titanium azide being the pre-catalyst leading to the highest activity toward the coupling of CHO with CO_2 under low CO_2 pressure.

These systems were the first tetravalent NHC titanium catalysts reported for the copolymerization of CHO with CO_2.

List of publications

Paper I

"Copolymerization of Cyclohexene Oxide with CO_2 Catalyzed by Tridentate *N*-Heterocyclic Carbene Titanium(IV) Complexes"

Quadri C. Quadri and Erwan Le Roux

Dalton Transactions 2014, Vol. 43, pp 4242-4246

Paper II

"Structural Characterization of Tridentate *N*-Heterocyclic Carbene of Titanium(IV) Benzyloxide, Silyloxide, Acetate and Azide Complexes and Assessment of Their Efficacies for Catalyzing the Copolymerization of Cyclohexene Oxide with CO_2"

Coralie C. Quadri, Ralte Lalrempuia, Julie Hessevik, Karl. W. Törnroos and Erwan Le Roux

Organometallics 2017, Vol. 36, pp 4477-4489

Paper III

"Steric Factors on Unsymmetrical *O*-hydroxyaryl *N*-Heterocyclic Carbene Ligands Prevailing the Stabilization of Single Stereoisomer of Bis-Ligated Titanium Complexes"

Coralie C. Quadri, Ralte Lalrempuia, Karl. W. Törnroos and Erwan Le Roux

Submitted

Additional paper, not included in this thesis

Paper IV

"Di-μ-chlorido-bis{bis[*N*,*N*-bis(trimethylsilyl)amido]-titanium(III)}"

Coralie C. Quadri, Karl. W. Törnroos and Erwan Le Roux

IUCrData 2017, Vol 2, pp x171488- x171490

Selected abbreviations

Ad	Adamantyl
atm	Atmosphere
Bdi	β-Diiminate
Boxdipy	1,9-Bis(2-oxidophenyl)dipyrrinate
BTP	Benzotriazole phenolate
Cat.	Catalyst
C_6D_6	Benzene-d_6
$CDCl_3$	Chloroform-*d*
CHC	Cyclohexene carbonate
CHO	Cyclohexene oxide
CO_2	Carbon dioxide
Dep	2,6-Diethylphenyl
Diars	1,2-Bis(dimethylarsino)benzene
Dipp	2,6-Diisopropylphenyl
DMAD	Dipolarophile dimethyl acetylenedicarboxylate
DRIFT	Diffuse reflectance infrared fourier transform
ΔG_f	Free energy of formation
GHG	Greenhouse gas

Δ	Heat
Kbtsa	Potassium bis(trimethylsilyl)amide
IMe	Bis(2,4,6-trimethylphenyl)imidazol-2-ylidene
Mes	1,3,5-Trimethylphenyl
M_n	Number average molecular weight
M_w	Weight average molecular weight
NHC	*N*-heterocyclic carbene
NMR	Nuclear magnetic resonance
Nu	Nucleophile
OBn	Benzyloxide
O*i*Pr	Isopropoxide
TOF	Turnover frequency
TON	Turnover number
PCHC	Poly(cyclohexene-*alt*-carbonate)
PCHO	Poly(cyclohexene oxide)
PO	Polypropylene oxide
PPC	Poly(propylene-*alt*-carbonate)
PPN	Bis(triphenylphosphine)iminium chloride
PPO	Poly(propylene oxide)
Ph	Phenyl

ppm	Parts per million
ROP	Ring-opening polymerization
rt	Room temperature
Salan	N,N′-Disubstituted bis(aminophenoxide)
Salen	N,N′-Bis-(salicylidene)-1,2-ethylenediimine
Salphen	N,N'-Phenylenebis(salicylideneimine)
TBD	1,5,7-Triabicyclo[4,4,0]dec-5-ene
*t*Bu	*tert*-Butyl
T_g	Glass transition temperature
THF	Tetrahydrofuran
Tpp	Tetraphenylporphyrin

Table of Contents

1. Introduction

1.1. Carbon Dioxide as a Chemical Feedstock

1.1.1. Carbon Dioxide as C_1 Source

The use of intensive oil-based carbon resources leads to the release of carbon dioxide as a by-product, which is known to enhance greenhouse gases (GHGs) emissions. GHGs are considered a major cause of global warming and climate changes. Indeed due to anthropogenic sources, the accumulation of CO_2 gas in the atmosphere rose from 278 ppm in the preindustrial period to a current level of 387 ppm [1]. Motivated by more restrictive environmental regulations and economic constraints, the interest to reduce fossil carbon consumption and CO_2 emission is constantly growing. To reach these goals, different strategies have been developed: 1) reduce the use of energy derived from fossil fuels, 2) recover and store CO_2 from processes and 3) reuse CO_2 as a renewable carbon source. Together with the other technologies, CO_2 utilization is a promising alternative that is able to convert a "waste" into valuable products [2].

Carbon dioxide is an optimal raw material since it is renewable, nontoxic, non-flammable, safe, relatively cheap and naturally abundant [3]. The CO_2 utilization technology presents other advantages by: its contribution to prevent CO_2 emissions (several million tons each year), recycling carbon, preserving resources (reducing extraction of fossil-C), increasing the independence from fossil fuels and potentially substitute toxic chemicals used in current processes [1, 4, 5]. One of the big challenges facing the use of CO_2 as a reagent for chemical synthesis is its thermodynamic stability (ΔG_f = -393.5 kJ mol^{-1}), limiting its application [6]. To overwhelm this drawback, reactions employing CO_2 with highly reactive reagents have been explored and their reactions with metal complexes have been extensively studied [6, 7]. Indeed, the development started in the early 1970s by the investigation of reactions of CO_2 with organometallic compounds based on transition metals (Rh, Ru, Pt, Co) [8]. In 1975, the synthesis and solid state structure of the first side-on

complex (([κ^2-*C*,*O*]-CO_2)-bis(tricyclohexylphosphine)nickel) **1** was reported (Scheme 1.1) [9]. Following this discovery, other CO_2 complexes based on Rh **2** (Scheme 1.1), Fe, Nb, Mo and Co were structurally characterized, showing that transition metal complexes are able to coordinate CO_2 or act as catalysts in CO_2 fixation. Different coordination modes metal center to CO_2 are possible: the bonding of the metal center via the carbon atom (κ^1-*C*), an oxygen atom (κ^1-*O*), the C=O bond (κ^2-*C*,*O*) and the oxygens (κ^2-*O*,*O*) which can be described as a carboxylate [10-15].

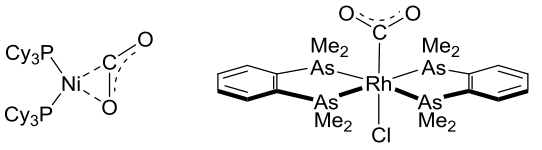

1 **2**

Scheme 1.1. Common coordination modes of CO_2 with a metal center ([κ^2-*C*,*O*]-CO_2)Ni(PCy_3)$_2$ **1** [9] and ([κ^1-*C*]-CO_2)Rh(Cl)(diars)$_2$ **2** [16].

For the last two decades, the interaction of CO_2 with transition metal complexes has been the subject of extensive studies, both experimental and theoretical, revealing potential pathways for catalytic reactions [17].

1.1.2. Carbon Dioxide Utilization

Carbon dioxide utilization is divided in four categories: 1) technological utilization (e.g. supercritical CO_2), 2) enhanced biological utilization (e.g. production of biomass), 3) production of fuels and 4) production of chemicals. On those domains, CO_2 as a C_1 feedstock has received a worldwide interest which results in applied examples as carbon source (fine chemistry), solvent in a variety of synthetic processes (supercritical CO_2) or co-reagent (for polymerization) [18-20].

Figure 1.1 illustrates the wide range of available molecules that can be produced from CO_2 as a co-reagent.

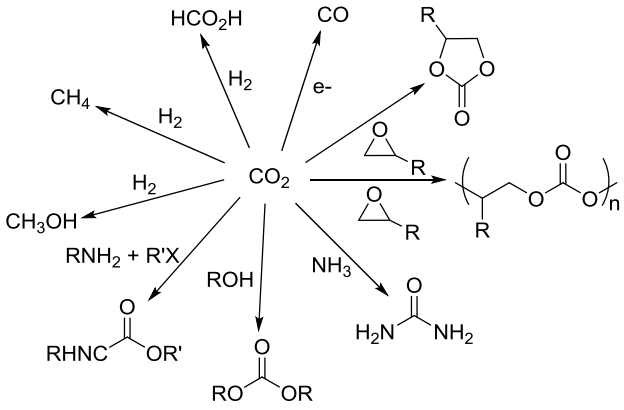

Figure 1.1. Possible applications of CO_2 in fuels and chemical synthesis.

Carbon dioxide can be used as a chemical feedstock for the production of fuels like formic acid, carbon monoxide, formaldehyde, methanol or hydrocarbons for example methane. CO_2 can also be used in the production of chemicals that involves the entire CO_2 molecule incorporation, providing compounds like urea, salicylic acid, carbamates, carboxylate, polyurethane, inorganic carbonate, hydrogen carbonate, cyclic/linear carbonate or polycarbonate [1, 7, 21-23].

Figure 1.2 summarizes the industrial production of CO_2 based chemicals. The total amount of CO_2 consumed is approximately 116 million tons per year, of which 94% is made up by the production of urea. However it is important to note that this particular process releases more gas than it consumes, reducing the current use of CO_2 as a feedstock for chemicals to only 0.36% of the global CO_2 emissions [24, 25].

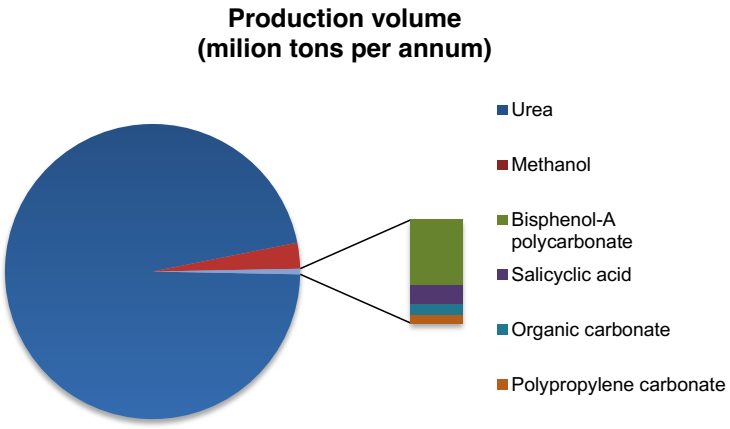

Figure 1.2. Industrial production volume of products made of CO_2, adapted from reference [25].

Today, there is a great interest in increasing the amount of CO_2 incorporated in other applications. Among them, the use of CO_2 as comonomer for its incorporation into polymers seems to be a promising approach for large-scale industrial applications of CO_2 utilization [26-30].

1.2. Copolymerization of Epoxide and Carbon Dioxide

1.2.1. Reaction and Applications

Carbone dioxide can be coupled with different high-energy profile molecules such as strained heterocyclic molecules, e.g. epoxides or oxetanes, aziridines and episulfides, generating polycarbonates, polyurethanes and polythiocarbonates, respectively [31]. Here we will focus on the use of epoxides as a comonomer, which is the most widely studied reaction, showing the highest potential for industrial applications. The coupling of CO_2 to an epoxide affords the formation of polycarbonates and/or cyclic carbonates [32, 33]. If there is no CO_2 insertion into the polymer chain, the formation of the homopolymer product is observed as a side product of the reaction. Among the different epoxides available, cyclohexene oxide (CHO) and propylene oxide (PO) are the most investigated ones (Scheme 1.2).

This alternative way for polycarbonates synthesis is of great interest since it can contribute to reduce the carbon footprint, replace most of the oil-based polymers [34, 35] and avoid the use of very toxic reagents such as bisphenol A and phosgene that are commonly used [36].

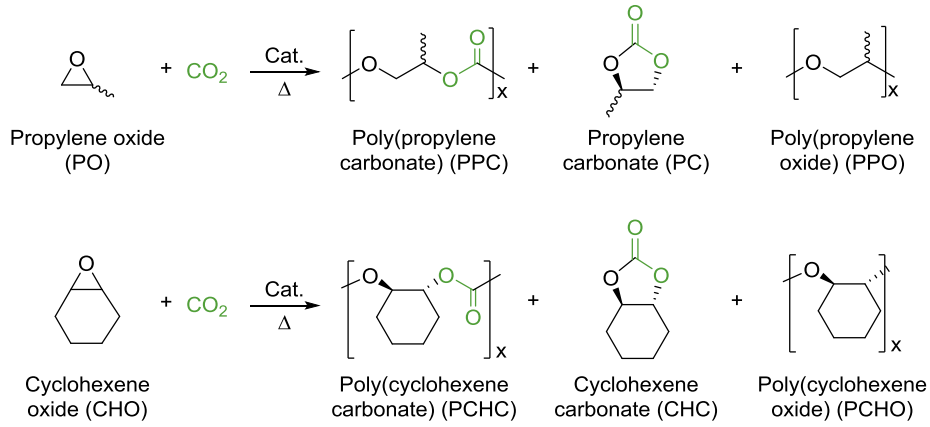

Scheme 1.2. CO_2/epoxides coupling into poly(carbonates), cyclic products and formation of polyethers.

Nowadays, aliphatic polycarbonates find applications as packaging materials and also in the synthesis of engineering thermoplastics and resins, pyrotechnics and interliners for safety glass [26, 27, 32, 37]. Poly(propylene-*alt*-carbonate) (PPC) has a glass transition temperature (T_g) of 35-40 ºC which hinders its application as a bulk material. However, PPC has the great property of decomposing uniformly and controllably to cyclic propylene carbonate below 250 ºC, making it an ideal candidate as a binder for ceramics, adhesives and propellants [32, 38]. One of the most promising applications of these aliphatic carbonates is as a mid-segment of polyurethanes [26, 39]. Poly(cyclohexene-*alt*-carbonate) (PCHC) shows similar decomposition temperature and properties as PPC making it also suitable in melt processing. In addition PCHC has a high T_g (150 ºC), similar to poly(styrene), giving it potential in lithographic processes for the construction of microfluidic devices [32, 37].

Cyclic carbonate products find industrial applications as polar aprotic solvents, substrates for small molecules synthesis, additives, antifoam agents for antifreeze and plasticizers [32, 40, 41]. Despite the feasibility of the examples described above, only a limited number of applications are exploited. The moderate thermal stability and low temperature needed for thermal deformation of these products, in addition to the high cost of the CO_2/epoxide copolymers have been slowing down the development of their industrial applications. Much higher levels of stereocontrol as well as regiocontrol of catalysts are required in order to improve the physical properties of aliphatic polycarbonates. Furthermore, the activity of the catalyst needs to be improved in order to reduce the cost of the material. Indeed, the low activity of the current industrial catalysts, the zinc/dicarboxylic acid, salen cobalt, zinc glutarate, double metal cyanide, nickel hydroxybenzenediamines or zinc bearing reduced Robson´s type ligand, is one of the reasons leading to their high price. To be suitable for such applications, polymers also encounter issues with the color of the end-polymer and the removal of (toxic) metal residues, particularly when the activity is low. In order to increase the use of CO_2/epoxides copolymers in different applications, the development of new catalytic systems is necessary.

1.2.2. Reaction Mechanism and Selectivity

The current and following sections will focus more specifically on the use and reactivity of CHO. To undergo the CO_2/epoxide copolymerization, various Lewis acidic metal halide, carboxylate, alkoxide and aryloxide complexes are typically used as catalysts. Although the complete understanding of the mechanism of the CO_2-epoxide coupling reaction is still under investigation, a general trend for a coordination-insertion mechanism has been proposed (Scheme 1.3).

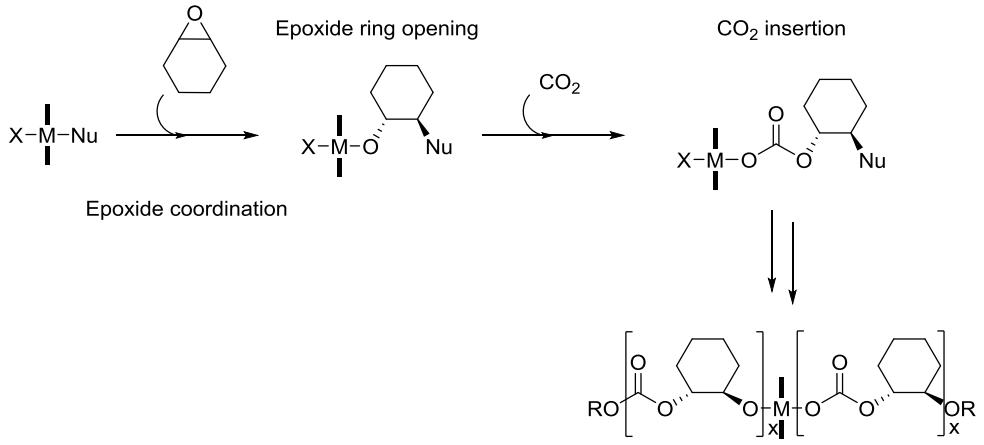

Scheme 1.3. Coordination-insertion mechanism for the copolymerization of CHO and CO_2.

The reaction is initiated by the epoxide coordination to the metal center and is followed by the attack of a nucleophilic cocatalyst or an anionic leaving group to one of the carbon atoms of the epoxide. Cocatalysts are divided in two categories according to their nature: anionic, the most common being onium salts such as [PPN]X (PPN = bis(triphenylphosphine)iminium with X = Cl, N_3, etc.) or [*n*Bu_4N]X and neutral with 4-(dimethylamino)pyridine (DMAP), *N*-methylimidazole (*N*-MeIm) and PPh_3 for instance. This first step, which showed to be the rate determining step, causes the epoxide ring-opening and the formation of a metal bound alkoxide. The nucleophilic group is called the initiation group and ends up at the chain end-group of the growing polymer. Several initiation pathways (e.g. epoxide coordination) have been proposed based on salen and salan metal complexes: the inter- and intramolecular monometallic and the intermolecular bimetallic mechanisms (Scheme 1.4) [42, 43].

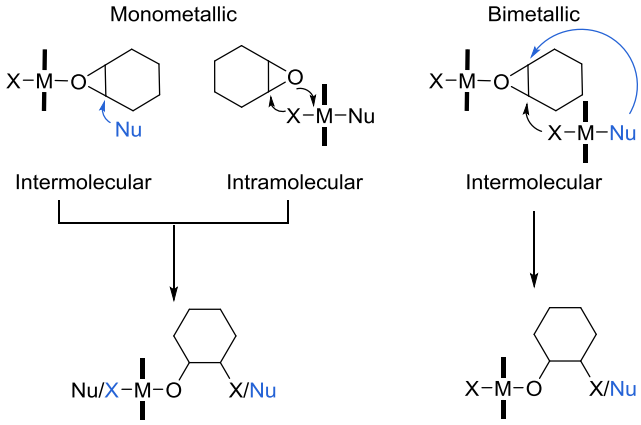

Scheme 1.4. Initiation mechanisms for the copolymerization of CHO and CO_2 proposed using salen and salan type ligand systems bearing a nucleophilic cocatalyst (Nu) and an anionic leaving group (X).

In the monometallic initiation pathway, the nucleophilic attack at the epoxide can be done by an intermolecular interaction of a nucleophilic cocatalyst (Nu) or an intramolecular interaction with an anionic leaving group (X) of the catalyst. In a bimetallic intermolecular initiation pathway, an activated nucleophile (either X or Nu) on one metal complex may ring open an epoxide that is coordinated to another metal complex [32-34, 42, 44-47]. The formed metal alkoxide undergoes CO_2 insertion into the metal oxygen leading to a metal carbonate. The rate of CO_2 insertion depends on the electronic and steric availability of the lone pairs on the oxygen atom of the alkoxide. More nucleophilic and less sterically encumbered metal alkoxides present a better interaction with the poorly electrophilic carbon center of CO_2 making it more active toward the insertion of CO_2 [34]. Then the propagation undergoes by nucleophilic attack of the metal carbonate to another coordinated epoxide molecule subsequently followed by another CO_2 insertion [32]. An example of mechanistic studies based on the (salen)CrCl complexes developed by Jacobsen [48] is described in Scheme 1.5 [33, 34].

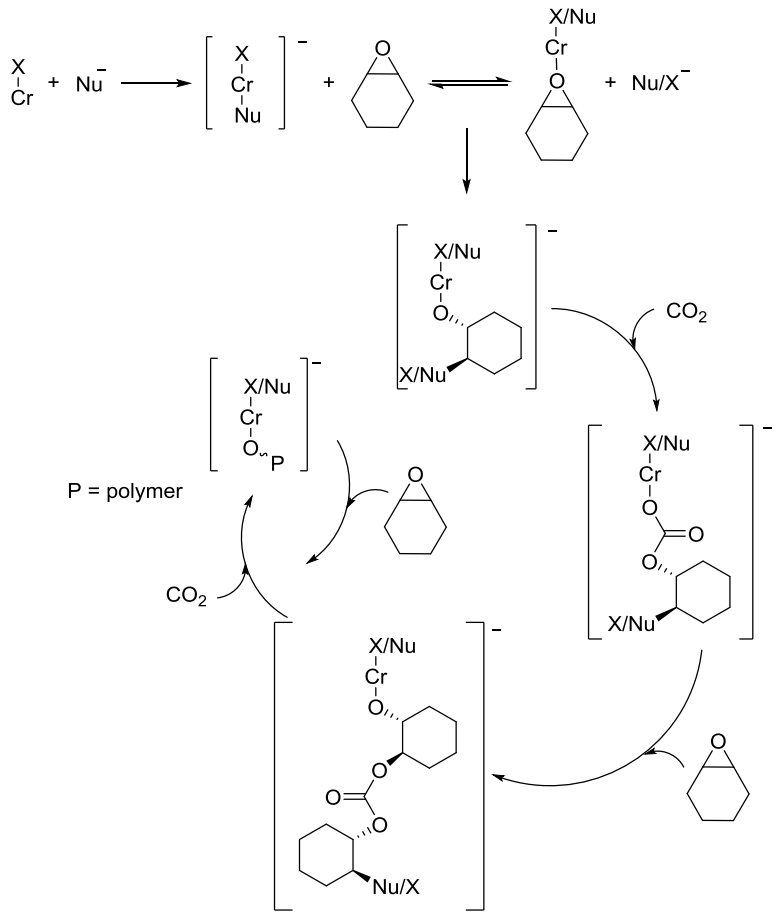

Scheme 1.5. Mechanism for CO_2/CHO copolymerization using (salen)CrCl in presence of an anionic cocatalyst (Nu), adapted from reference [34].

Upon the addition of an anionic cocatalyst *trans* to X, the formation of anionic six-coordinate active intermediate is observed [49] allowing the epoxide ring-opening by a monometallic inter- or intramolecular mechanism. Both nucleophilic cocatalyst (Nu) and anionic leaving group (X) have been identified in the copolymer end group making difficult to identify the favored initiation pathway(s).

In comparison, upon the addition of neutral cocatalyst to (salen)CrCl complex, neutral six-coordinate intermediate are formed and the initiation mechanism follows the bimetallic intermolecular pathway. Compared to its anionic analogue, the neutral six-coordinate intermediate proved to be less effective toward the CHO ring-opening and CO_2 insertion. In both cases, an addition of an excess of cocatalyst to the complex leads to the decrease of the catalytic activity, as there is a competition between the cocatalyst and the epoxide coordination [34].

In case of bimetallic complexes such as bimetallic β-diiminate (bdi) zinc catalyst, the mechanism follows an intramolecular bimetallic pathway, which does not necessitate the use of cocatalyst. The zinc alkoxide dimer inserts CO_2 to form carbonate complexes, the metal carbonate bound of one metal center then reacts with the coordinated epoxide on the second metal center [50].

The initiation-propagation steps are subsequently repeated to form copolymers until one or both of the monomers are consumed or the reaction is quenched and/or the catalyst is deactivated. If the catalyst used, possesses the ability to either catalyze the homopolymerization of the epoxide or undergo decarboxylation, then there are consecutive epoxide ring-opening and the formation of ether linkages instead of carbonates takes place. In addition, two possible chain transfers can occur during the coupling reaction, yielding by-products. The intramolecular back-biting described in Scheme 1.6 is responsible for the formation of cyclic compounds. The metal alkoxide or carbonate attacks the growing polymer chain leading to the formation of the thermodynamic product, the five-membered ring cyclic carbonate.

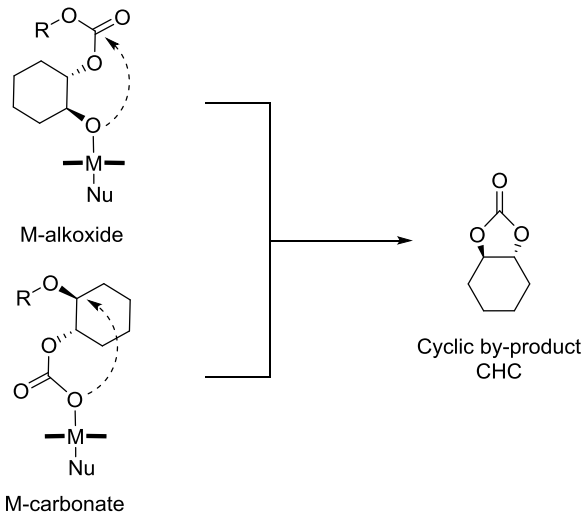

Scheme 1.6. Back-biting mechanism leading to cyclic carbonate compounds.

The back-biting reaction is often observed for aliphatic epoxides and/or in case of non-coordinative pathways and is favored at higher temperature. During a cooperative catalytic mechanism, the growing polymers are attached to the metal complex and therefore the back-biting side reactions are suppressed. But in the absence of multiple metal sites and/or the use of large cocatalysts favoring the dissociation of the growing polymer from the metal center (*e.g*. formation of "free" anionic polymer chain), cyclic compounds are the predominant products of the CO_2/epoxide copolymerization [32].

The other possible chain transfer is due to the interaction with external contaminants, typically protic compounds such as alcohol or water that react with the growing chain and afford a hydroxyl terminated copolymer and a new initiation site. The result of chain transfers causes a reduction in the number of repeat units and therefore of the molecular weight of the resulting polymers. Copolymerization is facing the recurrent challenge to avoid the formation of aforementioned undesired by-products.

1.2.3. Catalysts Development

The performance of a catalyst is evaluated by its productivity, its activity and by the quality of the produced polymer. The productivity and the activity are defined respectively by the turnover number (TON), which corresponds to the moles of epoxide consumed per mole of catalyst, and the turnover frequency (TOF), which is the TON per hour. The catalyst activity is considered as: TOF < 1 h^{-1}: very low, 1 < TOF < 10 h^{-1}: low, 10 < TOF < 100 h^{-1}: moderate, 100 < TOF < 1000 h^{-1}: high and TOF > 1000: very high. The quality of the material is characterized by the percentage of carbonate linkages, the percentage of selectivity (PCHC *vs* CHC), the number average (M_n) and weight average (M_w) molecular weights and the polydispersity index (PDI) of the polymer chains. In case of mono-substituted epoxide (e.g. PO), the polymer chain can present different regioselectivities: the substituents are on alternate carbon atoms (Head to Tail, HT linkages) or on consecutive carbon atoms (Head to Head, HH or Tail to Tail, TT linkages). In addition, the polymer chain can present different stereoselectivities also called tacticities: all the substituents have the same (isotactic), an alternating (syndiotactic) or a random (atactic) stereochemistry. The regio- and stereoselectivity of the polymer chain can have an important effect on its physical properties. Other important parameters to take into consideration are the reaction conditions: the temperature, the pressure of CO_2, and the use of additives (cocatalyst or solvent) necessary to activate the pre-catalyst [33].

1.2.3.1. Heterogeneous Catalysts

The reaction was reported for the first time in 1969 by Inoue and co-workers. The synthesis allows the production of PPC with high carbonate linkages (88%) by the copolymerization of PO and CO_2 catalyzed by $ZnEt_2/H_2O$ mixtures, which was a remarkable achievement in the field of CO_2 utilization [51]. Following this discovery, the groups of Inoue and Kuran investigated the use of $ZnEt_2$/di-or triprotic sources including primary amines, dihydric phenols, trihydric phenols, aminophenols, aromatic dicarboxylic acids, aromatic hydroxycarboxylic acids, diaminobenzene, and

thioresorcinol as active heterogeneous catalyst mixtures for PO/CO_2 copolymerization [32, 33]. These original catalysts exhibited extremely low activities (TOFs < 0.5 h^{-1}) associated often with a low regio- and/or stereoselectivity, affording polymers containing carbonate and ether linkages alongside the formation of side-products (cyclic carbonates). Moreover, these heterogeneous catalysts require high pressure, high temperature and long reaction times (several days) to produce appreciable amounts of polymers. Among heterogeneous catalysts, zing glutarate ($Zn[O_2C(CH_2)_3CO_2]$) is the most widely applied example showing high productivity and affording high molecular weight copolymers (conversion > 90%, TON = 70) [52]. Another class of promising heterogeneous catalysts is the double metal cyanides (DMCs), based on zinc and Fe or Co (for example: $Zn_3[CoCN)_6]_2$), which is also known to catalyze the homopolymerization, leading to low percentages of carbonate linkages (20-90% according to the polymer formed PPC/PCHC) [53, 54]. Other ZnO/fluorinated carboxylic acid precursors have also been investigated showing decent activity [55]. Despite their good productivity and stability, heterogeneous catalysts have been significantly less studied than their homogeneous homologues. Heterogeneous catalysts are the panacea of many industrial processes and in general preferred for polymerization in comparison with their homogeneous analogues (control of polymer morphology, granular size and avoidance of reactor fouling). Heterogenized catalysts also present important industrial advantages in term of stability and process development (handling ease, product separation and catalyst regeneration). However, the establishment of a relationship between structure and activity remains difficult owing to the weak homogeneity of their structure and weak concentration in active sites and therefore hampering a rational development of such systems [32].

1.2.3.2. Homogeneous Catalysts

In the last decade, homogeneous catalysts for the coupling of epoxides with CO_2 have been improved significantly. A wide range of catalysts has been successfully reported, leading to the production of polycarbonates. Homogeneous catalysts are

classified in two broad types, bimetallic (Scheme 1.7) and monometallic (Scheme 1.8) catalysts [56].

Different systems have been reported among bimetallic catalysts in which the use of a cocatalyst can be often avoided. An important investigated catalytic system is the highly active sterically encumbered β-diiminate (bdi) complexes type. [Zn(μ-OMe)(bdi)]$_2$ **3** exhibits unprecedented rates for the CHO/CO_2 copolymerization under mild reaction conditions (50 ºC, 7 bar, TOF = 2290 h^{-1}) but is inactive for the coupling of PO [32]. In these systems, the active catalysts are in equilibrium monomer *vs* dimer, and the non-active complexes are either the monomeric or dimeric forms, in this case substituents are relevant toward the activity. Other dimeric Zn complexes that proved to be active for the coupling of CHO and CO_2 are based on phenoxide ligands. Bis-2,6-difluorophenoxide dimeric Zn **4** showed to be an effective catalyst for the preparation of high molecular weight PCHCs (80 ºC, 55 bar, TOF = 16.5 h^{-1}, M_n = 42000 g mol^{-1}) [57]. Lee *et al*. reported in 2005 the use of bis(anilido-aldimine)-Zn catalyst. In this system, *N*-aryl *ortho* substituents show to be an important parameter for the activity of the complex toward the copolymerization of CHO and CO_2. Dinuclear μ-methyl sulfinato Zn complex bearing methyl and isopropyl groups **5** is active at low catalyst loading ([Zn]:[monomer] = 1:5600, 80 ºC, 12 bar, TOF = 200 h^{-1}) leading to high molecular weight and carbonate content polymers (M_n = 284000 g mol^{-1}, carbonate linkages = 91%) [58]. Tethered bdi-Zn catalysts type has been reported notably by Rieger *et al*.. For example complex **6**, bearing flexible methylene bridges between both bdi-Zn moieties and electron-withdrawing groups, leads to unprecedented activities ([Zn]:[monomer] = 1:8000, 100 ºC, 30 bar, TOF = 155000 h^{-1}) toward the formation of high molecular weight and carbonate content polymers (M_n = 280000 g mol^{-1}, carbonate linkages = 88%) [59].

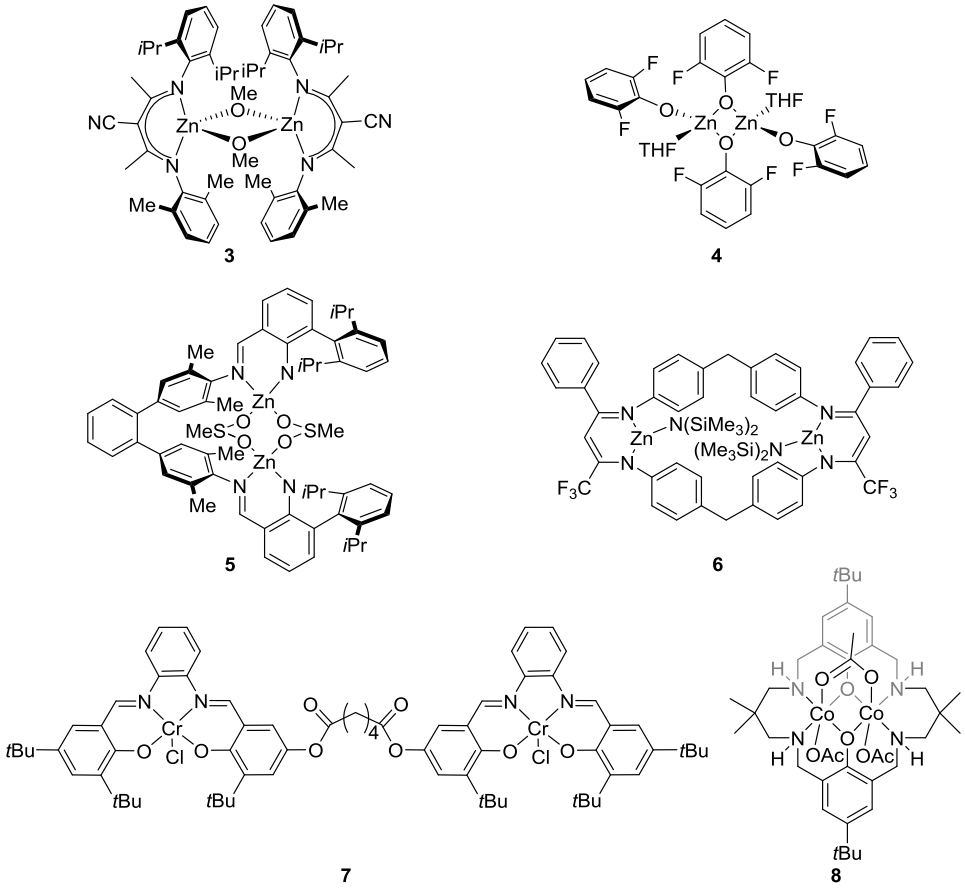

Scheme 1.7. Selected homogeneous bimetallic catalyst systems for CO_2/epoxide copolymerization: β-diiminate Zn **3** [60, 61], dimeric Zn phenoxide **4** [57], bis(anilido-aldimine) Zn **5** [58], tethered β-diiminate Zn **6** [59], tethered salphen Cr **7** [62] or dinuclear macrocyclic reduced "Robson" type **8** [56] systems.

More recently, Nozaki and Rieger groups respectively reported tethered (salen)M type (where M = Co, Cr) complexes for the copolymerization of PO and CO_2 [45, 62, 63]. When no cocatalyst is added, a bimetallic propagation mechanism is followed leading to a great improvement of the performance (differs by one to two orders of magnitude) compared to the monometallic counterparts. For example, the dimeric Cr-salphen with a four methylene linker **7** is active at low catalyst loading ([Cr]:[monomer] = 1:2000, 60 ºC, 40 bar, TOF = 82 h^{-1}), supporting the fact that two

metal sites are involved in the mechanism [62]. Dinuclear metal coordinated by a macrocyclic, reduced “Robson” type ancillary ligand was first developed on Zn and later on Mg or Co metal center leading to unprecedented activity for the coupling of CO_2 with CHO under low CO_2 pressure. Cobalt proved to be the most active and selective metal center investigated, especially compared to the zinc analogues. The mixed valence Co(II)/Co(III) complex **8** is active under mild conditions (80 ºC, 1 bar, TOF = 159 h^{-1}) but the activity increases significantly at higher temperature and pressure (100 ºC, 10 bar, TOF = 3700 h^{-1}) [56].

Monometallic catalysts are divided in two sub-categories: binary components including a cocatalyst in addition to the complex and single components also called bifunctional catalysts where the complex bears the cocatalyst (Scheme 1.8).

In 1978, Inoue reported the first single-site catalyst for the epoxide and CO_2 copolymerization. The system is based on a tetraphenylporphyrin (tpp) framework initially developed on aluminum, leading for example to complex **9**, and then extended to other metal centers like Co, Mn and Cr. These catalysts combined with an appropriate cocatalyst are moderately active, producing the first monodisperse polycarbonates with narrow PDIs but with low molecular weight and in long reaction times [64-67]. Among these metals, (tpp)MnOAc was reported in 2003 as the first successful example of catalyst enhancing the coupling of CHO with CO_2 under 1 bar of CO_2 (80 ºC, 24 h, conversion = 14%) [68]. However the catalytic activity is greatly improved by increasing the reaction time (90 h) or the CO_2 pressure (50 bar). Discrete Zn but also Al and Cd based catalysts mainly supported by phenoxide ligands were developed and showed to be active for the production of polymers [69-71]. Also, rare-earth alkyl/hydride precursors have been investigated showing decent activity [72, 73].

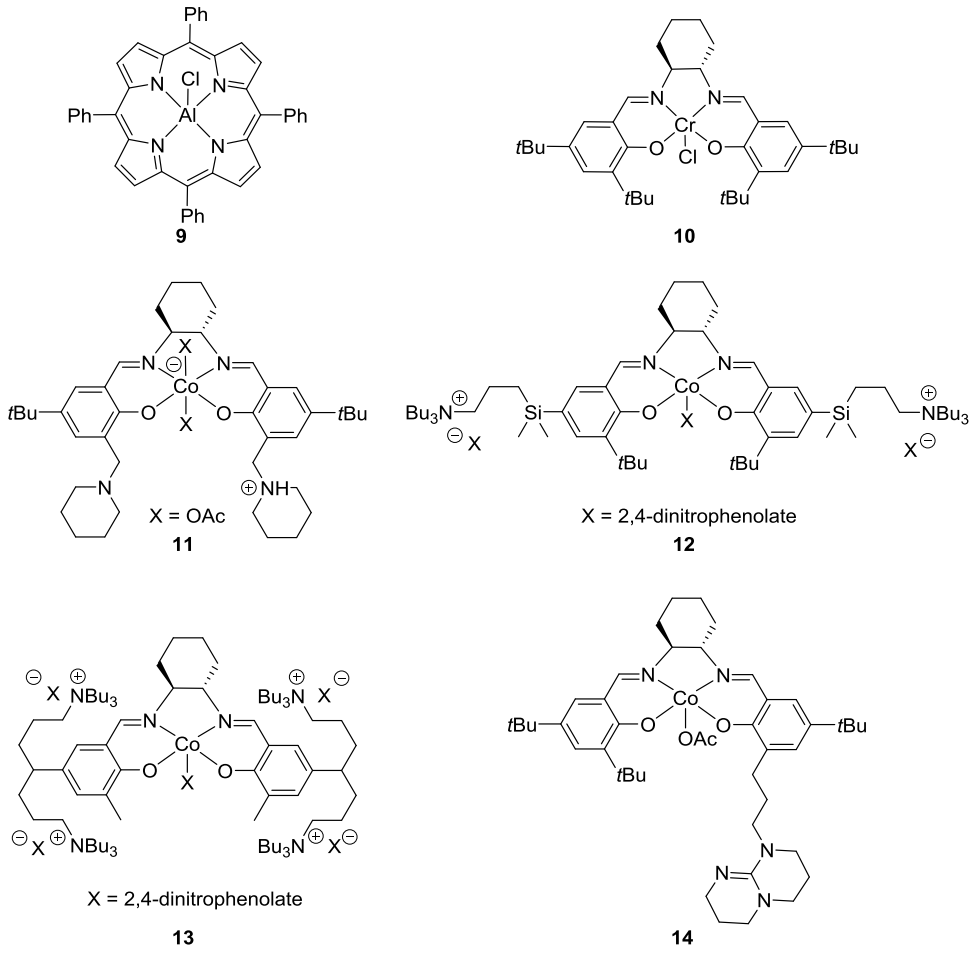

Scheme 1.8. Selected homogeneous monometallic catalyst systems for CO_2/epoxide copolymerization, binary component: porphyrin (tpp) Al **9** [64] or salen Cr **10** [48] systems and single component (salen)Co^{III} bearing: piperidinium **11** [74], quaternary ammonium salt **12** and **13** [75, 76] and TBD **14** [77] appended group.

Another class of intensively studied homogeneous catalytic systems is based on salicylaldimine (salen) framework. Jacobsen *et al*. and Darensbourg *et al*. were the first to report chromium salen complexes as active, stereoselective and stable catalysts for the production of polycarbonates. To date (salen)$M^{III}X$ (M = Cr **10** or Co) complexes combined with a cocatalyst (typically the onium salt [PPN]Cl) are

considered as the most successful systems for CO_2-epoxide coupling and have been developed extensively [34, 39, 78]. Detailed studies have shown that the use of one or two equivalents of an ionic cocatalyst is necessary to activate the pre-catalyst and form the active six-coordinate intermediate enhancing the formation of polycarbonates. In the past decades many examples of (salen)$Co^{III}X$ have been reported with various X nucleophiles as well as ligands bearing a wide range of substituents. Typically these catalysts are active at moderate temperature, highly selective (> 99%) and showing moderate yields (< 50%). This last property is mainly due to the increase in viscosity while the polymer is growing. The change of the reaction medium viscosity limits increasingly the epoxide diffusion to the metal center. In addition to Co and Cr, other metal centers as Al or Mn salen or salan complexes have been investigated [34, 79-90].

Following this development, we recently assisted to a breakthrough with the synthesis of an advanced class of single component salen complexes bearing appended functionalized cocatalyst groups. These systems are highly stereoselective (formation of polycarbonate over cyclic carbonate) and active, mainly for the production of PPC. In 2006, Nozaki *et al*. reported the first example of a cobalt salen complex with a piperidinium end-capping arm **11** [74]. The functionalized arm has the ability to shuffle protons between the amines and the growing polymer chain, avoiding the back-biting reaction even at high temperature. This bifunctional catalyst allows keeping a good selectivity (99%) toward the polymer synthesis and increases grandly the conversion until 80% ([Co]:[monomer] = 1:2000, 60 ºC, 20 bar, TOF = 610 h^{-1}). Following this new ligand design approach, Lee *et al*. published in 2007 a cobalt salen complex bearing one or two quaternary ammonium salts bound at the 5-position of each phenyl ring of the ligand, combining the catalyst and the cocatalyst in a single component **12**-**13** [75, 76, 91]. Complex **13** presents the highest activity for the copolymerization of CO_2 and PO reported, even at diluted catalyst concentration ([Co]:[monomer] = 1:25000, 80 ºC, 20 bar, TOF = 26000 h^{-1}) affording high molecular weight copolymers (M_n = 114000 g mol^{-1}). Another example of these highly productive bifunctional complexes are the asymmetric (salen)CoX complexes developed by Lu *et al*. where the 3-position of one of the ligand's phenyl ring bears a

sterically hindered organic defined as TBD (1,5,7-triabicyclo[4,4,0]dec-5-ene) **14** [77, 92]. Complex **14** leads to the formation of high molecular weights PPC (M_n = 112300 g mol^{-1}) with a TOF = 7139 h^{-1} in similar conditions as Lee's catalysts (([Co]:[monomer] = 1:25000, 90 ºC, 20 bar).

Single-component catalysts are considered to be among the most active catalyst to date. Such class of catalytic systems are stable, active at high temperature (up to 90 ºC), selective (> 90%), allow to decrease greatly the catalyst loading without impacting the initiation rate and achieve TOF between 1300 and 20000 h^{-1}. The success of these catalysts lies in the proximity of the cocatalyst to the metal center circle, thereby avoiding the growing chain to detach from it. Indeed, the charged polymer chain is electrostatically attracted to ammonium salts preventing any back-biting, making them resistant to possible contaminants (water, alcohols), and therefore stabilize the active metal center.

Compounds based on Cr, Co, and Zn metals have shown significant activity for the copolymerization of CO_2 and epoxides. However, harmless metals must be furthermore considered and explored [32, 33].

1.2.3.3. Recent Advances on "Sustainable" Catalysts

Despite the success of tetravalent group 4 metals in the ring-opening polymerization (ROP) of cyclic ethers [93], the use of catalytic systems based on group 4 elements for the reaction of CO_2 with epoxides has only recently emerged [94]. Indeed, in addition to their reactivity, the use of element as Ti or Zr are attractive metals for the synthesis of sustainable polymers as they are abundant in the earth's crust, listed as non-endangered elements and present a low toxicity [95].

Nozaki *et al*. opened the way with their investigation on active tetravalent metal (Ti, Zr, Ge and Sn) complexes, supported by a tetradentate trisanionic boxdipy ligand (boxdipy = 1,9-bis(2-oxidophenyl)dipyrrinate) mimicking salen-type ligands **15** (Scheme 1.9) [96]. Boxdipy-Ti^{IV}, after activation by [PPN]Cl salt, showed decent

activity and high selectivity toward CHO/CO_2 copolymerization ([Ti]:[monomer] = 1:2000, 60 ºC, 20 bar, TOF = 76 h^{-1}) producing high molecular weight PCHCs rich in carbonate linkages (M_n = 13000 g mol^{-1}, carbonate linkages = 99%).

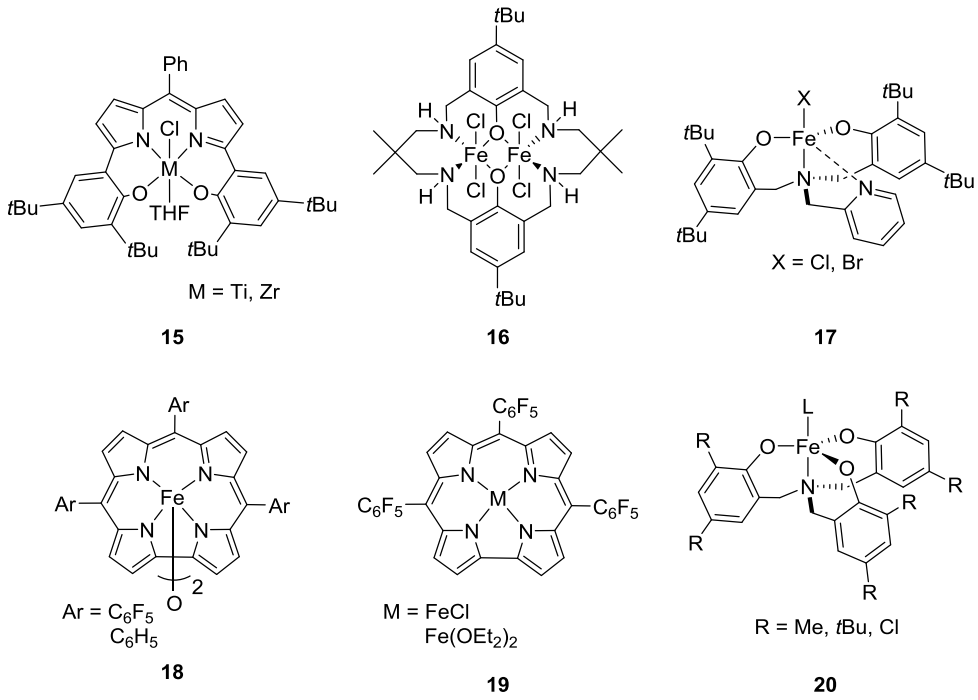

Scheme 1.9. Sustainable precursors active in copolymerization of CO_2 with epoxides: boxdipy titanium(IV) **15** [96], bimetallic iron(III) macrocyclic reduced "Robson" type ligand **16** [97], pyridylamino-bis(phenolate) **17** [98], iron-corrole **18** and **19** [99] and iron amino triphenolate **20** [100] catalysts.

In parallel, a first catalyst based on Fe was reported by Williams´s group [97]. Iron is another potential element as it is the most abundant transition metal. This novel di-iron(III) macrocyclic reduced "Robson" type ligand **16** (Scheme 1.9), without the addition of cocatalyst, yields PCHCs with high carbonate linkages and moderate molecular weight (carbonate linkages = 93%, M_n = 2000 g mol^{-1}) under mild conditions ([Fe]:[monomer] = 1:1000, 80 ºC, 1 bar, TOF = 6 h^{-1}). Other iron based catalysts were developed for the coupling of epoxide with CO_2 as pyridylamino-

bis(phenolate) **17** [98], corrole **18** and **19** [99] and amino triphenolate **20** [100] complexes.

1.3. Aims

The overall objective of this thesis was to develop novel catalysts for the copolymerization of epoxide/CO_2 in line with elements that are abundant, non-endangered and presenting a low toxicity.

More specifically, the thesis focuses on the research of new multidentate ligands and complexes of titanium based on the recent discovery of Nozaki´s group, showing for the first time that group 4 metal complexes (particularly Ti) have a great propensity toward the copolymerization of CO_2 and epoxides. Iron is discarded here, as its catalytic results did not show, so far, high selectivity and activity. Different *mer*/planar-ligands to mimic Nozaki's titanium-based system (Scheme 1.9) were considered such as tetradentate (salen, salan), tridentate NHC and bidentate NHC ligands (Scheme 1.10).

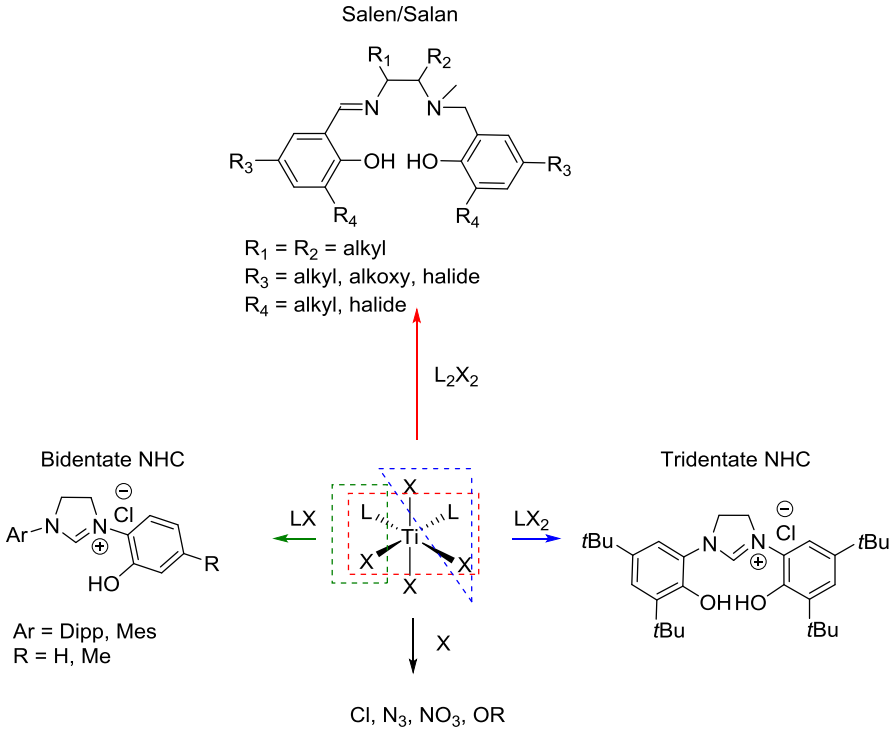

Scheme 1.10. Multidentate ligands of titanium-based considered as precursor for the polymerization of epoxides for CO_2.

After a short and unsuccessful period of investigations on salen-Ti complexes for the CO_2 and epoxide copolymerization, we turned our focus on the use of analogues oxygen–functionalized NHC group 4 compounds.

To date, few examples of mono, di and tridentate complexes based on early transition metals have been reported [101-103] (Scheme 1.11). Among the tridentate examples, NHC incorporating an imidazolium linked bis(phenol) group 4 complexes **21** - **23** were developed first by Aihara *et al*. [104], followed by Zhang's group [105-107]. The *mer*-tridentate bis(aryloxide)/phenolate NHC group 4 complexes **24** - **29** were developed by Bellemin-Laponnaz *et al*. [108, 109]. These catalytic systems based on Ti and Zr metals exhibit high activities and high control over the ring-opening polymerization (ROP) of *rac*-lactide.

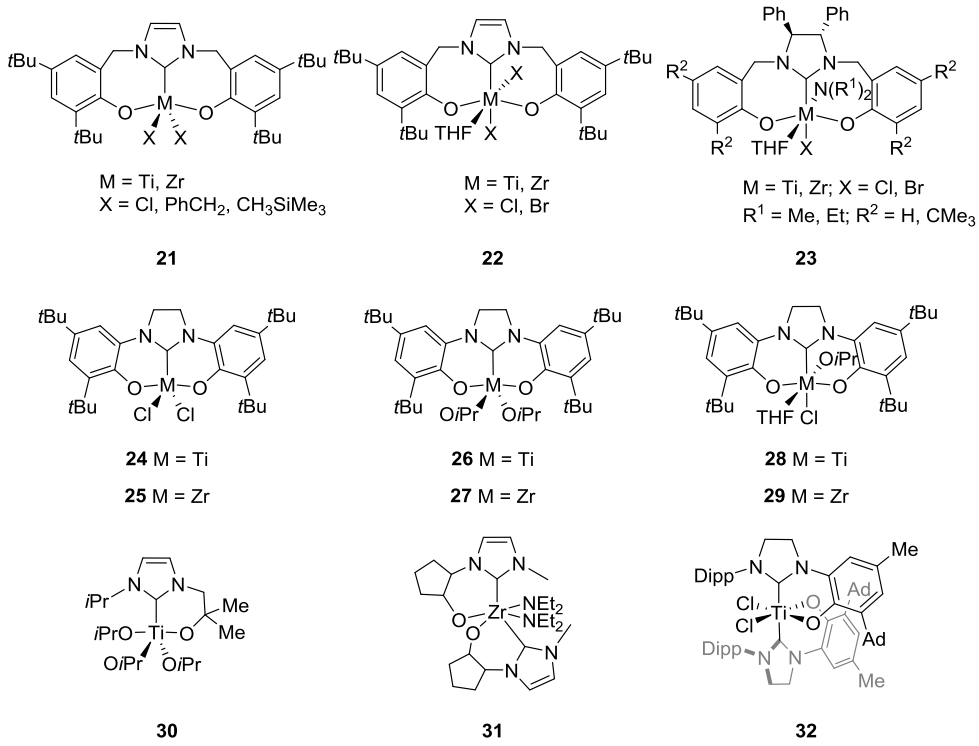

Scheme 1.11. NHC group 4 compounds, tridentate: NHC incorporating an imidazolium linked bis(phenol) complexes of Ti and Zr **21**-**23** [104-107], bis-chloride Ti **24** and Zr **25**, bis-isopropoxide Ti **26** and Zr **27**, chloride isopropoxide Ti **28** and Zr **29** [108] and bidentate: alkoxy Ti(IV) **30** [110], cyclopentenyl-2-alkoxy Zr(IV) **31** [111] and bis-ligated phenolate Ti(IV) (with Dipp = 2,6-diisopropylphenyl and Ad = adamantyl) **32** [112].

Few examples of bidentate NHC group 4 complexes have been reported. In 2005, Arnold *et al*. developed the remarkably air stable alkoxy functionalized NHC with oxygen-coordinated arms **30** [110, 113]. Other complexes have been developed as the bis(imidazolidene-N-methyl-N'-cyclopentenyl-2-alkoxy)zirconium diamide **31** [111] and the bis-ligated phenolate NHC group 4 compounds **32** [112, 114, 115]. These bidentate complexes showed to be active catalysts for the polymerization of *rac*-lactide [110] and the polymerization of ethylene, styrene and propylene [111, 112, 115].

Our initial success (Paper I) [116] combined with boxdipy-Ti/Zr systems initiated other investigations from our research group and others in developing new group 4 catalysts (Scheme 1.12).

In 2014, Wang *et al*. reported salen titanium as catalyst for the coupling of CHO and CO_2 [117]. Whereas (salen)$Ti^{IV}Cl_2$ **33** upon [PPN]Cl addition, proved to be only active for the production of *cis*-cyclic carbonate, (salalen)$Ti^{IV}Cl$ **34** allows the formation of completely alternating PCHCs ([Ti]:[monomer] = 1:1000, 60 ºC, 40 bar, TOF = 12 h^{-1}, carbonate linkages = 99%, PCHC/CHC = 98/2). Following this work, Wang´s group developed trivalent salalen titanium complexes **35** which, with the use of [PPN]Cl, proved to be highly active and selective for the production of PCHCs ([Ti]:[monomer] = 1:1000, 120 ºC, 40 bar, TOF = 577 h^{-1}, carbonate linkages = 99%, PCHC/CHC = 99/1) [118]. Other salen type, salen Zr(IV) **36** and bis(salphen) (salphen = N,N'-phenylenebis(salicylideneimine) ligands with group 4 systems for the coupling of CHO and CO_2 have been reported by Mandal *et al*. [119, 120]. Bis(salphen) with titanium(IV) **37** is active for the reaction with the use of a cocatalyst ([Ti]:[monomer] = 1:1000, 50 ºC, 35 bar, TOF = 123 h^{-1}, carbonate linkages = 74%) [120]. Following the work on complexes **24**, **26** and **28** (Scheme 1.11), our group investigated sterically (un)encumbered *mer*-tridentate NHC titanium **38** and **39** as catalysts for the CHO/CO_2 coupling [121]. However these catalysts are active at low CO_2 pressure (60 °C, $P_{CO2} \leq 1$ bar, TOF = 6 h^{-1}), they are less stable and efficient than their structural bulky analogues. The last examples reported are group 4 metals ligated with BTP (benzotriazole phenolate) type ligands developed by Chuang *et al*.. These catalysts showed to have a moderate activity and selectivity to afford completely alternating PCHCs: bimetallic $(BTP)_2Zr$ alkoxide complex **40** ([Zr]:[monomer] = 1:200, 100 ºC, 20 bar, TOF = 6.8 h^{-1}, carbonate linkages = 79%) [122] and BTP complex, where Zr proved to be the most active metal center leading to complex **41** ([Zr]:[monomer] = 1:500, 100 ºC, 20 bar, TOF = 9.5 h^{-1}, carbonate linkages = 70%) [123].

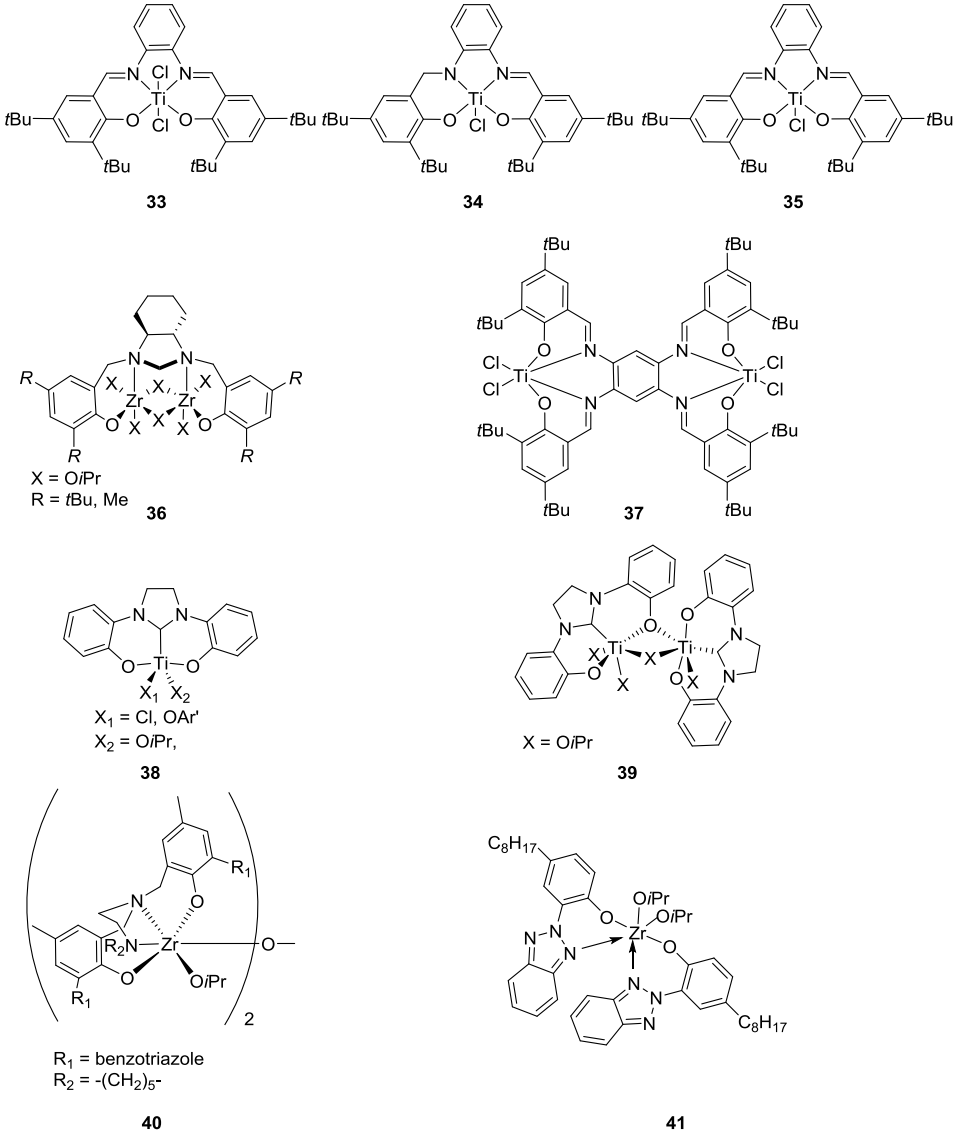

Scheme 1.12. Published group 4 catalysts for the CO_2/epoxide copolymerization during the course of this project: (salen)$Ti^{IV}Cl_2$ **33**, (salalen)$Ti^{IV}Cl$ **34** [117], (salalen)$Ti^{IV}Cl$ **35** [118], salan-type diamine bis(phenolato) Zr(IV) **36**, Bis(salphen) with titanium(IV) **37** [120], (un)encumbered *mer*-tridentate Ti^{IV} **38** and **39** [121], Bimetallic $(BTP)_2Zr$ alkoxide **40** [122] and BTP Zr(IV) alkoxide **41** [123].

2. Summary of main results

2.1. Synthesis and Characterization of Multidentate *N*-Heterocyclic Carbene Titanium Complexes

NHCs display strong σ-donor and weak to moderate π-acceptor electronic properties and constitute an important class of chelating ligands for transition metals, taking over the earlier use of phosphines as ancillary ligands. In addition to the unique electronic properties of NHCs, the ease of substituent´s variability at the nitrogen atom makes them suitable ligands to bind with a wide range of metals, giving them a huge potential as catalysts in organic transformations and polymerizations [101, 124]. Most of the current applied systems are based on late transition metal complexes, despite the great potential of early transition NHC complexes for catalytic applications.

The first group 4 NHC adducts reported, were the monodentate $(IMe)_2MCl_4$, synthetized from metal halide (where M = Ti, Zr and Hf) in 1994. However, the development of these complexes has been under investigated due to the ease of dissociation of the $M\text{-}C_{carbene}$ bond. Indeed, the carbene with its soft character dissociates easily from the electron deficient metal center, especially for group 4 transition metals in high oxidation states. To overcome this limitation, a plethora of multidentate NHC donor systems bearing anionic ligands have been developed in the past decade, *i.e*. containing armed chelating functional groups based on carbon, nitrogen and oxygen [103, 125-127]. The coordination of these NHC derivative ligands to early transition metals enable to ensure an efficient chelation and lead to robust and stable complexes [102, 103]. The stability of NHC complexes from undesired dissociation is also controlled by anchoring substituents, the use of ancillary ligands restricting the bite angle steric size avoids the degradation of the complex [128].

An overview of the classical synthetic approaches developed to obtain group 4 NHC containing functional groups complexes have been reported by Zhang et *al*. [102]. There are two main approaches. The first is *via* the deprotonation of the azolium salts to obtain the free (or M-NHC where M = Li, Na, K) NHC intermediate, followed by its coordination to halide metal precursors. Free carbene species are usually difficult to isolate due to their poor stability, but can be formed *in situ* before their coordination with group 4 metal sources, at low temperature. The second route is *via* amine, toluene, alcohol or HCl elimination by the direct addition of the metal precursor to the imidazolium salt to afford group 4 metal NHC complexes.

2.1.1. Synthesis of Tridentate *N*-Heterocyclic Carbene Titanium Complexes by Direct Addition

The synthesis and characterization of the symmetrical 1,3-bis(3,5-di-*tert*-butyl-2-hydroxyphenyl) imidazolinium chloride salt, [κ^3-$^{t\mathrm{Bu}}$*O,C,O*]-NHC ligand **42** and complexes ([κ^3-$^{t\mathrm{Bu}}$*O,C,O*]-NHC)Ti(THF)(O*i*Pr)Cl **28**, ([κ^3-$^{t\mathrm{Bu}}$*O,C,O*]-NHC)Ti(Cl)$_2$ **24** and ([κ^3-$^{t\mathrm{Bu}}$*O,C,O*]-NHC)Ti(O*i*Pr)$_2$ **26** was described by Dagorne *et al*. [108, 129]. Complex **28** was obtained by direct addition of Ti(O*i*Pr)$_4$ to the imidazolidinium salt **42** *via* isopropanol elimination (Scheme 2.1). Complex **24** was synthesized *via* a different synthetic route developed in our group. To the imidazolium salt **42** was added directly the titanium precursor $TiCl_4$ in toluene and the reaction was allowed to stir at reflux overnight, thus avoiding the need of a base to neutralize HCl (Scheme 2.1). This new approach for the synthesis of titanium NHC complex by the direct addition of titanium halide to **42** leads to higher yield (92%) compared to (O*i*Pr)$_3$TiCl precursor (84%).

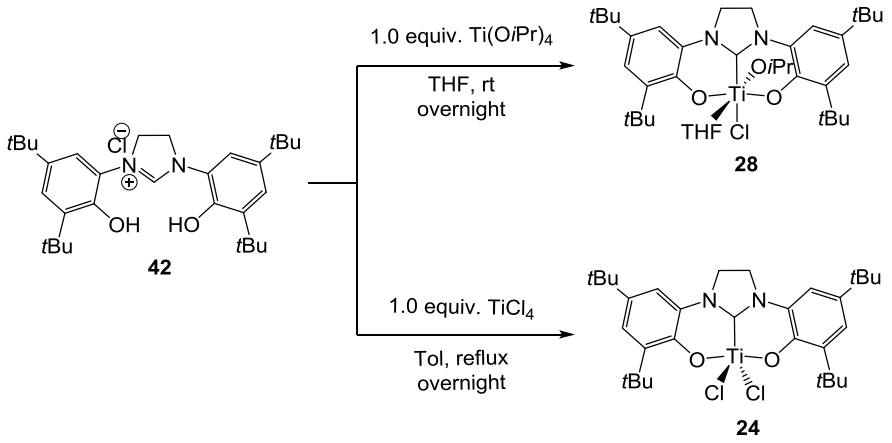

Scheme 2.1. Syntheses of tridentate bis-aryloxy NHC titanium chloride isopropoxide **28** and bis-chloride **24** complexes.

2.1.2. Reactivity of Tridentate *N*-Heterocyclic Carbene Titanium Complexes

The modification of the coligand X of ([κ^3-^{tBu}*O*,*C*,*O*]-NHC)Ti(X)$_2$ complexes was shown to be accessible *via* a typical salt metathesis procedure from the halide or alkoxide metal precursor. Complex **26** was synthesized by reaction of precursor **28** with one equiv. of lithium isopropoxide [108]. Compound **26** showed to be an adequate precursor that could be modified for example by its treatment with one equiv. of *tert*-butoxysilanol or a large excess of trimethylsilylazide to afford ([κ^3-^{tBu}*O*,*C*,*O*]-NHC)Ti(O*i*Pr)(OSi(O*t*Bu)$_3$) **43** and ([κ^3-^{tBu}*O*,*C*,*O*]-NHC)Ti(N$_3$)$_2$ **44** complexes respectively, in high yield (Scheme 2.2).

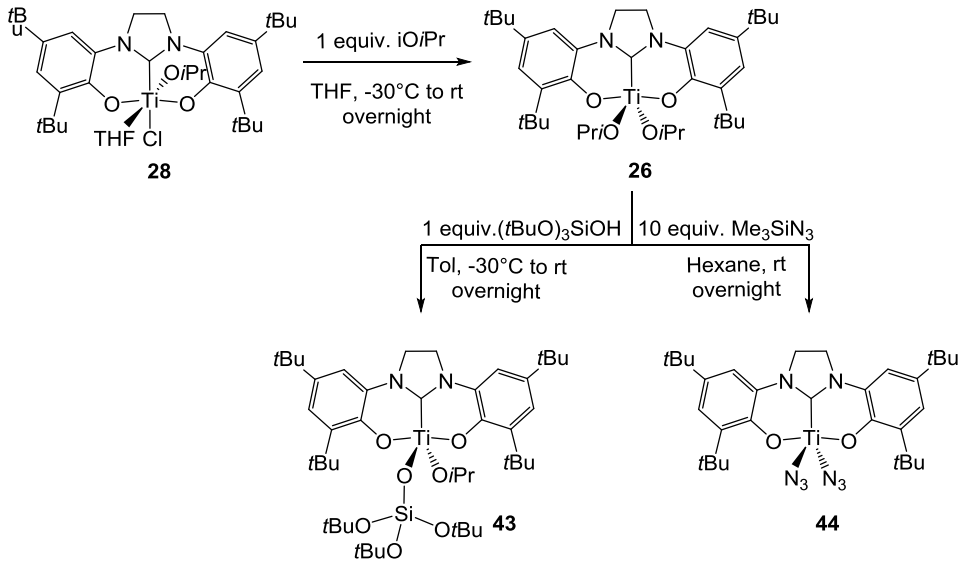

Scheme 2.2. Syntheses of tridentate bis-aryloxide NHC titanium bis-isopropoxide **26**, silyloxide/isopropoxide **43** and azide **44** complexes.

Bis-chloride NHC complex **24** was also applied as a complex precursor (Scheme 2.3). The reaction of **24** with a base followed by (*t*BuO)$_3$SiOH, with lithium benzyloxide salt or with sodium acetate under appropriate conditions generates the corresponding ([κ^3-$^{t\mathrm{Bu}}$*O*,*C*,*O*]-NHC)Ti(Cl)(OSi(O*t*Bu)$_3$)(THF)) **45**, ([κ^3-$^{t\mathrm{Bu}}$*O*,*C*,*O*]-NHC)Ti(OBn)$_2$ **46** and ([κ^3-$^{t\mathrm{Bu}}$*O*,*C*,*O*]-NHC)Ti(η^2-Ac)$_2$ **47** compounds, in good yield.

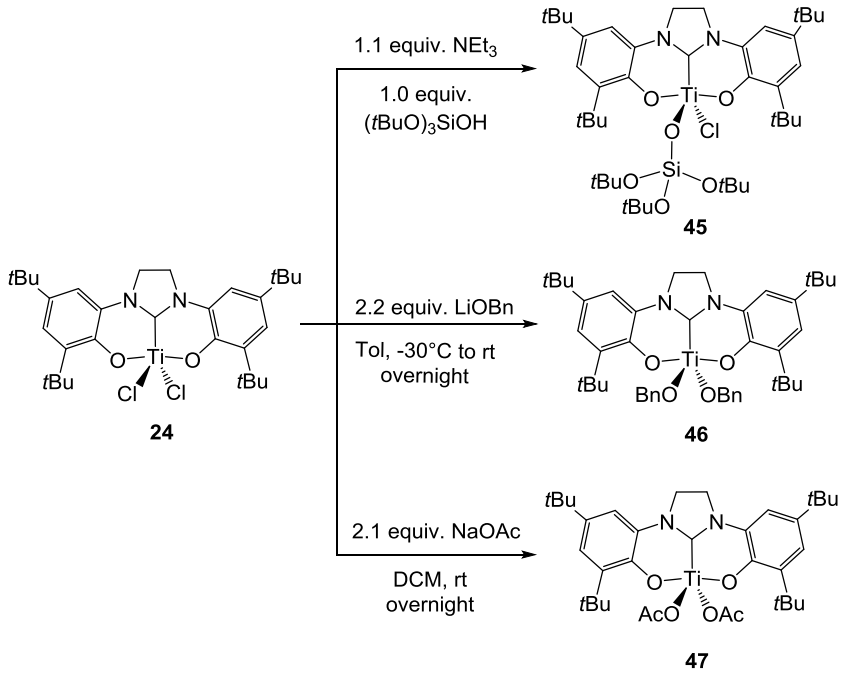

Scheme 2.3. Syntheses of tridentate bis-aryloxy NHC titanium silyloxide chloro **45** benzyloxide **46** and acetate **47** complexes.

All the new compounds were fully characterized by $^{1}H/^{13}C$ NMR and DRIFT spectroscopy and elemental analysis. In addition, complexes **43**, **44-THF** (Figure 2.1), **45-THF**, **46** and **47** (Figure 2.2) were structurally characterized by single crystal X-ray analysis.

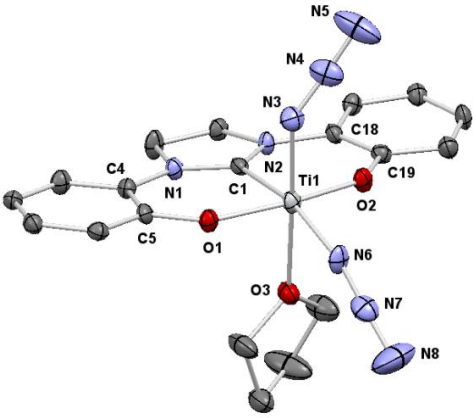

Figure 2.1. Crystal structure of **44-THF** adapted from Paper II [130]. Hydrogen atoms, toluene molecule and *t*Bu groups were removed for clarity.

The formation of complex **44** was also put in evidence by its reaction with an alkyne [131]. The [3+2] cycloaddition reaction of the dipolarophile dimethyl acetylenedicarboxylate (DMAD) (aka "*i-click*") with the azido ligands leads to the formation of the triazolato (Tz) complex ([κ^3-$^{t\mathrm{Bu}}$*O,C,O*]-NHC)Ti($C_2(CO_2Me)_2$) **48** (Scheme 2.4).

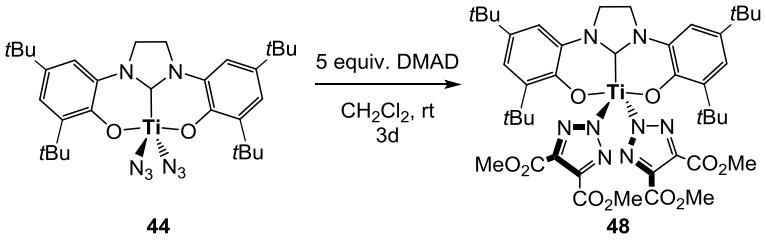

Scheme 2.4. Reactivity of tridentate NHC titanium azide with alkyne.

Tridentate NHC titanium complexes are usually five or six-coordinate adopting octahedral (**28**) or trigonal bipyramidal (**24**, **26**, **43**-**46**, **48**) geometries. Interestingly complex **47** having two oxygen moieties belonging to the NHC ligand and four others from the carboxylate ligands is a rare example of seven-coordinate titanium metal complex as illustrated in Figure 2.2.

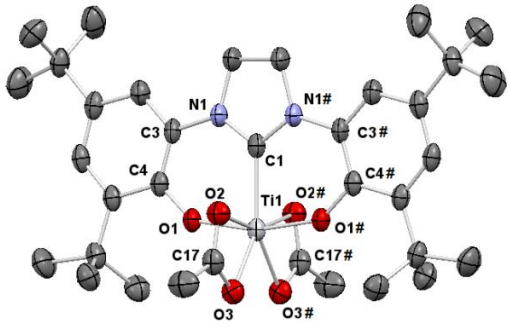

Figure 2.2. Crystal structure of **47** adapted from Paper II [130]. Hydrogen atoms were omitted for clarity.

This uncommon coordination is represented by a pentagonal bipyramid geometry where Ti-$C_{carbene}$ bond appears to have the shortest distance reported for multidentate oxygen-functionalized NHC titanium(IV) complexes (Ti-$C_{carbene}$ length = 2.148 Å). Attempts were performed to synthesize NHC-titanium(III) complex from either Ti(III) precursor or ([*O,C,O*]-NHC)Ti^{IV} derivatives with a reducing reagent. The addition of imidazolidinium chloride salt direct or after its deprotonation with KH to $TiCl_3(THF)_3$ precursor affords intractable reaction mixtures in contrast to other reported procedures for NHC-Ti^{III} [132-137]. The well-established approach to reduce complexes using one equiv. of $LiBEt_3H$ as reducing agent [113, 136-139] at -78 ºC in toluene proves to not be selective for the reduction of complex **24**, but affords after work up, a mixture of products. A green compound was extracted from toluene, which did not show any signals in NMR spectra, presumably being a paramagnetic Ti(III) compound and an insoluble brown compound was identified as the tetravalent complex ([κ^5-$^{t\mathrm{Bu}}$*O,N,C,N,O*]-imidazolidine)Ti(Cl)(THF) **49** (Scheme 2.5).

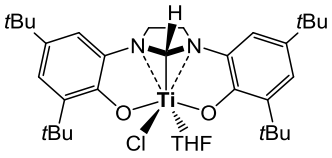

49

Scheme 2.5. Tetravalent imidazolidine titanium complex **49**.

This compound was fully characterized by $^{1}H/^{13}C$ NMR and DRIFT spectroscopy and elemental analysis and its molecular structure was determined by single X-ray analysis. The hydride transfer to the $C_{carbene}$ atom was observed through the ^{1}H and ^{13}C NMR data with respectively chemical resonances of δ 3.95 and 103.7 ppm for the CH formed and the disappearance of the characteristic ^{13}C signal of $C_{carbene}$. Although the obtained crystals of **49** have a limited quality, the connectivity around the titanium center can be determined upon doubts, confirming the formation of the imidazolidine titanium **49**. The solid-state structure of complex **49** shows a seven-coordinate metal center adopting a distorted square face monocapped trigonal prism geometry. However this reactivity has not been reported for NHC titanium complexes, similar alkyl transfers have been reported, notably Lewis base assisted benzyl migration on isolated or putative bidentate NHC-group 4 complexes [140-142], where the formation of the seven-coordinate complexes is engendered by the electrophilic nature of the $C_{carbene}$.

2.1.3. Synthesis of Bidentate *N*-Heterocyclic Carbene Titanium Complexes via Double Deprotonation

The route for the synthesis of versatile aryl substituted NHC ligands to give [κ^2-*O*,*C*] chelate ligand developed by Grubbs *et al*. was used to develop a new set of *o*-hydroxyaryl unsymmetrically *N*-substituted NHC ligands (Scheme 2.6) [114].

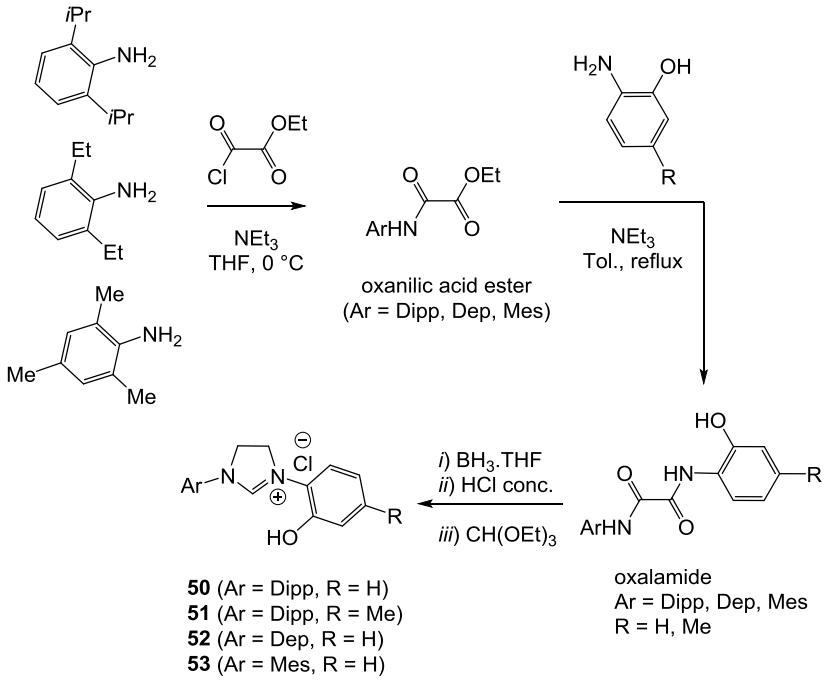

Scheme 2.6. Synthetic route for unsymmetrical *o*-hydroxyaryl substituted imidazolidinium salts **50**-**53** (with Dipp = 2,6-diisopropylphenyl, Dep = 2,6-diethylphenyl and Mes = 1,3,5-trimethylphenyl).

Ethyl chlorooxoacetate was treated with an aryl amine in presence of trimethylamine to afford the corresponding oxanilic acid ester. This compound was then reacted with the desired aminophenol leading to the oxalamide. At this point carbonyl functions were reduced using a borane-THF solution followed by the protonation of the amide functions by concentrated HCl. Finally, the cyclization of the heterocycle was achieved by treatment with triethylorthoformate to afford the carbene precursors **50**-**53**. The new intermediate compounds and ligands were characterized by $^{1}H/^{13}C$ NMR and DRIFT spectroscopy and elemental analysis.

The route followed for the coordination of bidentate *o*-hydroxyaryl unsymmetrically substituted NHC to titanium was reported by Grubbs *et al*. [112]. Ligands **50-53** were doubly deprotonated using two equivalents of potassium bis(trimethylsilyl)amide (Kbtsa) for 10 min prior to the reaction with a solution of $TiCl_4$ for 2 h. Free NHC ligands or alkali metal-NHC complexes are known to be difficult to isolate due to their poor stability, however, they can be formed *in situ* before their coordination with the metal source. The double deprotonation of **50** and **51** followed by their coordination to $TiCl_4$ precursor leads to the formation of $([\kappa^2\text{-}^{Dipp}C,O]NHC)_2TiCl_2$ **54** and $([\kappa^2\text{-}^{Dipp,(4\text{-}Me)}C,O]NHC)_2TiCl_2$ **55** complexes as dark red solids, in quantitative yield (Scheme 2.7).

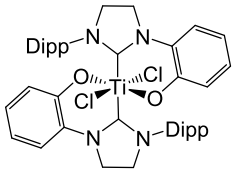

54

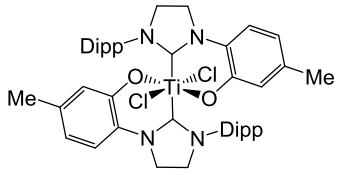

55

Scheme 2.7. Bidentate *o*-hydroxyaryl NHC titanium chloride complexes **54** and **55**.

Attempts using $Ti(OiPr)_4$ as titanium precursor by direct addition under different temperature conditions (room temperature to reflux) and solvents (toluene, THF) did not lead to the coordination of the carbene to the metal center. It is also interesting to note that despite our efforts to synthesize the mono-ligated complex, the treatment of the "free" NHC ligands **50** and **51** with one equiv. of $TiCl_4$, only afford a unique stereoisomer of bis-ligated NHC titanium. The new synthesized complexes **54** and **55** were characterized by $^1H/^{13}C$ NMR and DRIFT spectroscopy. The molecular structure of **54** was also determined by single X-ray analysis displaying a slightly distorted octahedral geometry, similar to the reported 1-(2,6-diisopropylphenyl)-3-(2-hydroxy-3-(adamant-1-yl)-5-methylphenyl)-4,5-dihydro-imidazolyl titanium(IV) dichloride complex $([\kappa^2\text{-}^{Dipp,(3\text{-}Ad,5\text{-}Me)}C,O]NHC)_2TiCl_2$ **32** [112] (Figure 2.3).

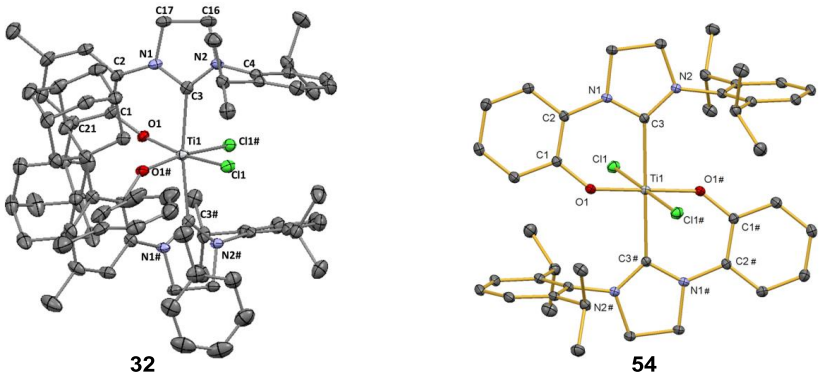

Figure 2.3. Crystal structure of **32** adapted from [112] and of **54** adapted from Paper III. Hydrogen atoms and a co-crystallized solvent dichloromethane molecule are omitted for clarity.

In both complexes, the neutral NHC moieties situated in *trans* to each other occupy the axial positions and the anionic aryloxide the equatorial positions. However, unlike ([κ^2-$^{Dipp,(3\text{-}Ad,5\text{-}Me)}$*C,O*]NHC)$_2$TiCl$_2$ **32** having the two oxygen and the two chloride atoms located *cis* to one another, complex **54** possesses the two oxygen and the two chloride atoms *trans* to each other. In the case of ([κ^2-$^{Dipp,(3\text{-}Ad,5\text{-}Me)}$*C,O*]NHC)$_2$TiCl$_2$ **32**, the *cis* configuration observed is favored to avoid the steric interaction between the Dipp and Ad bulky substituents. Although the coordination mode of **54** is similar to reported bis-ligated salicylaldimine titanium complexes [143], the lack of bulky substituents on the aryloxy ring leads to the thermodynamically stable *trans* configuration. Crystal structures of **32** and **54** were used to calculate the percent buried volume (%V_{bur}, *via* Sam*V*ca 2.0 calculations) and visualize steric maps of the complexes [144, 145]. This additional study showed that the *trans* configuration is greatly favored by the coordination of the second NHC ligand bearing a H as *ortho* substituent on the aromatic ring thus avoiding the collision of the two Dipp groups. On the contrary, the *cis* configuration is preferred with an *ortho* bulky substituent.

Following the same procedure as **50** and **51**, the double deprotonation of *o*-hydroxyaryl imidazolidinium chloride salts **52** and **53** followed by their treatment with $TiCl_4$ precursor gives only intractable mixture of compounds, suggesting the

formation of different isomers. A similar steric study, as for **32** and **54**, was conducted on **52** and **53**. Unlike in the case of *ortho* bulky *i*Pr groups on the *N*-Dipp substituent (leading to the single stereoisomer *trans* configuration in complex **54**), the presence of less hindered *N*-aryl substituent in imidazolidinium chloride salts **52** and **53** could not suppress the formation of other isomers.

2.2. Applications in Catalysis: Copolymerization of Cyclohexene Oxide and Carbon Dioxide

All the reported complexes (**24**, **26**, **28**, **43**-**47**, **49**, **54** and **55**) were evaluated as pre-catalyst for the coupling of CHO and CO_2. Typically, the reaction is run with a CHO:Ti ratio equal to 2500 (8 μmol of precursor, 8 μmol of [PPN]X cocatalyst, 20 mmol of CHO), with a CO_2 pressure of 0.5 bar and a temperature of 60 ºC.

All the tridentate bis-aryloxy NHC titanium(IV) complexes activated by [PPN]X are able to catalyze the copolymerization of CHO with CO_2 along with excellent selectivity in atactic PCHCs (≥ 99%) without the formation of side-products. Interestingly, ([κ^5-$^{t\mathrm{Bu}}$*O*,*N*,*C*,*N*,*O*]-imidazolidine]Ti(Cl)(THF) complex **49** shows no catalytic activity under these reaction conditions, demonstrating the importance of the $NHC_{carbene}$-type ligand in the reactivity of the titanium metal center.

Bidentate *o*-hydroxyaryl unsymmetrically substituted NHC titanium(VI) complexes **54** and **55** show no polycarbonates formation or other side-products such as cyclohexene carbonate or homopolymer. The unreactivity of these complexes toward the copolymerization is possibly due to the steric congestion around the metal center hindering the coordination either of the nucleophile (from the cocatalyst) to form the putative anionic active specie or the CHO to the titanium center.

2.2.1. Polymers Properties

Polymers were characterized by ^{1}H and ^{13}C NMR spectroscopy allowing the determination of the conversion and the selectivity. All the PCHCs formed showed to have a high degree of carbonate linkages (≥ 99%) and a moderate TOF included between 20 and 39 h^{-1}. The stereostructure was deduced by the model developed by Nozaki [146] from the ^{13}C spectra of the PCHCs, showing an atactic configuration for all the polymers produced [84, 146]. A general trend of the obtained PCHCs gives a narrow but bimodal polydiversity attesting that polymerization occurs in a control manner. Also, the molecular weights measured for these PCHCs are lower than the expected theoretical values due to the presence of a moisture contaminant and/or the possible monomer enchainment on both *trans* and *cis* side of the Ti-$C_{carbene}$ bond [67, 85, 147-150].

2.2.2. Study of the Reaction Conditions

2.2.2.1. Pressure and Temperature

Different pressures and temperatures were investigated for the optimization of the reaction conditions. Carbon dioxide pressure was studied from 2 to 25 bar. No significant changes in activity and/or selectivity were observed for our systems similarly to boxdipy titanium catalyst [96]. It is important to note that it was the first example of tetravalent titanium catalytic system working at pressure close to atmospheric pressure providing completely alternating polycarbonates (selectivity ≥ 99 %) with TOF included from 20 to 39 h^{-1}. The temperature of the copolymerization reaction was varied between 30 to 80 °C. An increase of the temperature allows an increase of the overall yield of the reaction (homogeneity of the reaction mixture is improved by higher temperature). However, above a certain temperature (*i.e.* 60 °C) an increase of the yield is still observed but accompanied by a decrease of the molecular weight of the produced polymer chains. In addition, the tridentate NHC titanium complexes proved to be robust toward high temperature and pressure conditions.

2.2.2.2. Catalyst Loading

An increase of the catalyst concentration from 2 mM to 8 mM (4 mM in typical reaction) leads to an increase of the overall yield of the reaction. Stagnation is observed at higher catalyst loading due to mass transfer problem as a consequence of the solidification of the reaction mixture. This phenomenon was also observed for other catalytic systems [33, 43, 147]. To overcome this problem, a co-solvent was used improving the copolymer yield until a concentration of 6.6 mM. At higher catalyst dilution the production of PCHCs significantly drops. Similar to salen type Cr(III) [PPN]X activated system, the mechanism is dependent on the concentration of catalyst and epoxide indicating that the reaction proceeds presumably via a cooperative intermolecular mechanism of the epoxide ring-opening [43, 81, 150, 151]. The incoming nucleophile binds to the titanium metal center to form the active species. The formed active compound is either behaving as a whole nucleophile or releasing a nucleophile allowing the intermolecular ring-opening to a coordinated CHO.

2.2.2.3. Nature of the Cocatalyst

Without the addition of a cocatalyst to the tridentate NHC titanium complexes, only the formation of PCHO was observed, pre-catalysts do not permit the insertion of CO_2 molecule into the polymeric chain. These polyethers produced in low yield are composed of long chains (M_n = 56 - 83 kg mol^{-1}) rich in ether linkages ($\geq$ 99%).

Different cocatalysts were tested in combination with tridentate NHC titanium complexes. The anionic [PPN]Cl salt, a bulky cation associated to an anion with a poor leaving group ability, was proved to be the most efficient cocatalyst, achieving high activities and good selectivity [42]. The coordination of [PPN]Cl to Lewis acid metal center is described as a reversible exchange process which creates an increase of the electron density on the metal center [152, 153]. Previous studies on salen catalytic systems have shown that this process enhances the formation of anionic six-coordinate *trans*-(salen)MX_2 and labilizes the ligand on the *trans* position to the

coordination site [152, 153]. These observations were also made for titanium(IV) tridentate NHC catalytic systems. The activation of the five- and six-coordinate neutral complexes by onium salts [PPN]X (where X = Cl, N_3, NO_2) allowed the production of PCHCs, without the formation of side products. Recrystallization of the active species proved to be impossible, due to the dissociation of the onium salt from the complex. Preliminary investigation by NMR spectroscopy of complexes **24**, **26** and **28** upon the addition of [PPN]Cl were performed (Figure 2.4).

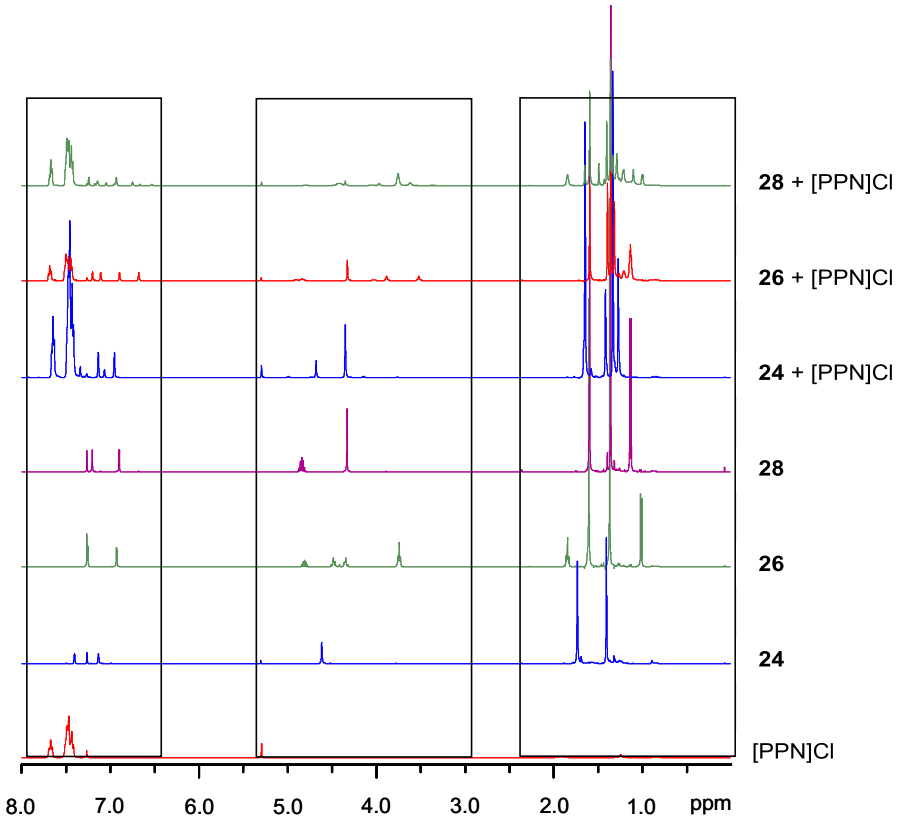

Figure 2.4. ^{1}H NMR spectra of complexes **24**, **26**, **28**, and [PPN]Cl and complexes **24**, **26** and **28** after activation with 1 equiv. of [PPN]Cl in $CDCl_3$. Adapted from Paper I [116].

The observed chemical shifts show an increase of the electron density on titanium metal center indicating most probably the formation of the six-coordinate intermediates **56**, **58**, **59** and **60** (Scheme 2.8).

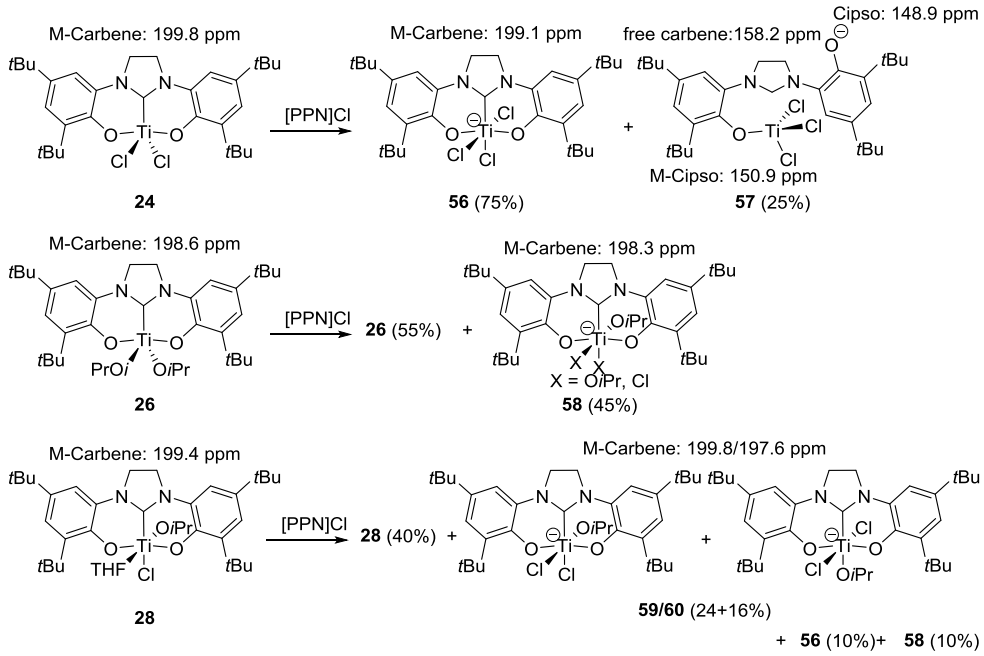

Scheme 2.8. Proposed initiation mechanism after activation with [PPN]Cl on **24**, **26** and **28** complexes adapted from Paper I [116].

Different equivalents of cocatalyst/catalyst were evaluated determining the optimized ratio of one equivalent. The use of a substoichiometric amount most probably provokes a decrease of concentration of anionic six-coordinate intermediates thus causing a decrease of the overall activity of the systems [67, 82, 151]. An addition of an excess of [PPN]Cl has a detrimental effect on the formation of polymer, which was already observed for salen type systems [150]. Interestingly the use of [nBu$_4$N]Cl salt did not lead to the formation of polymer, showing the importance of using a more sterically encumbered and less interacting [PPN]$^+$ cation for the formation of active anionic species [154]. The use of the more nucleophilic anionic cocatalyst [PPN]N$_3$ showed to have a small beneficial effect on the productivity and the TOF of the

complexes bearing encumbered coligands (isopropoxide **26** and **28**, silyloxide **43** and **45**, benzyloxide **46** and acetate **47**). On the contrary, its application to complexes with less-hindered coligands (chloride **24** and azide **44**) leads to a small decrease of CHO conversion due to, a slightly favored degradation of the active species for Cl and a lower concentration and stabilization of the active intermediate for N_3. A reduced activity and yield were observed when using [PPN]NO_2. In the class of neutral bases, the use of the known DMAP or PPh_3 to the tridentate NHC complexes did not allow the formation of polycarbonate or cyclic carbonate.

2.2.2.4. Nature of the Coligand

The effect of the initiating coligand was evaluated based on tridentate bis-aryloxy NHC complexes ([κ^3-$^{t\mathrm{Bu}}$*O*,*C*,*O*]-NHC)Ti$(X)_2$L. A summary of the result of the copolymerization of CO_2 with CHO catalyzed by complexes **24**, **26**, **28**, **43**-**47** is presented in Table 2.1.

Table 2.1. Summary of the main results for the copolymerization of CHO with CO_2 catalyzed by tridentate bis-aryloxy NHC titanium(IV) complexes

Run[a]	Complex/Cocat.[b]	Yield[c] (%)	Selectivity [d] (PCHC %)	TOF[e] (h^{-1})	M_n[f] (kg mol^{-1})	M_w/M_n[f]
1	**24**/[PPN]Cl	27	≥99	29	5.7	1.30
2	**26**/[PPN]Cl	27	≥99	28	8.0	1.37
3	**28**/[PPN]Cl	32	≥99	20	6.2	1.46
4	**43**/[PPN]Cl	23	≥99	24	8.0	1.75
5	**44**/[PPN]Cl	37	≥99	39	3.7	1.49
6	**45**/[PPN]Cl	27	≥99	29	8.2	1.77
7	**46**/[PPN]Cl	23	≥99	23	4.1	1.48
8	**47**/[PPN]Cl	32	≥99	33	4.0	1.92

[a] Polymerization procedure: 8 μmol of precursor, 8 μmol of cocatalyst, 20 mmol of CHO (CHO:Ti = 2500:1), P_{CO2} < 0.5 bar at 60 °C. [b] Catalyst pre-formation 15 min at 30 °C and dried for 2 h under vacuum. [c] Yield determined gravimetrically. [d] Measured by ^{1}H NMR spectroscopy in chloroform-*d* on the crude product. [e] Turnover frequency of CHO to PCHC. [f] Determined by GPC-SEC in THF at 30 °C against polystyrene standard.

A slightly enhanced activity for catalytic systems based on complexes bearing azide, isopropoxide and acetate ligands were observed compared to other coligand types, with a maximum TOF reached of 39 h^{-1} for the azide complex **44** (Table 2.1 Run 5). Comparable to previous systems [80, 84, 85, 154, 155], the presence of more nucleophilic initiator decreases the initiation time of the ring-opening allowing the complex to achieve higher activities. In the case of the poor nucleophile Cl, a significant decrease of the concentration of the active anionic center was observed by dissociation of the NHC aryloxy upon activation, dropping the catalyst activity. In the contrary with strong nucleophile, the moderate hindered isopropoxide, and acetate or

the azide coligands are more effective for the ring-opening of the coordinated CHO. The presence of very bulky coligands limits the accessibility of the incoming Cl atom needed to form the active six-coordinate intermediate. Variations lie in the differences on steric and electronic level of the incoming nucleophile and coligand.

3. Conclusion

Tridentate NHC-titanium silyloxide, azide, benzyloxide and acetate complexes were obtained *via* salt metathesis from the chloride or isopropoxide precursors. The new compounds were fully characterized and their molecular structures were identified. A unique seven-coordinate Ti(IV) metal center is observed in the acetate complex which adopts a pentagonal bipyramid geometry and presents the shortest Ti-$C_{carbene}$ distance reported for multidentate oxygen-functionalized NHC-titanium(IV) complexes. The formation of the azide complex was confirmed by its cycloaddition with a functionalized alkyne to afford the triazolato complex. Attempts to synthetize NHC-titanium(III), *via* the coordination of $TiCl_3(THF)_3$ precursor or by the reduction of titanium(IV), were unsuccessful. Instead, *via* a hydride transfer, the unexpected seven-coordinate imidazolidine-titanium(IV) was formed.

A set of new *o*-hydroxyaryl unsymmetrically *N*-substituted NHC ligand was synthetized, coordinated after double deprotonation to titanium(IV) precursor to afford bis-ligated NHC titanium complexes and fully characterized. *N*-aryl substituents showed to have a determinant effect for the obtaining of a single stereoisomer. In addition the *ortho*-substituent on the *N*-aryloxy has a determinant effect on the preferred *cis versus trans* configuration. The lack of bulky substituents on the aryloxy ring leads to the thermodynamically stable *trans* configuration complex.

All the developed complexes were evaluated for the copolymerization of CHO and CO_2. Tridentate NHC-titanium(IV) complexes are highly active towards the completely alternating copolymerization of cyclohexene oxide with CO_2, while the imidazolidine-titanium(IV) and the bidentate NHC-titanium(IV) complexes showed no activity.

The use of stoichiometric amount of bulky anionic [PPN]X salt as a cocatalyst is determinant for the formation of active anionic six-coordinate intermediates. The overall yield of the reaction is positively affected by an increasing of temperature and catalyst loading while it is independent toward the CO_2 pressure variation, indicating a cooperative intermolecular mechanism of the reaction.

In this work, we reported a new class of catalysts based on titanium NHC ligands, active under low CO_2 pressure ($\leq$ 0.5 bar), for the copolymerization of CHO and CO_2.

4. Further work

Following the finding of a new class of catalysts for the copolymerization of CO_2 with epoxide, group 4 NHC complexes should be further developed, based on different metal centers and bearing a wide range of NHC ligands (e.g. with different backbone and bearing substituents with different steric properties) to improve their catalytic performance and tune the properties of the polymers formed.

In parallel, further studies of the reactivity of such complexes as well as mechanistic studies of the catalytic systems should be solved as it is essential to get a deeper understanding of the mechanism reaction.

Titanium NHC complexes were investigated for the copolymerization of CO_2 and CHO and other comonomers could be studied as the common PO or promising alternatives with the use of bio-epoxides, such as (+)-limonene oxide, isoprene oxide or α-pinene oxide.

As titanium NHC complexes showed to be active in the copolymerization of epoxide and CO_2 and ethylene polymerization, it would be interesting to extend the use of these systems to other catalytic applications.

5. References

1. Aresta, M., *Carbon Dioxide as Chemical Feedstock*. Wiley-VCH Verlag GmbH & Co. KGaA. 2010.
2. Aresta, M., Dibenedetto, A., and Angelini, A., *Catalysis for the Valorization of Exhaust Carbon: from CO_2 to Chemicals, Materials, and Fuels. Technological Use of CO_2*. Chemical Reviews, 2014. **114**(3): 1709-1742.
3. Arakawa, H., Aresta, M., Armor, J.N., Barteau, M.A., Beckman, E.J., Bell, A.T., *et al*., *Catalysis Research of Relevance to Carbon Management: Progress, Challenges, and Opportunities*. Chemical Reviews, 2001. **101**(4): 953-996.
4. Peters, M., Köhler, B., Kuckshinrichs, W., Leitner, W., Markewitz, P., and Müller, T.E., *Chemical Technologies for Exploiting and Recycling Carbon Dioxide into the Value Chain*. ChemSusChem, 2011. **4**(9): 1216-1240.
5. Bolm, C., Beckmann, O., and Dabard, O.A.G., *The Search for New Environmentally Friendly Chemical Processes*. Angewandte Chemie International Edition, 1999. **38**(7): 907-909.
6. Aresta, M. and Dibenedetto, A., *Utilisation of CO_2 as a Chemical Feedstock: Opportunities and Challenges*. Dalton Transactions, 2007(28): 2975-2992.
7. Sakakura, T., Choi, J.-C., and Yasuda, H., *Transformation of Carbon Dioxide*. Chemical Reviews, 2007. **107**(6): 2365-2387.
8. Volpin, M.E., *The Reactions of Organometallic Compounds of Transition Metals with Molecular Nitrogen and Carbon Dioxide*. Pure and Applied Chemistry, 1972(30): 607-626.
9. Aresta, M., Nobile, C.F., Albano, V.G., Forni, E., and Manassero, M., *New Nickel-Carbon Dioxide Complex: Synthesis, Properties and Crystallographic Characterization of (Carbon Dioxide)-Bis(tricyclohexylphosphine)nickel*. Journal of the Chemical Society, Chemical Communications 1975(15): 636-637.
10. Cokoja, M., Bruckmeier, C., Rieger, B., Herrmann, W.A., and Kühn, F.E., *Transformation of Carbon Dioxide with Homogeneous Transition-Metal Catalysts: A Molecular Solution to a Global Challenge?* Angewandte Chemie International Edition, 2011. **50**(37): 8510-8537.
11. Gibson, D.H., *Carbon Dioxide Coordination Chemistry: Metal Complexes and Surface-Bound Species. What Relationships?* Coordination Chemistry Reviews, 1999. **185-186**(Supplement C): 335-355.
12. Leitner, W., *The Coordination Chemistry of Carbon Dioxide and its Relevance for Catalysis: a Critical Survey*. Coordination Chemistry Reviews, 1996. **153**(Supplement C): 257-284.
13. Gibson, D.H., *The Organometallic Chemistry of Carbon Dioxide*. Chemical Reviews, 1996. **96**(6): 2063-2096.
14. Behr, A., *Carbon Dioxide as an Alternative C_1 Synthetic Unit: Activation by Transition-Metal Complexes*. Angewandte Chemie International Edition in English, 1988. **27**(5): 661-678.
15. Palmer, D.A. and Van Eldik, R., *The Chemistry of Metal Carbonato and Carbon Dioxide Complexes*. Chemical Reviews, 1983. **83**(6): 651-731.
16. Calabrese, J.C., Herskovitz, T., and Kinney, J.B., *Carbon Dioxide Coordination Chemistry. 5. The Preparation and Structure of the Rhodium Complex $Rh(\eta^1\text{-}CO_2)(Cl)(diars)_2$*. Journal of the American Chemical Society, 1983. **105**(18): 5914-5915.

17. Yin, X. and Moss, J.R., *Recent Developments in the Activation of Carbon Dioxide by Metal Complexes*. Coordination Chemistry Reviews, 1999. **181**(1): 27-59.
18. Aresta, M. and Dibenedetto, A., *The Contribution of the Utilization Option to Reducing the CO_2 Atmospheric Loading: Research Needed to Overcome Existing Barriers for a Full Exploitation of the Potential of the CO_2 Use*. Catalysis Today, 2004. **98**(4): 455-462.
19. Leitner, W., *Homogeneous Catalysts for Application in Supercritical Carbon Dioxide as a 'Green' Solvent.* Comptes Rendus de l'Académie des Sciences - Series IIC - Chemistry, 2000. **3**(7): 595-600.
20. Cooper, A.I., *Polymer Synthesis and Processing using Supercritical Carbon Dioxide*. Journal of Materials Chemistry, 2000. **10**(2): 207-234.
21. Quadrelli, E.A., Centi, G., Duplan, J.-L., and Perathoner, S., *Carbon Dioxide Recycling: Emerging Large-Scale Technologies with Industrial Potential*. ChemSusChem, 2011. **4**(9): 1194-1215.
22. Omae, I., *Recent Developments in Carbon Dioxide Utilization for the Production of Organic Chemicals*. Coordination Chemistry Reviews, 2012. **256**(13–14): 1384-1405.
23. Olajire, A.A., *Valorization of Greenhouse Carbon Dioxide Emissions into Value-Added Products by Catalytic Processes*. Journal of CO_2 Utilization, 2013. **3–4**: 74-92.
24. Meessen, J.H. and Petersen, H., *Urea*, in *Ullmann's Encyclopedia of Industrial Chemistry*. 2000, Wiley-VCH Verlag GmbH & Co. KGaA.
25. Otto, A., Grube, T., Schiebahn, S., and Stolten, D., *Closing the Loop: Captured CO_2 as a Feedstock in the Chemical Industry*. Energy & Environmental Science, 2015. **8**: 3283-3297.
26. *http://www.empowermaterials.com*. December 2017.
27. *https://www.novomer.com*. December 2017.
28. *https://www.norner.no/greentech/plastics-from-co2*. December 2017.
29. *http://www.covestro.com*. December 2017.
30. *http://www.econic-technologies.com*. December 2017.
31. Kuran, W., *Coordination Polymerization of Heterocyclic and Heterounsaturated Monomers*. Progress in Polymer Science, 1998. **23**(6): 919-992.
32. Coates, G.W. and Moore, D.R., *Discrete Metal-Based Catalysts for the Copolymerization of CO_2 and Epoxides: Discovery, Reactivity, Optimization, and Mechanism*. Angewandte Chemie International Edition, 2004. **43**(48): 6618-6639.
33. Kember, M.R., Buchard, A., and Williams, C.K., *Catalysts for CO_2/epoxide copolymerisation*. Chemical Communications, 2011. **47**(1): 141-163.
34. Darensbourg, D.J., *Making Plastics from Carbon Dioxide: Salen Metal Complexes as Catalysts for the Production of Polycarbonates from Epoxides and CO_2*. Chemical Reviews, 2007. **107**(6): 2388-2410.
35. Koning, C., Wildeson, J., Parton, R., Plum, B., Steeman, P., and Darensbourg, D.J., *Synthesis and Physical Characterization of Poly(cyclohexane carbonate), Synthesized from CO_2 and Cyclohexene Oxide*. Polymer, 2001. **42**(9): 3995-4004.
36. Serini, V., *Polycarbonates*, in *Ullmann's Encyclopedia of Industrial Chemistry*. **2000**, Wiley-VCH Verlag GmbH & Co. KGaA.
37. Thorat, S.D., Phillips, P.J., Semenov, V., and Gakh, A., *Physical Properties of Aliphatic Polycarbonates Made from CO_2 and Epoxides*. Journal of Applied Polymer Science, 2003. **89**(5): 1163-1176.

38. Wang, S.J., Du, L.C., Zhao, X.S., Meng, Y.Z., and Tjong, S.C., *Synthesis and Characterization of Alternating Copolymer from Carbon Dioxide and Propylene Oxide*. Journal of Applied Polymer Science, 2002. **85**(11): 2327-2334.
39. Darensbourg, D.J. and Wilson, S.J., *What's New with CO_2? Recent Advances in its Copolymerization with Oxiranes*. Green Chemistry, 2012. **14**(10): 2665-2671.
40. Shaikh, A.-A.G. and Sivaram, S., *Organic Carbonates*. Chemical Reviews, 1996. **96**(3): 951-976.
41. Clements, J.H., *Reactive Applications of Cyclic Alkylene Carbonates*. Industrial & Engineering Chemistry Research, 2003. **42**(4): 663-674.
42. Klaus, S., Lehenmeier, M.W., Anderson, C.E., and Rieger, B., *Recent Advances in CO_2/Epoxide Copolymerization—New Strategies and Cooperative Mechanisms*. Coordination Chemistry Reviews, 2011. **255**(13–14): 1460-1479.
43. Dean, R.K., Dawe, L.N., and Kozak, C.M., *Copolymerization of Cyclohexene Oxide and CO_2 with a Chromium Diamine-bis(phenolate) Catalyst*. Inorganic Chemistry, 2012. **51**(16): 9095-9103.
44. Childers, M.I., Longo, J.M., Van Zee, N.J., LaPointe, A.M., and Coates, G.W., *Stereoselective Epoxide Polymerization and Copolymerization*. Chemical Reviews, 2014. **114**(16): 8129-8152.
45. Nakano, K., Hashimoto, S., and Nozaki, K., *Bimetallic Mechanism Operating in the Popolymerization of Propylene Oxide with Carbon Dioxide Catalyzed by Cobalt-Salen Complexes*. Chemical Science, 2010. **1**(3): 369-373.
46. Trott, G., Saini, P.K., and Williams, C.K., *Catalysts for CO_2/Epoxide Ring-Opening Copolymerization*. Philosophical Transactions of the Royal Society A 2016. **374**(2061).
47. Li, B., Wu, G.-P., Ren, W.-M., Wang, Y.-M., Rao, D.-Y., and Lu, X.-B., *Asymmetric, Regio- and Stereo-Selective Alternating Copolymerization of CO_2 and Propylene Oxide Catalyzed by Chiral Chromium Salan Complexes*. Journal of Polymer Science Part A: Polymer Chemistry, 2008. **46**(18): 6102-6113.
48. Jacobsen, E.N., *Asymmetric Catalysis of Epoxide Ring-Opening Reactions*. Accounts of Chemical Research, 2000. **33**(6): 421-431.
49. Darensbourg, D.J. and Moncada, A.I., *Mechanistic Insight into the Initiation Step of the Coupling Reaction of Oxetane or Epoxides and CO_2 Catalyzed by (salen)CrX Complexes*. Inorganic Chemistry, 2008. **47**(21): 10000-10008.
50. Moore, D.R., Cheng, M., Lobkovsky, E.B., and Coates, G.W., *Mechanism of the Alternating Copolymerization of Epoxides and CO_2 Using β-Diiminate Zinc Catalysts: Evidence for a Bimetallic Epoxide Enchainment.* Journal of the American Chemical Society, 2003. **125**(39): 11911-11924.
51. Inoue, S., Koinuma, H., and Tsuruta, T., *Copolymerization of Carbon Dioxide and Epoxide with Organometallic Compounds*. Macromolecular Chemistry and Physics, 1969. **130**(1): 210-220.
52. Ree, M., Bae, J.Y., Jung, J.H., and Shin, T.J., *A New Copolymerization Process Leading to Poly(propylene carbonate) with a Highly Enhanced Yield from Carbon Dioxide and Propylene oxide*. Journal of Polymer Science Part A: Polymer Chemistry, 1999. **37**(12): 1863-1876.
53. Chen, S., Hua, Z., Fang, Z., and Qi, G., *Copolymerization of Carbon Dioxide and Propylene Oxide with Highly Effective Zinc Hexacyanocobaltate(III)-Based Coordination Catalyst*. Polymer, 2004. **45**(19): 6519-6524.
54. Chen, S., Qi, G.-R., Hua, Z.-J., and Yan, H.-Q., *Double Metal Cyanide Complex Based on $Zn_3[Co(CN)_6]_2$ as Highly Active Catalyst for Copolymerization of Carbon*

Dioxide and Cyclohexene Oxide. Journal of Polymer Science Part A: Polymer Chemistry, 2004. **42**(20): 5284-5291.

55. Super, M., Berluche, E., Costello, C., and Beckman, E., *Copolymerization of 1,2-Epoxycyclohexane and Carbon Dioxide Using Carbon Dioxide as Both Reactant and Solvent*. Macromolecules, 1997. **30**(3): 368-372.
56. Kember, M.R., White, A.J.P., and Williams, C.K., *Highly Active Di- and Trimetallic Cobalt Catalysts for the Copolymerization of CHO and CO_2 at Atmospheric Pressure*. Macromolecules, 2010. **43**(5): 2291-2298.
57. Darensbourg, D.J., Wildeson, J.R., Yarbrough, J.C., and Reibenspies, J.H., *Bis 2,6-difluorophenoxide Dimeric Complexes of Zinc and Cadmium and Their Phosphine Adducts: Lessons Learned Relative to Carbon Dioxide/Cyclohexene Oxide Alternating Copolymerization Processes Catalyzed by Zinc Phenoxides*. Journal of the American Chemical Society, 2000. **122**(50): 12487-12496.
58. Lee, B.Y., Kwon, H.Y., Lee, S.Y., Na, S.J., Han, S.-i., Yun, H.*, et al*., *Bimetallic Anilido-Aldimine Zinc Complexes for Epoxide/CO_2 Copolymerization*. Journal of the American Chemical Society, 2005. **127**(9): 3031-3037.
59. Kissling, S., Lehenmeier, M.W., Altenbuchner, P.T., Kronast, A., Reiter, M., Deglmann, P.*, et al*., *Dinuclear Zinc Catalysts with Unprecedented Activities for the Copolymerization of Cyclohexene Oxide and CO_2*. Chemical Communications, 2015. **51**(22): 4579-4582.
60. Cheng, M., Lobkovsky, E.B., and Coates, G.W., *Catalytic Reactions Involving C_1 Feedstocks: New High-Activity Zn(II)-Based Catalysts for the Alternating Copolymerization of Carbon Dioxide and Epoxides*. Journal of the American Chemical Society, 1998. **120**(42): 11018-11019.
61. Allen, S.D., Moore, D.R., Lobkovsky, E.B., and Coates, G.W., *High-Activity, Single-Site Catalysts for the Alternating Copolymerization of CO_2 and Propylene Oxide*. Journal of the American Chemical Society, 2002. **124**(48): 14284-14285.
62. Vagin, S.I., Reichardt, R., Klaus, S., and Rieger, B., *Conformationally Flexible Dimeric Salphen Complexes for Bifunctional Catalysis*. Journal of the American Chemical Society, 2010. **132**(41): 14367-14369.
63. Klaus, S., Vagin, S.I., Lehenmeier, M.W., Deglmann, P., Brym, A.K., and Rieger, B., *Kinetic and Mechanistic Investigation of Mononuclear and Flexibly Linked Dinuclear Complexes for Copolymerization of CO_2 and Epoxides*. Macromolecules, 2011. **44**(24): 9508-9516.
64. Aida, T., Ishikawa, M., and Inoue, S., *Alternating Copolymerization of Carbon Dioxide and Epoxide Catalyzed by the Aluminum Porphyrin-Quaternary Organic Salt or -Triphenylphosphine System. Synthesis of Polycarbonate with Well-Controlled Molecular Weight*. Macromolecules, 1986. **19**(1): 8-13.
65. Mang, S., Cooper, A.I., Colclough, M.E., Chauhan, N., and Holmes, A.B., *Copolymerization of CO_2 and 1,2-Cyclohexene Oxide Using a CO_2-Soluble Chromium Porphyrin Catalyst*. Macromolecules, 1999. **33**(2): 303-308.
66. Stamp, L.M., Mang, S.A., Holmes, A.B., Knights, K.A., de Miguel, Y.R., and McConvey, I.F., *Polymer Supported Chromium Porphyrin as Catalyst for Polycarbonate Formation in Supercritical Carbon Dioxide*. Chemical Communications, 2001(23): 2502-2503.
67. Sugimoto, H. and Kuroda, K., *The Cobalt Porphyrin−Lewis Base System: A Highly Selective Catalyst for Alternating Copolymerization of CO_2 and Epoxide under Mild Conditions*. Macromolecules, 2007. **41**(2): 312-317.
68. Sugimoto, H., Ohshima, H., and Inoue, S., *Alternating Copolymerization of Carbon Dioxide and Epoxide by Manganese Porphyrin: The First Example of Polycarbonate*

Synthesis from 1-atm Carbon Dioxide. Journal of Polymer Science Part A: Polymer Chemistry, 2003. **41**(22): 3549-3555.

69. Darensbourg, D.J. and Holtcamp, M.W., *Catalysts for the Reactions of Epoxides and Carbon Dioxide*. Coordination Chemistry Reviews, 1996. **153**(0): 155-174.
70. Darensbourg, D.J., Holtcamp, M.W., Struck, G.E., Zimmer, M.S., Niezgoda, S.A., Rainey, P.*, et al*., *Catalytic Activity of a Series of Zn(II) Phenoxides for the Copolymerization of Epoxides and Carbon Dioxide*. Journal of the American Chemical Society, 1998. **121**(1): 107-116.
71. Darensbourg, D.J., Niezgoda, S.A., Draper, J.D., and Reibenspies, J.H., *Mechanistic Aspects of the Copolymerization of CO_2 and Epoxides by Soluble Zinc Bis(phenoxide) Catalysts as Revealed by Their Cadmium Analogues*. Journal of the American Chemical Society, 1998. **120**(19): 4690-4698.
72. Cui, D., Nishiura, M., and Hou, Z., *Alternating Copolymerization of Cyclohexene Oxide and Carbon Dioxide Catalyzed by Organo Rare Earth Metal Complexes*. Macromolecules, 2005. **38**(10): 4089-4095.
73. Cui, D., Nishiura, M., Tardif, O., and Hou, Z., *Rare-Earth-Metal Mixed Hydride/Aryloxide Complexes Bearing Mono(cyclopentadienyl) Ligands. Synthesis, CO_2 Fixation, and Catalysis on Copolymerization of CO_2 with Cyclohexene Oxide*. Organometallics, 2008. **27**(11): 2428-2435.
74. Nakano, K., Kamada, T., and Nozaki, K., *Selective Formation of Polycarbonate over Cyclic Carbonate: Copolymerization of Epoxides with Carbon Dioxide Catalyzed by a Cobalt(III) Complex with a Piperidinium End-Capping Arm*. Angewandte Chemie International Edition, 2006. **45**(43): 7274-7277.
75. Noh, E.K., Na, S.J., S, S., Kim, S.-W., and Lee, B.Y., *Two Components in a Molecule: Highly Efficient and Thermally Robust Catalytic System for CO_2/Epoxide Copolymerization*. Journal of the American Chemical Society, 2007. **129**(26): 8082-8083.
76. S, S., Min, J.K., Seong, J.E., Na, S.J., and Lee, B.Y., *A Highly Active and Recyclable Catalytic System for CO_2/Propylene Oxide Copolymerization*. Angewandte Chemie International Edition, 2008. **47**(38): 7306-7309.
77. Ren, W.-M., Liu, Z.-W., Wen, Y.-Q., Zhang, R., and Lu, X.-B., *Mechanistic Aspects of the Copolymerization of CO_2 with Epoxides Using a Thermally Stable Single-Site Cobalt(III) Catalyst*. Journal of the American Chemical Society, 2009. **131**(32): 11509-11518.
78. Lu, X.-B. and Darensbourg, D.J., *Cobalt Catalysts for the Coupling of CO_2 and Epoxides to Provide Polycarbonates and Cyclic Carbonates*. Chemical Society Reviews, 2012. **41**(4): 1462-1484.
79. Hansen, K.B., Leighton, J.L., and Jacobsen, E.N., *On the Mechanism of Asymmetric Nucleophilic Ring-Opening of Epoxides Catalyzed by (Salen)CrIII Complexes*. Journal of the American Chemical Society, 1996. **118**(44): 10924-10925.
80. Darensbourg, D.J., Mackiewicz, R.M., Rodgers, J.L., Fang, C.C., Billodeaux, D.R., and Reibenspies, J.H., *Cyclohexene Oxide/CO_2 Copolymerization Catalyzed by Chromium(III) Salen Complexes and N-Methylimidazole: Effects of Varying Salen Ligand Substituents and Relative Cocatalyst Loading*. Inorganic Chemistry, 2004. **43**(19): 6024-6034.
81. Darensbourg, D.J. and Yarbrough, J.C., *Mechanistic Aspects of the Copolymerization Reaction of Carbon Dioxide and Epoxides, Using a Chiral Salen Chromium Chloride Catalyst*. Journal of the American Chemical Society, 2002. **124**(22): 6335-6342.
82. Darensbourg, D.J., Bottarelli, P., and Andreatta, J.R., *Inquiry into the Formation of Cyclic Carbonates during the (Salen)CrX Catalyzed CO_2/Cyclohexene Oxide*

Copolymerization Process in the Presence of Ionic Initiators. Macromolecules, 2007. **40**(21): 7727-7729.

83. Darensbourg, D.J. and Billodeaux, D.R., *Aluminum Salen Complexes and Tetrabutylammonium Salts: A Binary Catalytic System for Production of Polycarbonates from CO_2 and Cyclohexene Oxide*. Inorganic Chemistry, 2005. **44**(5): 1433-1442.
84. Cohen, C.T., Thomas, C.M., Peretti, K.L., Lobkovsky, E.B., and Coates, G.W., *Copolymerization of Cyclohexene Oxide and Carbon Dioxide Using (Salen)Co(III) Complexes: Synthesis and Characterization of Syndiotactic Poly(cyclohexene carbonate)*. Dalton Transactions, 2006(1): 237-249.
85. Cohen, C.T., Chu, T., and Coates, G.W., *Cobalt Catalysts for the Alternating Copolymerization of Propylene Oxide and Carbon Dioxide: Combining High Activity and Selectivity*. Journal of the American Chemical Society, 2005. **127**(31): 10869-10878.
86. Qin, Z., Thomas, C.M., Lee, S., and Coates, G.W., *Cobalt-Based Complexes for the Copolymerization of Propylene Oxide and CO_2: Active and Selective Catalysts for Polycarbonate Synthesis*. Angewandte Chemie International Edition, 2003. **42**(44): 5484-5487.
87. Tian, D., Liu, B., Gan, Q., Li, H., and Darensbourg, D.J., *Formation of Cyclic Carbonates from Carbon Dioxide and Epoxides Coupling Reactions Efficiently Catalyzed by Robust, Recyclable One-Component Aluminum-Salen Complexes*. ACS Catalysis, 2012. **2**(9): 2029-2035.
88. Lu, X.-B. and Wang, Y., *Highly Active, Binary Catalyst Systems for the Alternating Copolymerization of CO_2 and Epoxides under Mild Conditions*. Angewandte Chemie International Edition, 2004. **43**(27): 3574-3577.
89. Lu, X.-B., Shi, L., Wang, Y.-M., Zhang, R., Zhang, Y.-J., Peng, X.-J*., et al*., *Design of Highly Active Binary Catalyst Systems for CO_2/Epoxide Copolymerization: Polymer Selectivity, Enantioselectivity, and Stereochemistry Control*. Journal of the American Chemical Society, 2006. **128**(5): 1664-1674.
90. Cohen, C.T. and Coates, G.W., *Alternating Copolymerization of Propylene Oxide and Carbon Dioxide with Highly Efficient and Selective (salen)Co(III) Catalysts: Effect of Ligand and Cocatalyst Variation*. Journal of Polymer Science Part A: Polymer Chemistry, 2006. **44**(17): 5182-5191.
91. Na, S.J., S, S., Cyriac, A., Kim, B.E., Yoo, J., Kang, Y.K*., et al*., *Elucidation of the Structure of a Highly Active Catalytic System for CO_2/Epoxide Copolymerization: A salen-Cobaltate Complex of an Unusual Binding Mode*. Inorganic Chemistry, 2009. **48**(21): 10455-10465.
92. Ren, W.-M., Zhang, X., Liu, Y., Li, J.-F., Wang, H., and Lu, X.-B., *Highly Active, Bifunctional Co(III)-Salen Catalyst for Alternating Copolymerization of CO_2 with Cyclohexene Oxide and Terpolymerization with Aliphatic Epoxides*. Macromolecules, 2010. **43**(3): 1396-1402.
93. Sauer, A., Kapelski, A., Fliedel, C., Dagorne, S., Kol, M., and Okuda, J., *Structurally Well-Defined Group 4 Metal Complexes as Initiators for the Ring-Opening Polymerization of Lactide Monomers*. Dalton Transactions, 2013. **42**(25): 9007-9023.
94. Le Roux, E., *Recent Advances on Tailor-Made Titanium Catalysts for Biopolymer Synthesis*. Coordination Chemistry Reviews, 2016. **306, Part 1**: 65-85.
95. North, M., *Sustainable Catalysis: Without Metals or Other Endangered Elements, Parts 1 and 2*. 2015, The Royal Society of Chemistry.

96. Nakano, K., Kobayashi, K., and Nozaki, K., *Tetravalent Metal Complexes as a New Family of Catalysts for Copolymerization of Epoxides with Carbon Dioxide*. Journal of the American Chemical Society, 2011. **133**(28): 10720-10723.
97. Buchard, A., Kember, M.R., Sandeman, K.G., and Williams, C.K., *A Bimetallic iron(III) Catalyst for CO_2/Epoxide Coupling*. Chemical Communications, 2011. **47**(1): 212-214.
98. Taherimehr, M., Sertã, J.P.C.C., Kleij, A.W., Whiteoak, C.J., and Pescarmona, P.P., *New Iron Pyridylamino-Bis(Phenolate) Catalyst for Converting CO_2 into Cyclic Carbonates and Cross-Linked Polycarbonates*. ChemSusChem, 2015. **8**(6): 1034-1042.
99. Nakano, K., Kobayashi, K., Ohkawara, T., Imoto, H., and Nozaki, K., *Copolymerization of Epoxides with Carbon Dioxide Catalyzed by Iron–Corrole Complexes: Synthesis of a Crystalline Copolymer*. Journal of the American Chemical Society, 2013. **135**(23): 8456-8459.
100. Taherimehr, M., Al-Amsyar, S.M., Whiteoak, C.J., Kleij, A.W., and Pescarmona, P.P., *High Activity and Switchable Selectivity in the Synthesis of Cyclic and Polymeric Cyclohexene Carbonates with Iron Amino Triphenolate Catalysts*. Green Chemistry, 2013. **15**(11): 3083-3090.
101. Bellemin-Laponnaz, S. and Dagorne, S., *Group 1 and 2 and Early Transition Metal Complexes Bearing N-Heterocyclic Carbene Ligands: Coordination Chemistry, Reactivity, and Applications*. Chemical Reviews, 2014. **114**(18): 8747-8774.
102. Zhang, D. and Zi, G., *N-Heterocyclic Carbene (NHC) Complexes of Group 4 Transition Metals*. Chemical Society Reviews, 2015. **44**(7): 1898-1921.
103. Hameury, S., de Fremont, P., and Braunstein, P., *Metal Complexes with Oxygen-Functionalized NHC Ligands: Synthesis and Applications*. Chemical Society Reviews, 2017. **46**(3): 632-733.
104. Aihara, H., Matsuo, T., and Kawaguchi, H., *Titanium N-Heterocyclic Carbene Complexes Incorporating an Imidazolium-Linked Bis(Phenol)*. Chemical Communications, 2003(17): 2204-2205.
105. Zhang, D., Aihara, H., Watanabe, T., Matsuo, T., and Kawaguchi, H., *Zirconium Complexes of the Tridentate Bis(Aryloxide)-N-Heterocyclic Carbene Ligand: Chloride and Alkyl Functionalized Derivatives*. Journal of Organometallic Chemistry, 2007. **692**(1): 234-242.
106. Zhang, D., *Dinuclear Titanium(IV) Complexes Bearing Phenoxide-Tethered N-Heterocyclic Carbene Ligands with Cisoid Conformation through Control of Hydrolysis*. European Journal of Inorganic Chemistry, 2007. **2007**(30): 4839-4845.
107. Zhao, N., Hou, G., Deng, X., Zi, G., and Walter, M.D., *Group 4 Metal Complexes with New Chiral Pincer NHC-Ligands: Synthesis, Structure and Catalytic Activity*. Dalton Transactions, 2014. **43**(22): 8261-8272.
108. Romain, C., Brelot, L., Bellemin-Laponnaz, S., and Dagorne, S., *Synthesis and Structural Characterization of a Novel Family of Titanium Complexes Bearing a Tridentate Bis-phenolate-N-heterocyclic Carbene Dianionic Ligand and Their Use in the Controlled ROP of rac-Lactide*. Organometallics, 2010. **29**(5): 1191-1198.
109. Romain, C., Heinrich, B., Bellemin-Laponnaz, S., and Dagorne, S., *A Robust Zirconium N-Heterocyclic Carbene Complex for the Living and Highly Stereoselective Ring-Opening Polymerization of rac-Lactide*. Chemical Communications, 2012. **48**(16): 2213-2215.
110. Patel, D., Liddle, S.T., Mungur, S.A., Rodden, M., Blake, A.J., and Arnold, P.L., *Bifunctional Yttrium(III) and Titanium(IV) NHC Catalysts for Lactide Polymerisation*. Chemical Communications, 2006(10): 1124-1126.

111. Bocchino, C., Napoli, M., Costabile, C., and Longo, P., *Synthesis of Octahedral Zirconium Complex Bearing [NHC-O] Ligands, and its Behavior as Catalyst in the Polymerization of Olefins*. Journal of Polymer Science Part A: Polymer Chemistry, 2011. **49**(4): 862-870.
112. El-Batta, A., Waltman, A.W., and Grubbs, R.H., *Bis-ligated Ti and Zr Complexes of Chelating N-Heterocyclic Carbenes*. Journal of Organometallic Chemistry, 2011. **696**(13): 2477-2481.
113. Arnold, P.L., Zlatogorsky, S., Jones, N.A., Carmichael, C.D., Liddle, S.T., Blake, A.J., and Wilson, C., *Comparisons between Yttrium and Titanium N-Heterocyclic Carbene Complexes in the Search for Early Transition Metal NHC Backbonding Interactions*. Inorganic Chemistry, 2008. **47**(19): 9042-9049.
114. Waltman, A.W. and Grubbs, R.H., *A New Class of Chelating N-Heterocyclic Carbene Ligands and Their Complexes with Palladium*. Organometallics, 2004. **23**(13): 3105-3107.
115. Miyake, G.M., Akhtar, M.N., Fazal, A., Jaseer, E.A., Daeffler, C.S., and Grubbs, R.H., *Chelating N-Heterocyclic Carbene Group IV Complexes for the Polymerization of Ethylene and Styrene*. Journal of Organometallic Chemistry, 2013. **728**: 1-5.
116. Quadri, C.C. and Le Roux, E., *Copolymerization of Cyclohexene Oxide with CO_2 Catalyzed by Tridentate N-Heterocyclic Carbene Titanium(IV) complexes*. Dalton Transactions, 2014. **43**(11): 4242-4246.
117. Wang, Y., Qin, Y., Wang, X., and Wang, F., *Coupling Reaction between CO_2 and Cyclohexene Oxide: Selective Control from Cyclic Carbonate to Polycarbonate by Ligand Design of Salen/Salalen Titanium Complexes*. Catalysis Science & Technology, 2014. **4**(11): 3964-3972.
118. Wang, Y., Qin, Y., Wang, X., and Wang, F., *Trivalent Titanium Salen Complex: Thermally Robust and Highly Active Catalyst for Copolymerization of CO_2 and Cyclohexene Oxide*. ACS Catalysis, 2015. **5**(1): 393-396.
119. Mandal, M., Chakraborty, D., and Ramkumar, V., *Zr(IV) Complexes Containing Salan-Type Ligands: Synthesis, Structural Characterization and Role as Catalysts towards the Polymerization of ε-Caprolactone, rac-Lactide, Ethylene, Homopolymerization and Copolymerization of Epoxides with CO_2*. RSC Advances, 2015. **5**(36): 28536-28553.
120. Mandal, M. and Chakraborty, D., *Group 4 Complexes Bearing Bis(salphen) Ligands: Synthesis, Characterization, and Polymerization Studies*. Journal of Polymer Science Part A: Polymer Chemistry, 2016. **54**(6): 809-824.
121. Hessevik, J., Lalrempuia, R., Nsiri, H., Tornroos, K.W., Jensen, V.R., and Le Roux, E., *Sterically (Un)encumbered mer-Tridentate N-Heterocyclic Carbene Complexes of Titanium(IV) for the Copolymerization of Cyclohexene Oxide with CO_2*. Dalton Transactions, 2016.
122. Su, C.-K., Chuang, H.-J., Li, C.-Y., Yu, C.-Y., Ko, B.-T., Chen, J.-D., and Chen, M.-J., *Oxo-Bridged Bimetallic Group 4 Complexes Bearing Amine-Bis(benzotriazole phenolate) Derivatives as Bifunctional Catalysts for Ring-Opening Polymerization of Lactide and Copolymerization of Carbon Dioxide with Cyclohexene Oxide*. Organometallics, 2014. **33**(24): 7091-7100.
123. Chuang, H.-J. and Ko, B.-T., *Facilely Synthesized Benzotriazole Phenolate Zirconium Complexes as Versatile Catalysts for Copolymerization of Carbon Dioxide with Cyclohexene Oxide and Lactide Polymerization*. Dalton Transactions, 2015. **44**(2): 598-607.

124. Hopkinson, M.N., Richter, C., Schedler, M., and Glorius, F., *An Overview of N-Heterocyclic Carbenes*. Nature, 2014. **510**(7506): 485-496.
125. Poyatos, M., Mata, J.A., and Peris, E., *Complexes with Poly(N-heterocyclic carbene) Ligands: Structural Features and Catalytic Applications*. Chemical Reviews, 2009. **109**(8): 3677-3707.
126. Kuhl, O., *The Chemistry of Functionalised N-Heterocyclic Carbenes*. Chemical Society Reviews, 2007. **36**(4): 592-607.
127. Benhamou, L., Chardon, E., Lavigne, G., Bellemin-Laponnaz, S., and César, V., *Synthetic Routes to N-Heterocyclic Carbene Precursors*. Chemical Reviews, 2011. **111**(4): 2705-2733.
128. Díez-González, S., *N-Heterocyclic Carbenes From Laboratory Curiosities to Efficient Synthetic Tools*. 2011: Royal Sociery of Chemistry.
129. Bellemin-Laponnaz, S., Welter, R., Brelot, L., and Dagorne, S., *Synthesis and Structure of V(V) and Mn(III) NHC Complexes Supported by a Tridentate Bis-Aryloxide-N-Heterocyclic Carbene Ligand*. Journal of Organometallic Chemistry, 2009. **694**(5): 604-606.
130. Quadri, C.C., Lalrempuia, R., Hessevik, J., Törnroos, K.W., and Le Roux, E., *Structural Characterization of Tridentate N-Heterocyclic Carbene Titanium(IV) Benzyloxide, Silyloxide, Acetate, and Azide Complexes and Assessment of Their Efficacies for Catalyzing the Copolymerization of Cyclohexene Oxide with CO_2*. Organometallics, 2017. **36**(22): 4477-4489.
131. Chang, C.-W. and Lee, G.-H., *Synthesis of Ruthenium Triazolato and Tetrazolato Complexes by 1,3-Dipolar Cycloadditions of Ruthenium Azido Complex with Alkynes and Alkenes and Regiospecific Alkylation of Triazolates*. Organometallics, 2003. **22**(15): 3107-3116.
132. Downing, S.P. and Danopoulos, A.A., *Indenyl- and Fluorenyl-Functionalized N-Heterocyclic Carbene Complexes of Titanium and Vanadium*. Organometallics, 2006. **25**(6): 1337-1340.
133. Jones, N.A., Liddle, S.T., Wilson, C., and Arnold, P.L., *Titanium(III) Alkoxy-N-heterocyclic Carbenes and a Safe, Low-Cost Route to $TiCl_3(THF)_3$*. Organometallics, 2007. **26**(3): 755-757.
134. Downing, S.P., Guadaño, S.C., Pugh, D., Danopoulos, A.A., Bellabarba, R.M., Hanton, M.*, et al*., *Indenyl- and Fluorenyl-Functionalized N-Heterocyclic Carbene Complexes of Titanium, Zirconium, Vanadium, Chromium, and Yttrium*. Organometallics, 2007. **26**(15): 3762-3770.
135. Lorber, C. and Vendier, L., *Routes to New N-Heterocyclic Carbene Titanium(IV) Imido Complexes*. Organometallics, 2008. **27**(12): 2774-2783.
136. Sarazin, Y., Howard, R.H., Hughes, D.L., Humphrey, S.M., and Bochmann, M., *Titanium, Zinc and Alkaline-Earth Metal Complexes Supported by Bulky O,N,N,O-Multidentate Ligands: Syntheses, Characterisation and Activity in Cyclic Ester Polymerisation*. Dalton Transactions, 2006(2): 340-350.
137. Zhang, D. and Liu, N., *Titanium Complexes Bearing Bisaryloxy-N-heterocyclic Carbenes: Synthesis, Reactivity, and Ethylene Polymerization Study*. Organometallics, 2009. **28**(2): 499-505.
138. Durfee, L.D., Latesky, S.L., Rothwell, I.P., Huffman, J.C., and Folting, K., *Chemical and Electrochemical Reduction of Titanium(IV) Aryloxides*. Inorganic Chemistry, 1985. **24**(26): 4569-4573.
139. Zhang, D., *Unexpected Binuclear Bis(phenolato) Titanium (IV) {[(L)Ti(Ph)]2(μ-$OEt)_2$} Assisted by Carbon−Oxygen Bond Cleavage and Alkali-Metal-Containing*

Titanium(III) Complexes [Ti(L)$_2$·M(solv)$_2$] (M = Li, Na, K; solv = THF, DME). Organometallics, 2007. **26**(16): 4072-4075.

140. Despagnet-Ayoub, E., Henling, L.M., Labinger, J.A., and Bercaw, J.E., *Group 4 Transition-Metal Complexes of an Aniline–Carbene–Phenol Ligand*. Organometallics, 2013. **32**(10): 2934-2938.
141. Romain, C., Miqueu, K., Sotiropoulos, J.-M., Bellemin-Laponnaz, S., and Dagorne, S., *Non-Innocent Behavior of a Tridentate NHC Chelating Ligand Coordinated onto a Zirconium(IV) Center*. Angewandte Chemie International Edition, 2010. **49**(12): 2198-2201.
142. Romain, C., Specklin, D., Miqueu, K., Sotiropoulos, J.-M., Fliedel, C., Bellemin-Laponnaz, S., and Dagorne, S., *Unusual Benzyl Migration Reactivity in NHC-Bearing Group 4 Metal Chelates: Synthesis, Characterization, and Mechanistic Investigations*. Organometallics, 2015. **34**(20): 4854-4863.
143. Mitani, M., Mohri, J.-i., Yoshida, Y., Saito, J., Ishii, S., Tsuru, K.*, et al*., *Living Polymerization of Ethylene Catalyzed by Titanium Complexes Having Fluorine-Containing Phenoxy−Imine Chelate Ligands.* Journal of the American Chemical Society, 2002. **124**(13): 3327-3336.
144. Poater, A., Cosenza, B., Correa, A., Giudice, S., Ragone, F., Scarano, V., and Cavallo, L., *SambVca: A Web Application for the Calculation of the Buried Volume of N-Heterocyclic Carbene Ligands*. European Journal of Inorganic Chemistry, 2009. **2009**(13): 1759-1766.
145. Falivene, L., Credendino, R., Poater, A., Petta, A., Serra, L., Oliva, R.*, et al*., *SambVca 2. A Web Tool for Analyzing Catalytic Pockets with Topographic Steric Maps*. Organometallics, 2016. **35**(13): 2286-2293.
146. Nakano, K., Nozaki, K., and Hiyama, T., *Spectral Assignment of Poly[cyclohexene oxide-alt-carbon dioxide]*. Macromolecules, 2001. **34**(18): 6325-6332.
147. Darensbourg, D.J. and Mackiewicz, R.M., *Role of the Cocatalyst in the Copolymerization of CO_2 and Cyclohexene Oxide Utilizing Chromium Salen Complexes*. Journal of the American Chemical Society, 2005. **127**(40): 14026-14038.
148. Darensbourg, D.J. and Frantz, E.B., *Manganese(III) Schiff Base Complexes: Chemistry Relevant to the Copolymerization of Epoxides and Carbon Dioxide*. Inorganic Chemistry, 2007. **46**(15): 5967-5978.
149. Darensbourg, D.J. and Fitch, S.B., *Copolymerization of Epoxides and Carbon Dioxide. Evidence Supporting the Lack of Dual Catalysis at a Single Metal Site*. Inorganic Chemistry, 2009. **48**(18): 8668-8677.
150. Nakano, K., Nakamura, M., and Nozaki, K., *Alternating Copolymerization of Cyclohexene Oxide with Carbon Dioxide Catalyzed by (salalen)CrCl Complexes*. Macromolecules, 2009. **42**(18): 6972-6980.
151. Dean, R.K., Devaine-Pressing, K., Dawe, L.N., and Kozak, C.M., *Reaction of CO_2 with Propylene Oxide and Styrene Oxide Catalyzed by a Chromium(III) Amine-Bis(phenolate) Complex*. Dalton Transactions, 2013. **42**(25): 9233-9244.
152. Darensbourg, D.J., Mackiewicz, R.M., Phelps, A.L., and Billodeaux, D.R., *Copolymerization of CO_2 and Epoxides Catalyzed by Metal Salen Complexes*. Accounts of Chemical Research, 2004. **37**(11): 836-844.
153. Robert, C., de Montigny, F., and Thomas, C.M., *Tandem Synthesis of Alternating Polyesters from Renewable Resources*. Nature Communications, 2011. **2**: 586.
154. Darensbourg, D.J., Mackiewicz, R.M., Rodgers, J.L., and Phelps, A.L., *(Salen)CrIIIX Catalysts for the Copolymerization of Carbon Dioxide and Epoxides: Role of the Initiator and Cocatalyst*. Inorganic Chemistry, 2004. **43**(6): 1831-1833.

155. Liu, B., Zhao, X., Guo, H., Gao, Y., Yang, M., and Wang, X., *Alternating Copolymerization of Carbon Dioxide and Propylene Oxide by Single-Component Cobalt Salen Complexes with Various Axial Group*. Polymer, 2009. **50**(21): 5071-5075.

APPENDIX A: Paper I

"Copolymerization of Cyclohexene Oxide with CO_2 Catalyzed by Tridentate *N*-Heterocyclic Carbene Titanium(IV) Complexes"

Quadri C. Quadri and Erwan Le Roux

Dalton Transactions 2014, Vol. 43, pp 4242-4246

APPENDIX B: Paper II

"Structural Characterization of Tridentate *N*-Heterocyclic Carbene of Titanium(IV) Benzyloxide, Silyloxide, Acetate and Azide Complexes and Assessment of Their Efficacies for Catalyzing the Copolymerization of Cyclohexene Oxide with CO_2"

Coralie C. Quadri, Ralte Lalrempuia, Julie Hessevik, Karl. W. Törnroos and Erwan Le Roux

Organometallics 2017, Vol. 36, pp 4477-4489

APPENDIX C: Paper III

"Steric Factors on Unsymmetrical *O*-hydroxyaryl *N*-Heterocyclic Carbene Ligands Prevailing the Stabilization of Single Stereoisomer of Bis-Ligated Titanium Complexes"

Coralie C. Quadri, Ralte Lalrempuia, Karl. W. Törnroos and Erwan Le Roux

Submitted

Steric Factors on Unsymmetrical *O*-hydroxyaryl *N*-Heterocyclic Carbene Ligands Prevailing the Stabilization of Single Stereoisomer of Bis-Ligated Titanium Complexes

*Coralie C. Quadri, Ralte Lalrempuia, Karl W. Törnroos, Erwan Le Roux**

Department of Chemistry, University of Bergen, Allégaten 41, N-5007, Bergen, Norway.

Tel: +47 555 89491; E-mail: Erwan.LeRoux@uib.no

Abstract

Bis-ligated titanium(IV) metal complexes supported by bidentate unsymmetrical *o*-hydroxyaryl-substituted N-heterocyclic carbene ligands were synthesized and structurally identified. While the direct addition of the doubly deprotonated bulky imidazolidinium chloride salts [$^{Dipp,4\text{-}R}$NHC-H]Cl (with Dipp = 2,6-diisopropylphenyl, R = H (2-hydroxyphenyl), and R = Me (2-hydroxy-4-methyl-phenyl)) with chloro-titanium precursor favors the formation of single stereoisomer corresponding to the bis-ligated titanium complexes *trans*-([κ^2-C,O]-$^{Dipp,4\text{-}R}$NHC)$_2$TiCl$_2$ (R = H (2-hydroxyphenyl) for **4a^{H}**, and R = Me (2-hydroxy-4-methyl-phenyl) for **4a^{Me}**), the reactivity with sterically less hindered imidazolidinium chloride salts [^{Mes,H}NHC-H]Cl and [^{Dep,H}NHC-H]Cl as protio-ligands (with Mes = 2,4,6-trimethylphenyl and Dep = 2,6-diethylphenyl) did not afford to single stereoisomer of bis-ligated titanium complexes. These results combined with topographic steric maps as well as the buried volume descriptor (%V_{bur}) indicate that bidentate bulky *N*-Dipp-substituted NHC ligands offer some level of steric protection preventing the formation of other possible bis-ligated (C,O)-NHC-titanium stereoisomers.

Keywords

Titanium; Bidentate ligand; Unsymmetrical N-heterocyclic carbene; Bis-ligated titanium complex; Ethylene polymerization.

1. Introduction

Since the first isolation and characterization of the *N*-heterocyclic carbene (NHC) by Bertrand [1] and Arduengo [2], NHCs have gained outstanding importance as ancillary ligands throughout most of the late transition metals and provided an useful hand of robust and versatile organometallic compounds for homogeneous catalysis [3]. Although late transition metal complexes show strong metal carbene bonds and slow dissociation with most of the NHC ligands, many of the early transition and *f*-block metals show the opposite trend [4]. Thus, to reduce the tendency of the NHC to dissociate from transition metal, considerable research effort have been devoted toward the studies of multidentate anionic carbon, nitrogen, oxygen and sulfur functionalized-NHC ligands [3h, 5]. A series of anionic carbon (i.e. phenyl, cyclopentadienyl, indenyl, fluorenyl), nitrogen (i.e. amido), oxygen (i.e. alkoxide, aryloxide, enolate) and sulfur (thiolate) groups have been developed to act as tethers for holding the NHC moiety in a close proximity to oxophilic metal centers [3f, h, 4b, d, 4f-h]. For example, the use of multidentate oxygen-functionalized NHC ligands of group 4 has proven to be an effective synthetic method for developing robust catalysts for the oligomerization and (co-)polymerization of olefins [6], hydroamination/cyclization of primary aminoalkenes [7], ring-opening polymerization (ROP) of *rac*-lactide [8], and selective coupling of epoxides and CO_2 to either polycarbonates [9] or cyclic carbonates [9b]. Of particular interest, the bidentate *o*-hydroxyaryl substituted NHCs are structurally analogous to bidentate salicylaldimine ligands [10], and are amongst the most commonly studied ligand classes in coordination chemistry due to their ease of preparation, ability to stabilize various metals in different oxidation states, and particularly valuable for the fine-tuning of electronic and steric parameters in a large variety of catalytic organic and polymerization reactions [11]. Recent investigations on bis-ligated bidentate alkoxy/aryloxy-functionalized NHCs of group 4, when activated by MAO (methylaluminoxane), showed to be active in ethylene [6d, f, g, l], ethylene/1-octene and ethylene/norbordene [6d] (co-)polymerization, and stereoselective in propylene [6f, g] and styrene polymerization [6l] similarly to the class of salicylaldimine group 4 catalysts (aka phenoxy-imine, FI, Chart 1) [11e]. Following these leads, we sought to use bidentate *o*-hydroxyaryl substituted NHC-based ligands framework that are analogous to FI ligands in efforts to conceive a new class of catalysts not only for olefins polymerization, but also for the copolymerization of CO_2 and cyclohexene oxide (CHO) in order to extend our studies on active and highly selective catalysts based on tridentate bis(aryloxy) NHC ligand sets of group 4 [9]. In addition to complex developed by Grubbs, *i.e. cis*-([κ^2-C,O]-$^{Dipp,(3\text{-}Ad,5\text{-}Me)}$NHC)$_2$TiCl$_2$ (with 3-Ad, 5-Me = (2-hydroxy-3-(adamant-1-yl)-5-methylphenyl), and a Dipp moiety as *N*-aryl substituent, Chart 1) [6d][6l], a similar set of unsymmetrical *o*-hydroxyaryl NHC ligands was synthesized bearing sterically less-hindered substituents on the *N*-aryloxy moieties and with various *N*-aryl substituents such as Dipp, Mes and Dep groups, as well as their coordination behavior to titanium. Preliminary data concerning the ability of the isolated bis-ligated (C,O)-NHC-titanium complexes to initiate the ethylene polymerization are also presented.

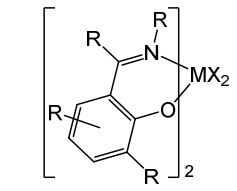

M = group 4 (FI catalysts)

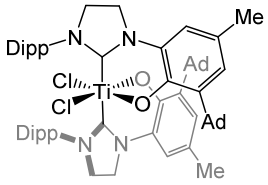

cis bis-ligated
[κ^2-C,O]-NHC titanium

Chart 1

2. Results and Discussion

*2.1. Synthesis of o-hydroxyaryl substituted imidazolidinium protio-ligands **3a-c***

The *o*-hydroxyaryl substituted imidazolidinium chloride salts [$^{Ar,4\text{-}H}$NHC-H]Cl **3a^{H}** (with Ar = Dipp) and **3c** (with Ar = Mes) were prepared according to the established procedure [12], and [$^{Dipp,4\text{-}Me}$NHC-H]Cl **3a^{Me}** and [$^{Dep,4\text{-}H}$NHC-H]Cl **3b** by adapting this literature procedure: ethyl chlorooxoacetate was reacted in THF with the appropriate arylamine **a-c** in presence of triethylamine at 0 °C to give the corresponding oxanilic acid esters **1a-c**, which were treated with the suitable aminoalcohols to afford quantitatively to oxalamides **2a-c** (Scheme 1). Subsequent reduction of **2a-c** with borane THF-adduct and acidification of ethylenediamine moieties followed by their cyclization with an excess of triethyl orthoformate affords to imidazolidinium protio-ligands **3a-c** in high overall yields (Scheme 1). Protio-ligand **3c** was further characterized by X-ray crystallography and crystallizes as a well-separated ion pair as found in other analogous imidazolidinium salt (Fig. S1, Table S1-3) [13]. The ^{1}H NMR spectra of imidazolidinium salt [$^{Dipp,4\text{-}Me}$NHC-H]Cl **3a^{Me}** and [$^{Dep,4\text{-}H}$NHC-H]Cl **3b** display the characteristic chemical resonances of the C*H*$_{imidazolidinium}$ proton (singlet at δ 9.05 and 8.96 ppm, respectively) and two broad triplets for the NC*H*$_2$ protons (apparent A_2B_2 system) of the *o*-hydroxyaryl unsymmetrically substituted imidazolidinium ring (centered at δ 4.59 ppm with υ_{AB} = 192 Hz and 4.64 ppm with υ_{AB} = 216 Hz, respectively), which are well-in-line with the reported data for **3a^{H}** and **3c** (Fig. S2-3) [12]. The ^{13}C NMR spectra of **3a^{Me}** and **3b** show typical chemical resonances at δ 156.6 and 157.2 ppm in chloroform-*d*, respectively, corresponding to the CH$_{imidazolidinium}$ carbons (Fig. S4-5). The IR spectra of both protio-ligands also exhibit stretches at 1624 ($\nu_{C=N}$) cm^{-1} characteristic of the imidazolidinium ring.

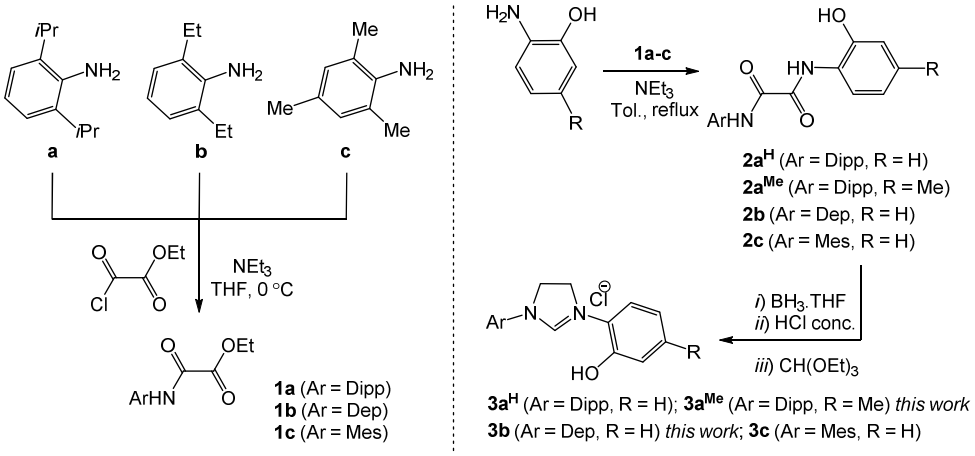

Scheme 1. Synthetic route for unsymmetrical *o*-hydroxyaryl substituted imidazolidinium salts **3a-c** [12].

2.2. Synthesis of bis-ligated o-hydroxyaryl substituted NHC titanium complexes ***4a^{H}*** *and* ***4a^{Me}***

Following the synthetic route reported previously by Grubbs [6d], the *o*-hydroxyaryl substituted imidazolidinium salts **3a^{H}** and **3a^{Me}** were doubly deprotonated by two equivalent of potassium bis(trimethylsilyl)amide (Kbtsa) for 10 min before to be treated with a 1M solution of $TiCl_4$ in toluene for 1 h affording to complexes **4a^{H}** and **4a^{Me}** as dark-red solids in quantitative yield (Scheme 2). Attempts using other synthetic methods for the syntheses of NHC-group 4 complexes [8b, 9a-c], such as the direct addition of imidazolidinium salts to Ti(O*i*Pr)$_4$ (alcohol elimination route) under different temperature conditions (room temperature to reflux) and solvents (toluene, THF), which should give in principle similar compounds, did not lead to the bis-ligated titanium complexes. It is interesting to note that the addition of one equivalent of deprotonated imidazolidinium salts **3a^{H}** or **3a^{Me}** to $TiCl_4$ mainly leads to the formation of bis-ligated NHC complexes of titanium as major products. The ^{1}H NMR spectra of **4a^{H}** and **4a^{Me}** show similar pattern, *i.e.* the disappearance of C$H_{\text{imidazolidinium}}$ proton and the appearance of a centrosymmetric multiplet assigned to the magnetically nonequivalent NCH_2 protons (geminal AA'BB' system) on the NHC ring, which is consistent with either a C_{2h} or C_{2v}-symmetry molecule in solution (Fig. S6-7). The ^{13}C NMR spectra of both complexes **4a^{H}** or **4a^{Me}** confirm the NHC$_{\text{carbene}}$ ligation to the titanium central atom with typical chemical resonances of the carbene at δ 206.7 and 206.6 ppm in benzene-d_6, respectively, (Fig. S8-9) [4g].

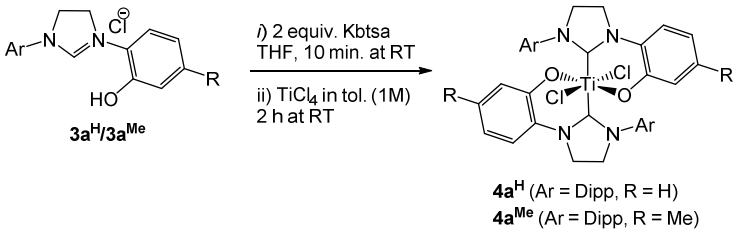

Scheme 2. Syntheses of bis-ligated *o*-hydroxyaryl NHC titanium complexes.

Single crystals of **4a^{H}** were obtained after few days from a saturated solution of the complex in dichloromethane at -30 °C. The molecular structure of **4a^{H}** was determined by single-crystal X-ray diffraction that confirms the chelation of two aryloxide-NHC ligands to titanium (Fig. 1). Compound **4a^{H}** crystallizes in the space group $P2_1/n$, corresponding to a C_{2h}-symmetry molecule which is consistent with the observed ^{1}H NMR spectroscopy in solution. As depicted in figure 1, the structure determined for **4a^{H}** shows that the titanium center adopts a nearly perfect octahedral geometry (Table 1). As previously reported for similar bis-ligated NHC titanium complex, *i.e. cis*-([κ^2-C,O]-$^{Dipp,(3\text{-}Ad,5\text{-}Me)}$NHC)$_2$TiCl$_2$ [6d], the two neutral NHC moieties are in *trans* position to each other (∠C$_{carbene}$-Ti-C$_{carbene}$ = 180.00(8)°) for complex **4a^{H}** and for the complex *cis*-([κ^2-C,O]-$^{Dipp,(3\text{-}Ad,5\text{-}Me)}$NHC)$_2$TiCl$_2$) at 178.0(9)° occupying the axial positions (Table 1 and Table S4-5). However unlike complex *cis*-([κ^2-C,O]-$^{Dipp,(3\text{-}Ad,5\text{-}Me)}$NHC)$_2$TiCl$_2$ having both two oxygen and two chloride atoms located in *cis* position (∠O$_{Ar}$-Ti-O$_{Ar}$ = 88.35(7)° and ∠Cl-Ti-Cl = 96.04(3)°, respectively), complex **4a^{H}** has the two oxygen and two chloride atoms in *trans* to each other (∠O$_{Ar}$-Ti-O$_{Ar}$ = 180.0° and ∠Cl-Ti-Cl = 180.0°). Contrary to complex *cis*-([κ^2-C,O]-$^{Dipp,(3\text{-}Ad,5\text{-}Me)}$NHC)$_2$TiCl$_2$ (which crystallizes as a C_2-symmetry molecule, enantiomer Λ), where the *cis*-configuration is favored to avoid the steric repulsion between Dipp and bulky Ad substituents [6d], complex **4a^{H}** is lacking of such bulky substituents, and thus leading to the most thermodynamically stable *trans* configuration as recently demonstrated by density functional theory calculation on bis-ligated alkoxy-functionalized NHC-Zr systems [6f, g]. Due to the more effective way that both NHC ligands wrap around titanium in **4a^{H}** in this *trans*-configuration, the overall bond lengths (*i.e.* Ti-C$_{carbene}$, and at least one of -Cl and –O bonds) are shorter, and one of the bite angles (∠O$_{Ar}$-Ti-C$_{carbene}$) is larger with a less pronounced deviation from planarity (∠O$_{Ar}$–C$_{Ar}$–N–C$_{carbene}$) for one of the NHC ligands compared to the complex *cis*-([κ^2-C,O]-$^{Dipp,(3\text{-}Ad,5\text{-}Me)}$NHC)$_2$TiCl$_2$ (Table 1).

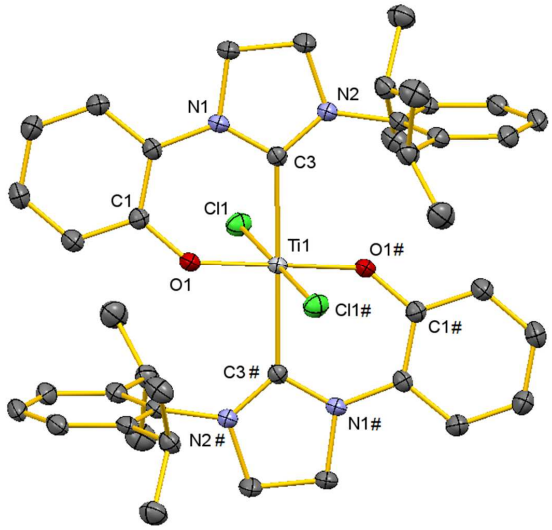

Fig. 1 Crystal structure of compound **4a^{H}** with anisotropic displacement parameter's set at the 50% probability level. Hydrogen atoms and a co-crystallized solvent dichloromethane molecule are omitted for clarity. Selected bond distances, bond angles and torsions angles are listed in table 1. Symmetry code #: 1-x+1, -y+1, -z+1.

Table 1

Selected Bond Distances, Bond Angles and Torsion Angles for Bis-Ligated ([κ^2-C,O]-^{Dipp,R}NHC)$_2$TiCl$_2$ complexes.

	trans-([κ^2-C,O]-$^{Dipp,4\text{-}H}$NHC)$_2$TiCl$_2$ (**4a^{H}**)	*cis*-([κ^2-C,O]-$^{Dipp,(3\text{-}Ad,5\text{-}Me)}$NHC)$_2$TiCl$_2$[a]
Bond lengths (Å)		
Ti-$C_{carbene}$	2.2597(18)/2.2597(18)	2.264(3)/2.275(3)
Ti-O_{Ar}	1.8578(12)/1.8579(12)	1.870(1)/1.842(1)
Ti-Cl	2.3269(5)/2.3269(5)	2.337(8)/2.297(6)
Bond Angles (deg)		
$C_{carbene}$-Ti-$C_{carbene}$	180.00(8)	178.0(9)
O_{Ar}-Ti-O_{Ar}	180.0	88.35(7)
O_{Ar}-Ti-$C_{carbene}$	82.40(6)/82.40(6)	82.45(8)/80.43(8)
Cl-Ti-Cl	180.0	96.04(3)
O_{Ar}-Ti-Cl	90.71(4)/89.29(4)	169.14(5)/88.32(5)
$C_{carbene}$-Ti-Cl	84.73(4)/95.27(4)	88.15(6)/83.54(6)
Torsion Angles (deg)		
O_{Ar}–C_{Ar}–N–$C_{carbene}$[b]	10.65/-10.65	1.95/-19.21

[a] Ref. [6d].

[b] O_{Ar}–C_{Ar}–N–$C_{carbene}$: O1–C1–N1–C3/O1#–C1#–N1#–C3# for **4a^{H}** and O1–C21–N2–C1/O2–C53–N4–C33.

Although the steric hindrance could be conceptualized for both *trans* and *cis* bis-ligated complexes, the availability of solid-state molecular structures allows to calculate the percent buried volume (%V_{bur}, *via* Samb*V*ca 2.0 calculations) and visualize the steric maps for further comparisons of each substituents on NHC ligands [14]. To make a best comparison of both complexes, the analyses were made only by considering ([κ²-C,O]-NHC)-Ti moiety and assuming a 3.5 Å radius of the sphere around the titanium for a Ti–$C_{carbene}$ length of 2.26 Å. Figure 2 shows minor differences between the two unsymmetrical NHC moieties with nearly identical steric map and %V_{bur} (37.0 *vs.* 36.5); thus, making it difficult to appreciate the steric profiles of these ligands using a value of 3.5 Å, which best defines the steric hindrance in the first coordination sphere around the metal. The differences between those two ligands become more marked when increasing the spherical radius around the metal to 5.0 Å allowing taking in account the bulky groups not bound to the metal. The C_{2h}-symmetry steric map of the NHC ligand in **4a^{H}**, with %V_{bur} of 33.4, shows a rather flat steric map with two small bulges located in the northern and western quadrants (corresponding to the *i*Pr groups of *N*-Dipp substituent), and two large hollows which can easily accommodate two Cl atoms in *trans* to each other in the empty southern (SW, SE) and northern quadrants (NE). In contrast, the C_2-symmetry steric map of *cis*-([κ²-C,O]-$^{Dipp,(3\text{-}Ad,5\text{-}Me)}$NHC)$_2$TiCl$_2$ with %V_{bur} of 38.0 shows a non-flat steric map particularly in the south-eastern quadrant imposed by the upward-pointing Ad substituent and two narrow hollows (SW and NE quadrants). From these steric maps, it is clear that the *trans*-configuration observed in these bis-ligated titanium complexes (**4a^{H}** and **4a^{Me}**) is largely favored by the embedment of the second NHC ligand bearing a H as *ortho* substituent on the aromatic ring, and when replaced by the more hindered Ad substituent, only the *cis*-configuration with the second Ad substituent pointing downward (SW quadrant) is allowed among other configurations.

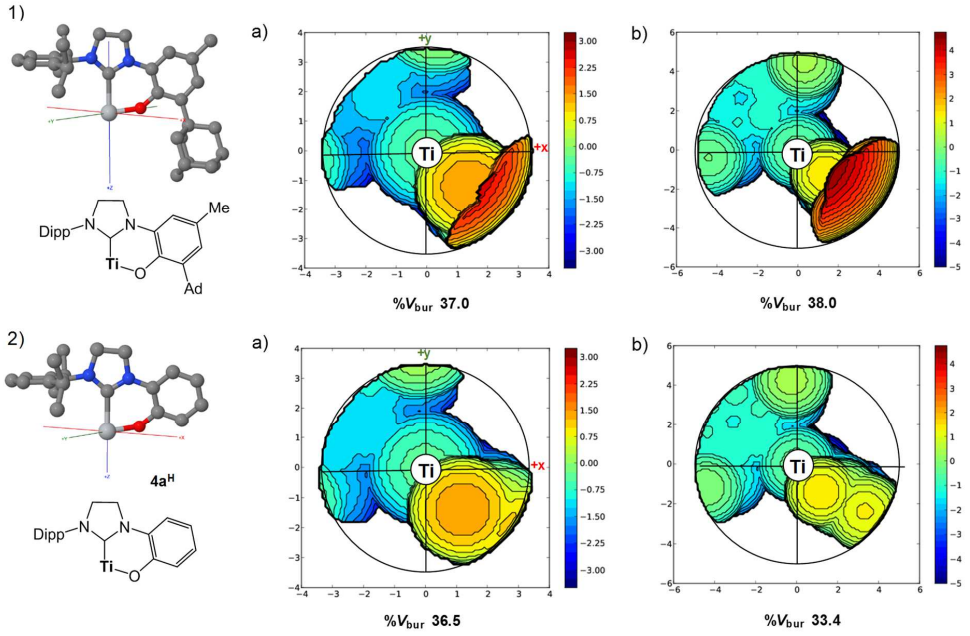

Fig. 2 Ball-and-stick representations and schemes (left) of bidentate ([κ²-C,O]-NHC)-Ti moiety: 1) from *cis*-([κ²-C,O]-$^{Dipp,(3\text{-}Ad,5\text{-}Me)}$NHC)$_2$TiCl$_2$ [6d] and 2) from complex **4a^{H}** with their respective steric maps (right) calculated with a sphere radius of: a) 3.5 Å and b) 5.0 Å [15]. The steric maps of these complexes are oriented in a Cartesian frame with a transverse xy-plane and a +z-axis pointing upward.

Following the same synthetic route described for the aforementioned complexes **4a^{H}** and **4a^{Me}**, the doubly deprotonated *o*-hydroxyaryl imidazolidinium salts **3b** and **3c** protio-ligands bearing less sterically hindered *N*-substituents (Dep and Mes, respectively) were treated by a solution of $TiCl_4$ consistently giving an intractable mixture of products. Although the disappearance of C*H*$_{imidazolidinium}$ and hydroxyl protons were observed for both mixtures in their respective ^{1}H NMR spectra, there are numerous overlapping multiple sets of signals which cannot straightforwardly be assigned but indicates that there are possibly formation of several stereoisomers. In order to rationalize the unsuccessful products isolation, we envisage that the steric map and the calculated %V_{bur} based on our modified X-ray data obtained for **4a^{H}** could adequately mimic the *N*-Mes substituent, *i.e.* by replacing the *i*Pr groups from the *N*-Dipp substituent by Me groups and give an insight trend of reactivity (Fig. 3). Interestingly, the simulated steric map of this bidentate NHC bearing *pseudo N*-Mes' substituent is substantially flat for both sphere radii of 3.5 and 5 Å in the NW and SE quadrants (with largely inferior %V_{bur}), with two large hollows in the adjacent quadrants. Through these steric maps and the previous ones, it can be deduced that the *ortho* bulky *i*Pr groups on the *N*-Dipp are the steric driving force leading mostly to *trans*-configuration complexes (in absence of *ortho* bulky group on the aromatic ring). When those *N*-aryl substituents are exchanged by less bulky groups (here Me), there is a drastic lack of steric hindrance to inhibit the formation of several species, which is leading most likely in our case, to the formation of many stereoisomers.

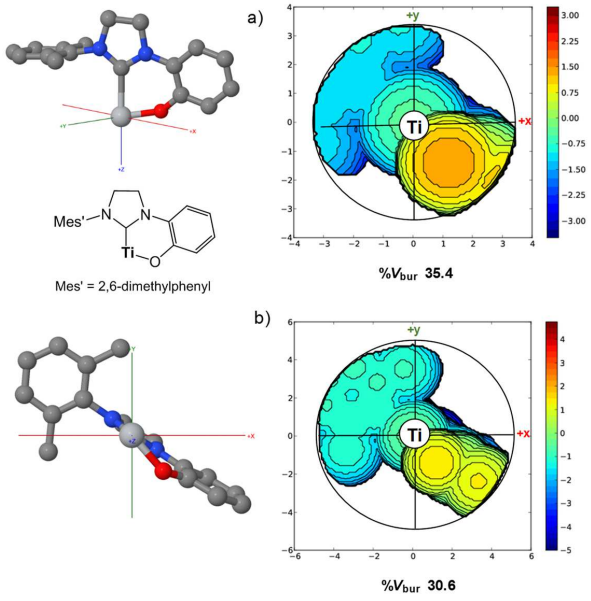

Fig. 3 Ball-and-stick representation, scheme (left) and projection (right) of the simulated steric map for a bidentate ([κ²-C,O]-$^{Mes',4\text{-}H}$NHC)-Ti moiety with a sphere radius of a) 3.5 Å and b) 5.0 Å [15]. The steric maps of these complexes are oriented in a Cartesian frame with a transverse xy-plane and a +z-axis pointing upward.

2.3. Polymerization Studies

Following previous studies on the copolymerization of epoxides and CO_2 catalyzed by group 4 metal complexes bearing benzotriazole alkoxide [16], bis(salphen) [17] ligands, showing structural similarities with our current 6-coordinate bis-ligated bidentate aryloxy NHC titanium complexes, and the highly selective catalysts based on the tridentate bis-aryloxy NHC complexes of group 4 [9a, c], we were interested in evaluating these complexes in the copolymerization of epoxides with CO_2. Copolymerization experiments of CHO with CO_2 were performed by using **4a^{H}**, **4a^{Me}** and *cis*-([κ²-C,O]-$^{Dipp,(3\text{-}Ad,5\text{-}Me)}$NHC)$_2$TiCl$_2$ compounds in the presence of most common co-catalysts such as [PPN]Cl, [PPN]N_3 and[Bu_4N]Cl to form the putative anionic catalysts [9]. The copolymerization of neat CHO with CO_2 shows no polycarbonate formation (conditions: 1 bar of CO_2 at 60 °C, ratio CHO:Ti = 2500) or other side-products such as cyclohexene carbonate or poly(cyclohexene oxide) ring-opening polymerization of CHO. The absence of activity is probably due to the steric congestion around the metal center and/or high stability avoiding the association of the co-catalysts nucleophile to form the "activated" species [9a, c] and/or the epoxide.

Due to the previous studies based on (non-)metallocene and phenoxy-imine catalysts development and their impact on the coordination polymerization of olefins for shaping tailored microstructure of polymers or synthetizing oligomers [11e, 18], systems based on functionalized NHC group 4 catalysts, especially the ones bearing multidentate and asymmetric auxiliary NHC ligands, have been recently explored for the α-olefins polymerization [6a-g, 6l, 19] and 1-hexene trimerization catalysis [6j]. More recently, a series of *C*$_2$-symmetric bidentate *o*-hydroxyaryl unsymmetrically substituted NHC ligands of group 4 were found moderately active in ethylene [6d, f, g, l], ethylene/1-octene and ethylene/norbordene [6d] (co-)polymerization , and stereoselective in propylene (isotactic up to ca. 70%) [6f, g] and styrene (syndiotactic up to ca. 99% in *rrrrrr* heptads) polymerization [6l]. The preliminary reported performance on *C*$_2$-symmetric and sterically hindered *cisoid* catalyst (*cis*-([κ²-C,O]-$^{Dipp,(3\text{-}Ad,5\text{-}Me)}$NHC)$_2$TiCl$_2$) in (co)polymerization show moderate and excellent stereoselectivity in α-olefins polymerization [6d, l], we were interested to evaluate the performance of the sterically less hindered **4a^{H}** and **4a^{Me}** catalysts with different spatial configuration (*transoid*). Thus, next to the *cis*-([κ²-C,O]-$^{Dipp,(3\text{-}Ad,5\text{-}Me)}$NHC)$_2$TiCl$_2$ catalyst, the newly synthesized compounds **4a^{H}** and **4a^{Me}** were examined for ethylene polymerization in the presence of 500 equiv. of MAO as co-catalyst. The preliminary polymerization results show that *trans*-**4a^{H}** and **4a^{Me}** catalysts have a moderate overall activity: 1206 and 1453 g_{PE} $mmol_{Ti}^{-1}$ h^{-1} (conditions: 40 bar of ethylene at room temperature and quenched after 5 min.), respectively, which are comparable to other group 4 systems [11e, 18]. However, the activities of both catalysts remain slightly superior to the benchmark catalyst *cis*-([κ²-C,O]-$^{Dipp,(3\text{-}Ad,5\text{-}Me)}$NHC)$_2$TiCl$_2$ (1131 g_{PE} $mmol_{Ti}^{-1}$ h^{-1}) under similar conditions [6d, l]. The difference in activity in this case is mostly assigned to the extremely bulky bidentate aryloxy NHC ligand wrapping the titanium center, notably with its Ad

substituent retarding the ethylene association to the metal rather than the *cis*/*transoid* configuration itself.

3. Conclusions

In summary, we have successfully synthesized a set of *o*-hydroxyaryl-substituted NHC ligands and the corresponding bis(aryloxide-NHC) titanium complexes. The bulky *N*-aryl substituent (such as Dipp *vs.* Mes and Dep) at the NHCs combined with the other *ortho*-substituent on the *N*-aryloxy moieties appear essential for leading to a single stereoisomer. Meaning that both steric factors have a significant effect on the configuration (*trans* or *cis*) of the final bis-ligated titanium complex, which can be fine-tuned by varying the size of the *N*-functional groups on the NHCs. The *cis*-bis(aryloxide-NHC) titanium complexes show moderate catalytic activities in ethylene polymerization, and the *N*-substituents at the NHCs and the configurations of the complexes have modest effect on the activity.

4. Experimental

4.1. General procedures

All operations were performed with rigorous exclusion of air and water, using standard Schlenk, high-vacuum and glovebox techniques (MB Braun MB200B-G; <1 ppm O_2, <1 ppm H_2O). Dichloromethane, hexane, THF and toluene were purified by using Grubbs columns (MB Braun Solvent Purification System 800). Benzene-d_6 and chloroform-*d* (99.96%) were obtained from Aldrich, dried over sodium or CaH_2, vacuum transferred, degassed and filtered prior to use. All other chemicals were purchased from Aldrich and used as received. The oxanilic acid ethyl esters (**1a** and **1c**), oxalamides (**2a^{H}** and **2c**), unsymmetrical *o*-hydroxyaryl substituted imidazolidinium chloride salts (**3a^{H}** and **3c**) and (*cis*-[κ^2-C,O]-$^{Dipp,3\text{-}Ad/5\text{-}Me}$NHC)$_2$TiCl$_2$ were prepared according to the literature procedures [6d, 12]. The imidazolidinium chloride salt **3c** was crystallized from acetonitrile/hexane (1/5) at -30 °C (CCDC reference code 1579164). The NMR spectra of air and moisture sensitive compounds were recorded using J. Young valve NMR tubes at 298 K on a *Bruker*-AVANCE-DMX400 spectrometer (5 mm BB, ^{1}H: 400.13 MHz; ^{13}C: 100.62 MHz) and a *Bruker*-BIOSPIN-AV500 and AV600 (5 mm BBO, ^{1}H: 500.13 MHz; ^{13}C: 125.77 MHz and 5 mm triple resonance inverse CryoProbe, ^{1}H: 600.13 MHz; ^{13}C: 150.91 MHz). ^{1}H and ^{13}C shifts are referenced to internal solvent resonances and reported in *parts per million* (ppm) relative to TMS. IR spectra were recorded on a Nicolet FT-IR Protégé 460 spectrometer with a DRIFT collector. The spectra were averaged over 64 scans; the resolution was ±4 cm^{-1}. Elemental analyses of C, H and N were performed on an Elementar Vario EL III instrument.

4.2. Unsymmetrical o-hydroxyaryl-substituted imidazolidinium protio-ligand syntheses

*4.2.1. 1-(2,6-diisopropylphenyl)-3-(2-hydroxy-4-methylphenyl)-4,5-dihydro-imidazolyl chloride salt (**3a^{Me}**)*

Compound *N*-(2,6-diisopropylphenyl)-oxanilic acid ethyl ester **1a** (1.71 g, 6.15 mmol) and 2-amino-5-methylphenol (1 equiv., 758 mg, 6.15 mmol) were dissolved in toluene (100 mL), and 0.86 mL of NEt_3 (1 equiv., 6.15 mmol) was added under inert atmosphere. The suspension was stirred and heated to reflux overnight. After cooling down the solution, a precipitate was obtained which was dissolved in EtOAc. The solution was washed with 2 M HCl (2x100 mL). The aqueous phase was then washed with EtOAc and the combined organic phases were washed with brine, dried over $MgSO_4$ and dried under vacuum. The solid was crystallized from warm toluene to afford *N*-(2,6-diisopropylphenyl)-*N'*-(2-hydroxy-4-methylphenyl)-oxalamide **2a^{Me}** (1.47 g, 67% yield). ^{1}H NMR (400.13 MHz, chloroform-*d*): δ 9.56 (s, 1H, N*H*), 8.81 (s, 1H, N*H*), 8.25 (s, 1H, O*H*), 7.37 (t, *J* = 7.8 Hz, 1H, Ar$_{Dipp}$-*H*), 7.24 (d, *J* = 8.2 Hz, 2H, Ar-*H*), 7.23 (d, *J* = 7.8 Hz, 1H, Ar$_{Dipp}$-*H*), 6.84 (s, 1H, Ar-*H*), 6.74 (d, *J* = 8.2 Hz, 1H, Ar-*H*), 3.02 (sept., *J* = 6.9 Hz, 2H, C*H*(CH_3)$_2$), 2.32 (s, 3H, Ar-C*H*$_3$), 1.22 (d, *J* = 6.9 Hz, 12H, CH(C*H*$_3$)$_2$) ppm.
Under inert atmosphere, to compound **2a^{Me}** (1.47 g, 4.15 mmol) was added 33.2 mL BH_3-THF (8 equiv., 1M in THF) and the mixture was heated to reflux overnight. After cooling down to room temperature, MeOH was added to the reaction mixture until gas evolution cease and then quenched by ≈ 1.5 mL of conc. HCl. The mixture was dried, dissolved in MeOH and these steps were repeated two more times. To this pale pink solid was added 15 mL of triethyl orthoformate and the solution was stirred at room temperature overnight. The solid was filtered off, washed with Et_2O and dried under vacuum to afford **3a^{Me}** as a white solid (1.20 g, 78% yield).^{1}H NMR (500.13 MHz, chloroform-*d*): δ 9.05 (s, 1H, NC*H*N), 7.47 (t, *J* = 7.8 Hz, 1H, Ar$_{Dipp}$-*H*), 7.35 (s, 1H, Ar-*H*), 7.24 (d, *J* = 7.8 Hz, 2H, Ar$_{Dipp}$-*H)*, 6.95 (d, *J* = 7.8, 1H, Ar-*H*), 6.62 (d, *J* = 7.8 Hz, 1H, Ar-*H*), 4.84 (bm, 2H, NC*H*$_2$), 4.36 (bm, 2H, NC*H*$_2$), 3.00 (sept., *J* = 6.8 Hz, 2H, C*H*(CH_3)$_2$), 2.18 (s, 3H, Ar-C*H*$_3$), 1.28 (d, *J* = 6.8 Hz, 6H, CH(C*H*$_3$)$_2$), 1.17 (d, *J* = 6.8 Hz, 6H, CH(C*H*$_3$)$_2$) ppm. ^{13}C NMR (125.77 MHz, chloroform-*d*): δ 156.6 (NCHN), 149.6 (*C$_{ipso}$*, O-Ar), 146.6 (*C$_q$*, Ar), 139.3 (*C$_q$*, Ar), 131.5 (*C$_q$*, Ar), 130.0 (*C$_q$*, Ar), 125.1 (*C*H, Ar), 120.5 (*C*H, Ar), 120.1 (*C*H, Ar), 119.8 (*C*H, Ar), 119.1 (*C*H, Ar), 52.5 (NCH_2), 51.0 (NCH_2), 28.9 (*C*H(CH_3)$_2$), 25.0 (CH(*C*H$_3$)$_2$), 24.3 (CH(*C*H$_3$)$_2$), 21.1 (Ar-*C*H$_3$) ppm. DRIFT (ν/cm^{-1}): 2970s, 2958s, 2868s, 1624vs, 1588w, 1553w, 1526w, 1494w, 1476w, 1457m, 1420m, 1385w, 1368w, 1335w, 1311m, 1292s, 1283m, 1263s, 1185w, 1166w, 945w, 879w, 812m, 764w, 593w, 487w, 456w. Anal. Calcd for $C_{22}H_{29}ClN_2O$: C, 68.98; H, 7.01; N 8.47. Found: C, 69.16; H, 7.26; N, 8.40.

*4.2.2. 1-(2,6-diethylphenyl)-3-(2-hydroxyphenyl)-4,5-dihydro-imidazolyl chloride (**3b**)*

2,6-diethylaniline (10 mL, 60.7 mmol) and triethylamine (1 equiv., 8.5 mL, 60.7 mmol) were dissolved in dry THF (80 mL). After cooling down the solution at 0 °C, 6.8 mL of ethyl chloroacetate (1 equiv., 60.7 mmol) was added dropwise leading to a formation of smoke and white solid. The solution was allowed to warm up at room temperature and stirred overnight. The solid was filtered off and the organic phase was washed with HCl 2M (2x100 mL). The aqueous phase was then washed with EtOAc and the combined organic phases were washed with brine, dry over $MgSO_4$ and dry under vacuum to afford *N*-(2,6-diethylphenyl)-oxanilic acid ethyl ester **1b** as white solid (11.23

g, 75% yield). ^{1}H NMR (500.13 MHz, chloroform-*d*): δ 8.40 (s, 1H, N*H*), 7.27 (t, *J* = 7.6 Hz, 1H, Ar$_{Dep}$-*H*), 7.15 (d, *J* = 7.6 Hz, 2H, Ar$_{Dep}$-*H*), 4.44 (q, *J* = 7.2 Hz, 2H, O-C*H*$_2$-CH$_3$), 2.59 (q, *J* = 7.6 Hz, 4H, C*H*$_2$-CH$_3$), 1.45 (t, *J* = 7.2 Hz, 3H, O-CH$_2$-C*H*$_3$), 1.20 (t, *J* = 7.6 Hz, 6H, CH$_2$-C*H*$_3$) ppm. ^{13}C NMR (125.77 MHz, chloroform-*d*): δ 161.0 (*C*O, carbimide), 155.4 (*C*O, ester), 141.1 5 (C_q, Ar), 130.9 (C_q, Ar), 128.6 (CH, Ar), 126.5 (CH, Ar), 63.7 (CH$_2$, O-*C*H$_2$-CH$_3$), 24.8 (CH$_2$, *C*H$_2$-CH$_3$), 14.3 (CH$_3$, O-CH$_2$-*C*H$_3$), 14.0 (CH$_3$, CH$_2$-*C*H$_3$) ppm.

Compound **1b** (10.96 g, 43.57 mmol) and 2-aminophenol (1 equiv., 4.80 mg, 43.97 mmol) were dissolved in toluene (100 mL), and 12.3 mL of NEt$_3$ (1 equiv., 87.9 mmol) was added under inert atmosphere. The suspension was stirred and heated to reflux overnight. After cooling down the solution a precipitate was obtained, which was dissolved in dichloromethane. The solution was washed with 2 M HCl (2x100 mL). The aqueous phase was then washed with dichloromethane and the combined organic phases were washed with brine, dried over MgSO$_4$ and dried under vacuum. The solid was crystallized from warm toluene to afford *N*-(2,6-diethylphenyl)-*N'*-(2-hydroxyphenyl)-oxalamide **2b** (10.06 g, 73% yield). ^{1}H NMR (500.13 MHz, chloroform-*d*): δ 9.68 (s, 1H, N*H*), 8.88 (s, 1H, N*H*), 8.06 (s, 1H, O*H*), 7.50 (dd, *J* = 8.1 Hz, *J* = 1.4 Hz, 1H, Ar$_{Dep}$-*H*), 7.30 (m, 1H, Ar-*H*), 7.18 (s, 1H, Ar$_{Dep}$-*H*), 7.17 (s, 1H, Ar$_{Dep}$-*H*), 7.15 (m, 1H, Ar-*H*), 6.97 (dd, *J* = 8.1 Hz, *J* = 1.4 Hz, 1H, Ar$_{Dep}$-*H*), 6.92 (m, 1H, Ar-*H*), 2.61 (q, *J* = 7.6 Hz, 4H, C*H*$_2$-CH$_3$), 1.21 (t, *J* = 7.6 Hz, 6H, CH$_2$-C*H*$_3$) ppm.

Following the procedure described for **3a^{Me}**, the reaction of **2b** (1.92 g, 6 mmol) and 49.2 mL of BH$_3$-THF (8 equiv., 1M in THF) yielded **3b** (1.6 g, 81% yield) as a white solid. ^{1}H NMR (500.13 MHz, chloroform-*d*): δ 8.96 (s, 1H, NC*H*N), 7.57 (d, *J* = 8.2 Hz, 1H, Ar$_{Dep}$-*H*), 7.41 (t, *J* = 7.8 Hz, 1H, Ar-*H*), 7.20 (d, *J* = 7.8 Hz, 2H, Ar$_{Dep}$-*H*), 7.10 (d, *J* = 7.8 Hz, Ar-*H*), 6.96 (t, *J* = 7.7 Hz, 1H, Ar-*H*), 6.77 (t, *J* = 7.7 Hz, 1H, Ar-*H*), 4.86 (bt, *J* = 10.4 Hz, 2H, NC*H*$_2$), 4.42 (bt, *J* = 10.4 Hz, 2H, NC*H*$_2$), 2.64 (q, *J* = 7.5 Hz, 4H, C*H*$_2$-CH$_3$), 1.22 (t, *J* = 7.5 Hz, 6H, CH$_2$-C*H*$_3$) ppm. ^{13}C NMR (125.77 MHz, chloroform-*d*): δ 157.2 (NCHN), 150.0 (C_{ipso}, O-Ar), 141.6 (C_q, Ar), 131.8 (C_q, Ar), 131.2 (C_q, Ar), 128.8 (*C*H, Ar), 127.6 (*C*H, Ar), 122.7 (*C*H, Ar), 120.3 (*C*H, Ar), 119.9 (*C*H, Ar), 118.9 (*C*H, Ar), 51.5 (N*C*H$_2$), 51.0 (N*C*H$_2$), 24.3 (CH$_2$, *C*H$_2$-CH$_3$), 15.2 (CH$_3$, CH$_2$-*C*H$_3$) ppm. DRIFT (ν/cm^{-1}): 2971s, 2959s, 2869s, 1624vs, 1588w, 1555w, 1525w, 1494w, 1476w, 1457m, 1421m, 1385w, 1368w, 1337w, 1313m, 1292s, 1284m, 1263s, 1186w, 1166w, 945w, 880w, 812m, 763w, 593w, 487w, 455w. Anal. Calcd for $C_{19}H_{23}ClN_2O$: C, 68.97; H, 7.01; N 8.47. Found: C, 68.79; H, 7.26; N, 8.36.

4.3. Preparation of bis-ligated o-hydroxyaryl substituted NHC titanium(IV) complexes

*4.3.1. 1-(2,6-diisopropylphenyl)-3-(2-hydroxyphenyl)-4,5-dihydro-imidazolyl titanium(IV) dichloride (**4a^H**)*

In a vial 1-(2,6-diisopropylphenyl)-3-(2-hydroxyphenyl)-4,5-dihydro-imidazolyl chloride salt **3a^H** (588.0 mg, 1.64 mmol) and potassium bis(trimethylsilyl)amide (2 equiv., 561.35 mg, 3.27 mmol) were dissolved in THF (3 mL), and the resulting yellow suspended mixture was stirred for 10 min at room temperature. To this mixture was added 0.82 mL of a solution of 1M titanium tetrachloride in toluene (0.5 equiv., 0.82 mmol) in 2 mL THF. The solution rapidly turned dark red and was allowed to stir for 2

h at room temperature. Subsequent centrifugation, filtration and evaporation to dryness afforded complex **4a^{H}** as a dark red solid in quantitative yield. Crystals of **4a^{H}** were obtained from a saturated solution of dichloromethane at -30°C for several days. ^{1}H NMR (500.13 MHz, benzene-d_6): δ 7.42 (t, J = 7.7 Hz, 2H, Ar$_{Dipp}$-H), 7.29 (d, J = 7.7 Hz, 4H, Ar$_{Dipp}$-H), 7.01 (m, 2H, Ar-H), 6.75 (m, 2H, Ar-H), 6.37 (dd, J = 8.1 Hz, J = 1.4 Hz, 2H, Ar-H), 5.26 (dd, J = 8.1 Hz, , J = 1.4 Hz, 2H, Ar-H), 3.47 (sept., J = 6.8 Hz, 4H, CH(CH$_3$)$_2$), 3.07 (m, 4H, NCH_2), 2.95 (m, 4H, NCH_2), 1.56 (d, J = 6.8 Hz, 12H, CH(CH_3)$_2$), 1.10 (d, J = 6.8 Hz, 12H, CH(CH_3)$_2$) ppm. ^{13}C NMR (125.77 MHz, benzene-d_6): δ 206.7 (N*C*N), 155.0 (C$_{ipso}$, O-Ar), 148.0 (C_q, Ar), 137.8 (C_q, Ar), 133.6 (C_q, Ar), 129.2 (*C*H, Ar), 125.3 (*C*H, Ar), 124.0 (*C*H, Ar), 119.3 (*C*H, Ar), 118.1 (*C*H, Ar), 116.7 (*C*H, Ar), 53.9 (N*C*H$_2$), 47.3 (N*C*H$_2$), 28.5 (*C*H(CH$_3$)$_2$), 26.2 (CH(*C*H$_3$)$_2$), 24.8 (CH(*C*H$_3$)$_2$) ppm. DRIFT (ν/cm^{-1}): 3065w, 3031w, 2961s, 2925m, 2867m, 1610m, 1587m, 1495vs, 1474vs, 1429s, 1408s, 1385w, 1363w, 1317s, 1288vs, 1236m, 1123w, 1056w, 996w, 912m, 879m, 806w, 750m, 671m, 640w, 453w, 438w, 418m. Anal. Calcd for $C_{42}H_{50}Cl_2N_4O_2Ti.2CH_2Cl_2$: C, 56.73; H, 5.84; N 6.01. Found: C, 57.04; H, 6.18; N 5.94.

*4.3.2. 1-(2,6-diisopropylphenyl)-3-(2-hydroxy-4-methylphenyl)-4,5-dihydro-imidazolyl titanium(IV) dichloride (**4a^{Me}**)*

Following the procedure described for **4a^{H}**, the reaction of 1-(2,6-diisopropylphenyl)-3-(2-hydroxy-4-mehtylphenyl)-4,5-dihydro-imidazolyl chloride salt **3a^{Me}** (350.8 mg, 0.94 mmol), potassium bis(trimethylsilyl)amide (2 equiv., 375.2 mg, 1.88 mmol) and titanium tetrachloride (0.5 equiv., 0.47 mL, 0.82 mmol) yielded **4a^{Me}** (323 mg, 87% yield) as a dark red solid. ^{1}H NMR (500.13 MHz, chloroform-d): δ 7.53 (t, J = 7.7 Hz, 2H, Ar$_{Dipp}$-H), 7.35 (d, J = 7.7 Hz, 4H, Ar$_{Dipp}$-H), 6.68 (d, J = 8.2 Hz, 2H, Ar-H), 6.50 (dd, J = 8.2 Hz, J = 1.7 Hz, 2H, Ar-H), 4.60 (d, 2H, J = 1.7 Hz, Ar-H), 4.10 (m, 4H, NCH_2), 3.79 (m, 4H, NCH_2), 3.27 (sept., J = 6.8 Hz, 4H, CH(CH$_3$)$_2$), 2.09 (s, 3H, Ar-CH_3), 1.27 (d, J = 6.8 Hz, 12H, CH(CH_3)$_2$), 1.16 (d, J = 6.8 Hz, 12H, CH(CH_3)$_2$) ppm. ^{13}C NMR (125.77 MHz, chloroform-d): δ 205.8 (N*C*N), 153.6 (C$_{ipso}$, O-Ar), 148.0 (C_q, Ar), 137.3 (C_q, Ar), 133.7 (C_q, Ar), 130.7 (C_q, Ar), 129.2 (*C*H, Ar), 125.0 (*C*H, Ar), 120.3 (*C*H, Ar), 118.1 (*C*H, Ar), 115.5 (*C*H, Ar), 54.0 (N*C*H$_2$), 48.0 (N*C*H$_2$), 28.3 (*C*H(CH$_3$)$_2$), 26.2 (CH(*C*H$_3$)$_2$), 24.5 (CH(*C*H$_3$)$_2$), 20.4 (Ar-*C*H$_3$) ppm. ^{13}C NMR (125.77 MHz, benzene-d_6): δ 206.6 (N*C*N), 154.9 (C$_{ipso}$, O-Ar), 148.3 (C_q, Ar), 138.0 (C_q, Ar), 133.6 (C_q, Ar), 131.3 (C_q, Ar), 129.2 (*C*H, Ar), 125.2 (*C*H, Ar), 119.8 (*C*H, Ar), 118.4 (*C*H, Ar), 116.1 (*C*H, Ar), 53.8 (N*C*H$_2$), 53.3 (N*C*H$_2$), 28.4 (*C*H(CH$_3$)$_2$), 26.1 (CH(*C*H$_3$)$_2$), 24.7 (CH(*C*H$_3$)$_2$), 20.7 (Ar-*C*H$_3$) ppm. DRIFT (ν/cm^{-1}): 3064w, 3032w, 2962s, 2925m, 2867m, 1615s, 1572m, 1506s, 1474vs, 1458s, 1420s, 1402s, 1363w, 1319s, 1292vs, 1234m, 1169m, 1147m, 1056w, 1009w, 960m, 909w, 864w, 804m, 760s, 734w, 663m, 590w, 428w, 415m.

4.4. General procedure for ethylene polymerization

In the glovebox, a vial was charged with a stirring bar, Ti catalyst (5 μmol) in 5 mL of toluene and 500 equiv. of MAO, and placed in an autoclave reactor. After addition of 40 bar of ethylene, the reaction was stirred 5 min and the pressure was released before to quench the reaction by 1 mL of acidified MeOH. Volatiles were removed under reduced

pressure, and polymer was washed with isopropanol and dried under vacuum for 2 h at 150 °C. The polymer yield was determined gravimetrically.

4.5. X-ray crystallography and crystal structure determination

Suitable crystals for diffraction experiments were selected in a glovebox and mounted in a minimum of Parabar 10312 oil (Hampton Research) in a nylon loop and then mounted under a nitrogen cold stream from an Oxford Cryosystems 700 series open-flow cryostat. Data collection was done on a Bruker AXS TXS rotating anode system with an APEXII Pt^{135} CCD detector using graphite-monochromated Mo K_α radiation (λ = 0.710 73 Å). Data collection and data processing were done using APEX2[20], SAINT[21], and SADABS[22] version 2012/1,whereas structure solution and final model refinement were done using SHELXS[23] version 2013/1 or SHELXT[24] version 2014/4 and SHELXL[25] version 2014/7. Crystal data: for **4**$^{\mathbf{aH}}$ obtained from a saturated solution in CH_2Cl_2. $C_{42}H_{50}Cl_2N_4O_2Ti.2(CH_2Cl_2)$, M = 931.51, crystal size: 0.125 x 0.100 x 0.050 mm^3, crystal habit/color: prism/dark red, monoclinic, space group $P2_1/n$ (No.14), a = 11.9657(7), b = 12.9163(8), c = 14.5572(9) Å, β = 99.1720(10)°, V = 2221.1(2) $Å^3$, Z = 2, ρ_{calc} = 1.393 $g.cm^{-3}$, $F(000)$ = 972, μ(Mo-K_α) = 0.595 mm^{-1}, λ = 0.71073 Å, T = 103(2) K. The 28755 reflections measured on a Bruker AXS APEXII Ultra CCD area detector system yielded 4739 unique data (2.050 < θ < 26.776°, R_{int} = 0.0485) [4739 observed reflections ($I > 2\sigma(I)$]. Goodness-of-fit on F^2 = 1.037, $R1$ = 0.0350, $wR2$ = 0.0894, R indices (all data) $R1$ = 0.0486, w$R2$ = 0.0980. CCDC reference code 1579165 contains the supplementary crystallographic data for **4**$^{\mathbf{aH}}$. These data can be obtained free of charge from The Cambridge Crystallographic Data Centre via www.ccdc.cam.ac.uk/data_request/cif.

4.6. %V_{Bur} and steric maps calculations

The %V_{Bur} values and steric maps were evaluated with the SambVca 2.0 package [26]. The radius of the sphere around the center atom was set to: 3.5 Å or 5 Å, distance from the center of the sphere: 2.26 Å, mesh spacing: 0.1 Å, H atoms omitted and atom radii: Bondi radii scaled by 1.17, as recommended by Cavallo.

Acknowledgements

The authors acknowledge the University of Bergen, L. Meltzers Høyskolefond (K. W. T.: bursary no. 2017/3273) and the Norwegian Research Council (FRINATEK grant no. 240333) for financial support. Prof. Dr. Nils Åge Frøystein and Dr. Marco Foscato are thanked for their fruitful discussions on NMR spectroscopy and calculations, respectively.

References

[1] A. Igau, H. Grutzmacher, A. Baceiredo, G. Bertrand, J. Am. Chem. Soc. 110 (1988) 6463-6466.

[2] (a) A.J. Arduengo, M. Kline, J.C. Calabrese, F. Davidson, J. Am. Chem. Soc. 113 (1991) 9704-9705; (b) A.J. Arduengo, H.V.R. Dias, R.L. Harlow, M. Kline, J. Am. Chem. Soc. 114 (1992) 5530-5534.
[3] (a) W.A. Herrmann, M. Elison, J. Fischer, C. Köcher, G.R.J. Artus, Angew. Chem., Int. Ed. Engl. 34 (1995) 2371-2374; (b) W.A. Herrmann, Angew. Chem., Int. Ed. 41 (2002) 1290-1309; (c) V. César, S. Bellemin-Laponnaz, L.H. Gade, Chem. Soc. Rev. 33 (2004) 619-636; (d) S.P. Nolan, Editor, N-Heterocyclic Carbenes in Synthesis, Wiley-VCH Verlag GmbH & Co. KGaA, (2006); (e) F. Glorius, Editor, N-Heterocyclic Carbenes in Transition Metal Catalysis, Springer-Verlag Berlin Heidelberg, (2007); (f) S. Díez-González, S.P. Nolan, Coord. Chem. Rev. 251 (2007) 874-883; (g) S. Díez-González, N. Marion, S.P. Nolan, Chem. Rev. 109 (2009) 3612-3676; (h) M. Poyatos, J.A. Mata, E. Peris, Chem. Rev. 109 (2009) 3677-3707; (i) K. Riener, S. Haslinger, A. Raba, M.P. Högerl, M. Cokoja, W.A. Herrmann, F.E. Kühn, Chem. Rev. 114 (2014) 5215-5272; (j) S.P. Nolan, Editor, N-Heterocyclic Carbenes: Effective Tools for Organometallic Synthesis, Wiley-VCH Verlag GmbH & Co. KGaA, (2014); (k) M.N. Hopkinson, C. Richter, M. Schedler, F. Glorius, Nature 510 (2014) 485-496.
[4] (a) D. Bourissou, O. Guerret, F.P. Gabbaï, G. Bertrand, Chem. Rev. 100 (2000) 39-92; (b) S.T. Liddle, I.S. Edworthy, P.L. Arnold, Chem. Soc. Rev. 36 (2007) 1732-1744; (c) D. Pugh, A.A. Danopoulos, Coord. Chem. Rev. 251 (2007) 610-641; (d) D. McGuinness, Dalton Trans. (2009) 6915-6923; (e) L.-A. Schaper, E. Tosh, W.A. Herrmann, RSC Catal. Ser 6 (2011) 166-195; (f) S. Bellemin-Laponnaz, S. Dagorne, Chem. Rev. 114 (2014) 8747-8774; (g) D. Zhang, G. Zi, Chem. Soc. Rev. 44 (2015) 1898-1921; (h) S. Hameury, P. de Fremont, P. Braunstein, Chem. Soc. Rev. 46 (2017) 632-733.
[5] (a) O. Kuhl, Chem. Soc. Rev. 36 (2007) 592-607; (b) L. Benhamou, E. Chardon, G. Lavigne, S. Bellemin-Laponnaz, V. César, Chem. Rev. 111 (2011) 2705-2733.
[6] (a) H. Aihara, T. Matsuo, H. Kawaguchi, Chem. Commun. (2003) 2204-2205; (b) D.S. McGuinness, V.C. Gibson, J.W. Steed, Organometallics 23 (2004) 6288-6292; (c) D. Zhang, Eur. J. Inorg. Chem. 2007 (2007) 4839-4845; (d) A. El-Batta, A.W. Waltman, R.H. Grubbs, J. Organomet. Chem. 696 (2011) 2477-2481; (e) T.G. Larocque, A.C. Badaj, S. Dastgir, G.G. Lavoie, Dalton Trans. 40 (2011) 12705-12712; (f) C. Bocchino, M. Napoli, C. Costabile, P. Longo, J. Polym. Sci. A Polym. Chem. 49 (2011) 862-870; (g) C. Costabile, C. Bocchino, M. Napoli, P. Longo, J. Polym. Sci. A Polym. Chem. 50 (2012) 3728-3735; (h) T.G. Larocque, G.G. Lavoie, J. Organomet. Chem. 715 (2012) 26-32; (i) E. Despagnet-Ayoub, L.M. Henling, J.A. Labinger, J.E. Bercaw, Dalton Trans. 42 (2013) 15544-15547; (j) S. Dagorne, S. Bellemin-Laponnaz, C. Romain, Organometallics 32 (2013) 2736-2743; (k) E. Despagnet-Ayoub, M.K. Takase, L.M. Henling, J.A. Labinger, J.E. Bercaw, Organometallics 34 (2015) 4707-4716; (l) G.M. Miyake, M.N. Akhtar, A. Fazal, E.A. Jaseer, C.S. Daeffler, R.H. Grubbs, J. Organomet. Chem. 728 (2013) 1-5.
[7] (a) J. Cho, T.K. Hollis, T.R. Helgert, E.J. Valente, Chem. Commun. (2008) 5001-5003; (b) J. Cho, T.K. Hollis, E.J. Valente, J.M. Trate, J. Organomet. Chem. 696

(2011) 373-377; (c) T.R. Helgert, T.K. Hollis, E.J. Valente, Organometallics 31 (2012) 3002-3009; (d) S. Barroso, S.R.M.M. de Aguiar, R.F. Munha, A.M. Martins, J. Organomet. Chem. 760 (2014) 60-66; (e) W.D. Clark, J. Cho, H.U. Valle, T.K. Hollis, E.J. Valente, J. Organomet. Chem. 751 (2014) 534-540; (f) W.D. Clark, K.N. Leigh, C.E. Webster, T.K. Hollis, Aust. J. Chem. 69 (2016) 573-582; (g) H.U. Valle, G. Akurathi, J. Cho, W.D. Clark, A. Chakraborty, T.K. Hollis, Aust. J. Chem. 69 (2016) 565-572.
[8] (a) D. Patel, S.T. Liddle, S.A. Mungur, M. Rodden, A.J. Blake, P.L. Arnold, Chem. Commun. (2006) 1124-1126; (b) C. Romain, L. Brelot, S. Bellemin-Laponnaz, S. Dagorne, Organometallics 29 (2010) 1191-1198; (c) C. Romain, B. Heinrich, S.B. Laponnaz, S. Dagorne, Chem. Commun. 48 (2012) 2213-2215; (d) N. Zhao, G. Hou, X. Deng, G. Zi, M.D. Walter, Dalton Trans. 43 (2014) 8261-8272.
[9] (a) C.C. Quadri, E. Le Roux, Dalton Trans. 43 (2014) 4242-4246; (b) J. Hessevik, R. Lalrempuia, H. Nsiri, K.W. Törnroos, V.R. Jensen, E. Le Roux, Dalton Trans. 45 (2016) 14734-14744; (c) R. Lalrempuia, F. Breivik, K.W. Törnroos, E. Le Roux, Dalton Trans. 46 (2017) 8065-8076; (d) Coralie C. Quadri, Ralte Lalrempuia, Julie Hessevik, Karl. W. Törnroos, E.L. Roux, Organometallics (2017) submitted.
[10] M. Calligarir, L. Randaccio, in: G. Wilkinson, R.D. Gillard, J. McCleverty (Eds.) Comprehensive Coordination Chemistry, Pergamon Press Ltd, Oxford, (1987), pp. 723-726.
[11] (a) C. Gennari, U. Piarulli, Chem. Rev. 103 (2003) 3071-3100; (b) H. Gröger, Chem. Rev. 103 (2003) 2795-2828; (c) M. North, D.L. Usanov, C. Young, Chem. Rev. 108 (2008) 5146-5226; (d) E. Wojaczyńska, J. Wojaczyński, Chem. Rev. 110 (2010) 4303-4356; (e) H. Makio, H. Terao, A. Iwashita, T. Fujita, Chem. Rev. 111 (2011) 2363-2449.
[12] A.W. Waltman, R.H. Grubbs, Organometallics 23 (2004) 3105-3107.
[13] N. Stylianides, A.A. Danopoulos, D. Pugh, F. Hancock, A. Zanotti-Gerosa, Organometallics 26 (2007) 5627-5635.
[14] (a) A. Poater, B. Cosenza, A. Correa, S. Giudice, F. Ragone, V. Scarano, L. Cavallo, Chem. – A Eur. J. 2009 (2009) 1759-1766; (b) L. Falivene, R. Credendino, A. Poater, A. Petta, L. Serra, R. Oliva, V. Scarano, L. Cavallo, Organometallics 35 (2016) 2286-2293.
[15] A. Poater, F. Ragone, R. Mariz, R. Dorta, L. Cavallo, Chem. – A Eur. J. 16 (2010) 14348-14353.
[16] (a) C.-K. Su, H.-J. Chuang, C.-Y. Li, C.-Y. Yu, B.-T. Ko, J.-D. Chen, M.-J. Chen, Organometallics 33 (2014) 7091-7100; (b) H.-J. Chuang, B.-T. Ko, Dalton Trans. 44 (2015) 598-607.
[17] M. Mandal, D. Chakraborty, J. Polym. Sci. Part A: Polym. Chem. 54 (2016) 809-824.
[18] (a) V.C. Gibson, S.K. Spitzmesser, Chem. Rev. 103 (2003) 283-316; (b) H.H. Brintzinger, D. Fischer, R. Mülhaupt, B. Rieger, R.M. Waymouth, Angew. Chem. Int. Ed. 34 (1995) 1143-1170; (c) G.W. Coates, Chem. Rev. 100 (2000) 1223-1252;

(d) C. Redshaw, Y. Tang, Chem. Soc. Rev. 41 (2012) 4484-4510; (e) G.J.P. Britovsek, V.C. Gibson, D.F. Wass, Angew. Chem. Int. Ed. 38 (1999) 428-447.
[19] D. Zhang, N. Liu, Organometallics 28 (2009) 499-505.
[20] Bruker-AXS: APEX2. Version 2014.11-0. Madison, Wisconsin, USA. 2014.
[21] Bruker-AXS: SAINT. Version 7.68A. Madison, Wisconsin, USA, 2010.
[22] L. Krause, R. Herbst-Irmer, G.M. Sheldrick, D. Stalke, J. Appl. Crystallogr. 48 (2015) 3-10.
[23] G. M. Sheldrick, XS. Version 2013/1. Georg-August-Universität Göttingen, Göttingen, Germany, 2013.
[24] G. Sheldrick, Acta Crystallogr., Sect. A: Found. Adv. 71 (2015) 3-8.
[25] G. Sheldrick, Acta Crystallogr., Sect. C: Cryst. Struct. Chem. 71 (2015) 3-8.
[26] The %V_{bur} and steric maps were calculated using the web-based SambVca 2.0 program (https://www.molnac.unisa.it/OMtools/sambvca2.0/index.html)

Supporting Information

Steric Factors on Unsymmetrical *O*-hydroxyaryl *N*-Heterocyclic Carbene Ligands Prevailing on the Stabilization of Single Stereoisomer of Bis-Ligated Titanium Complexes

Coralie C. Quadri, Ralte Lalrempuia, Karl. W. Törnroos, Erwan Le Roux*

Department of Chemistry, University of Bergen, Allégaten 41, N-5007, Bergen, Norway.

Tel: +47 555 89491; E-mail: Erwan.LeRoux@uib.no

Content:

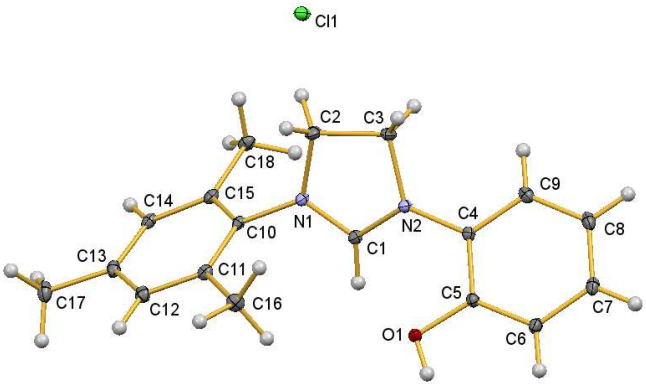

Figure S1. Crystal structure of 1-(2,4,6-trimethylphenyl)-3-(2-hydroxyphenyl)-4,5-dihydro-imidazolyl chloride salt **3c**.

Table S1. Crystal structure and refinement data for **3c**.

Compound	**3c**
Chemical formula	$C_{18}H_{21}ClN_2O$
Formula weight	316.82
Crystal size	0.341 x 0.231 x 0.070
Temperature/K	103(2)
Wavelength/Å	0.71073
Crystal system	Monoclinic
Space group	$P2_{1/c}$ (No.14)
a/ Å	12.3644(11)
b/ Å	8.8966(8)
c/ Å	14.9065(13)
α/ °	90
β/ °	94.3230(10)
γ / °	90
V/ Å^3	1635.1(3)
Z	4
ρ_{calcd}/ g cm^{-3}	1.287
Absorption coeff./ mm^{-1}	0.237
F(000)	672
Θ Range for data collection/ °	2.668 to 32.038
Reflections collected	25989
Independent reflections	5655 [R(int) = 0.0265]
Completeness to Θ/ %	98.6
Data/restraints/parameters	5655/0/206
Goodness-of-fit on F^2	1.080
Final R_1 indices [$I>2\sigma(I)$]	R1 = 0.0429, wR2 = 0.1135
R indices (all data)	R1 = 0.0459, wR2 = 0.1166
Largest diff. peak; hole/e Å^{-3}	0.676 and -0.201

Table S2. Selected bond lengths [Å] and angles [°] for **3c**.

O(1)-C(5)	1.3538(11)	C(13)-C(14)	1.3962(14)
O(1)-H(1O)	0.84(2)	C(13)-C(17)	1.5067(14)
N(1)-C(1)	1.3141(11)	C(14)-C(15)	1.3982(13)
N(1)-C(10)	1.4341(12)	C(15)-C(18)	1.5065(14)
N(1)-C(2)	1.4802(12)		
N(2)-C(1)	1.3204(11)	C(5)-O(1)-H(1O)	104.9(14)
N(2)-C(4)	1.4167(11)	C(1)-N(1)-C(10)	124.74(8)
N(2)-C(3)	1.4752(12)	C(1)-N(1)-C(2)	109.69(7)
C(1)-H(1)	0.9500	C(10)-N(1)-C(2)	124.06(7)
C(2)-C(3)	1.5346(14)	C(1)-N(2)-C(4)	125.99(8)
C(4)-C(9)	1.3931(13)	C(1)-N(2)-C(3)	109.43(8)
C(4)-C(5)	1.4069(13)	C(4)-N(2)-C(3)	123.93(8)
C(5)-C(6)	1.3980(12)	N(1)-C(1)-N(2)	113.48(8)
C(6)-C(7)	1.3921(14)	N(1)-C(1)-H(1)	123.3
C(7)-C(8)	1.3888(16)	N(2)-C(1)-H(1)	123.3
C(8)-C(9)	1.3937(14)	C(9)-C(4)-N(2)	120.11(8)
C(10)-C(11)	1.4028(13)	C(5)-C(4)-N(2)	119.50(8)
C(10)-C(15)	1.4048(12)	O(1)-C(5)-C(4)	117.94(8)
C(11)-C(12)	1.3946(13)	C(11)-C(10)-C(15)	122.16(8)
C(11)-C(16)	1.5065(13)	C(11)-C(10)-N(1)	118.79(8)
C(12)-C(13)	1.3974(14)	C(15)-C(10)-N(1)	119.05(8)

Symmetry transformations used to generate equivalent atoms:

Table S3. Torsion angles [°] for **3c**.

C(10)-N(1)-C(1)-N(2)	-169.84(8)	C(1)-N(2)-C(4)-C(9)	140.25(9)
C(2)-N(1)-C(1)-N(2)	-3.42(11)	C(3)-N(2)-C(4)-C(9)	-29.55(13)
C(4)-N(2)-C(1)-N(1)	-178.62(8)	C(1)-N(2)-C(4)-C(5)	-42.42(13)
C(3)-N(2)-C(1)-N(1)	-7.58(11)	C(3)-N(2)-C(4)-C(5)	147.78(9)
C(1)-N(1)-C(2)-C(3)	12.14(10)	C(9)-C(4)-C(5)-O(1)	179.52(8)
C(10)-N(1)-C(2)-C(3)	178.67(8)	N(2)-C(4)-C(5)-O(1)	2.20(12)
C(1)-N(2)-C(3)-C(2)	14.50(11)	N(2)-C(4)-C(5)-C(6)	-176.79(8)
C(4)-N(2)-C(3)-C(2)	-174.24(8)	C(1)-N(1)-C(10)-C(11)	59.35(12)
N(1)-C(2)-C(3)-N(2)	-15.27(10)	C(1)-N(1)-C(10)-C(15)	-120.65(10)

Symmetry transformations used to generate equivalent atoms: #1 -x+1,-y+1,-z+1

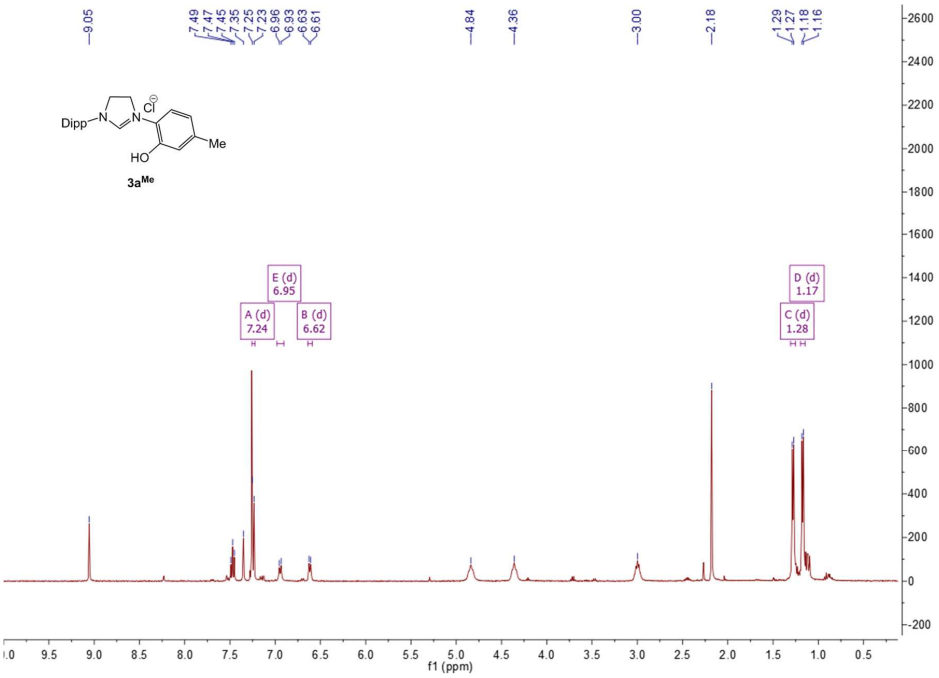

Figure S2. ^{1}H NMR spectrum of **3a^{Me}**.

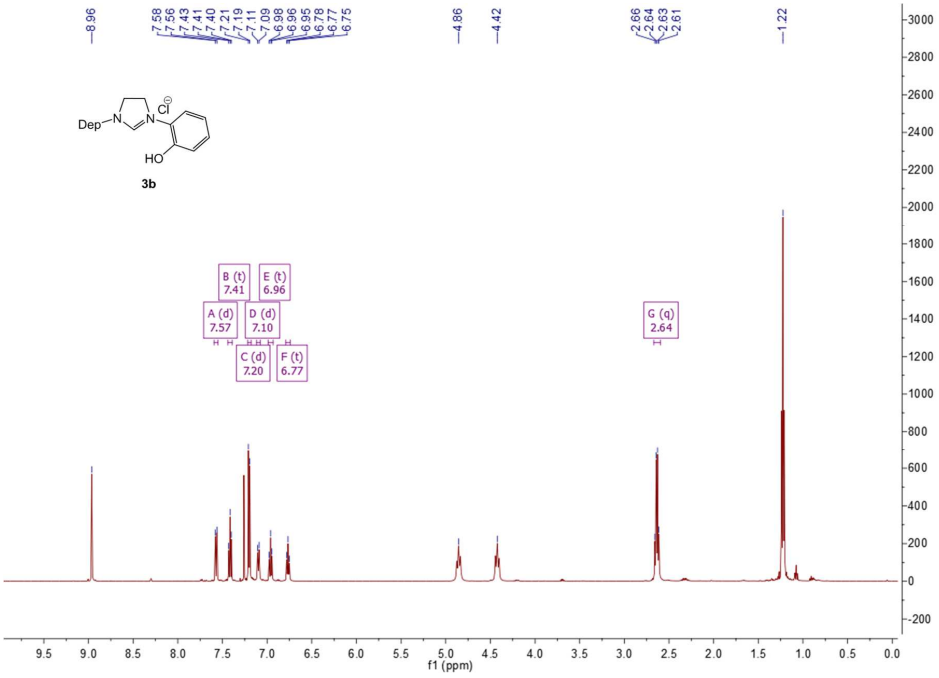

Figure S3. ^{1}H NMR spectrum of **3b**.

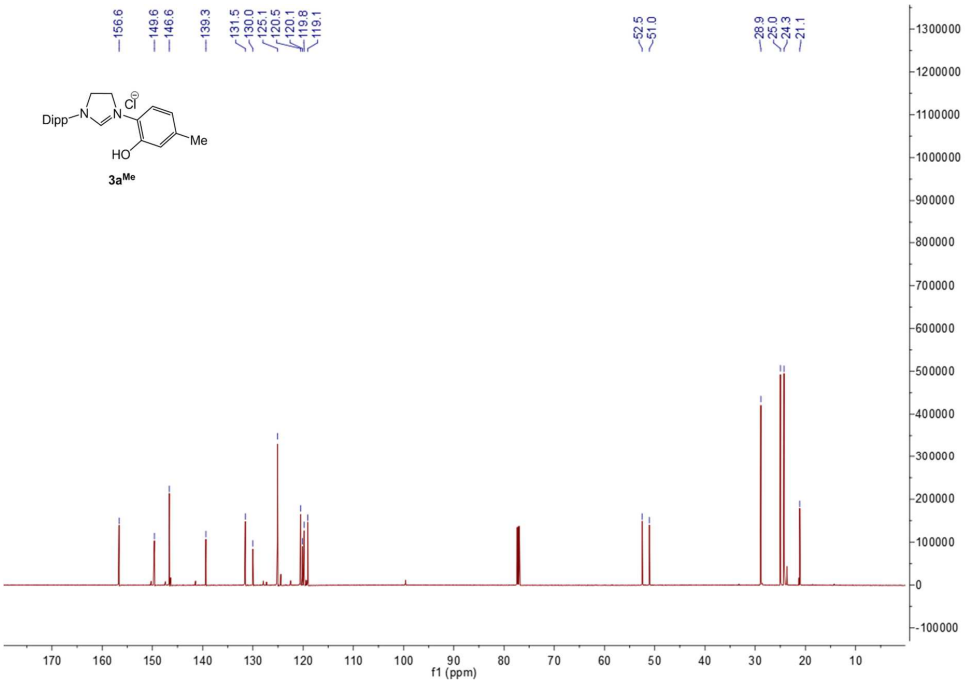

Figure S4. ^{13}C NMR spectrum of **3a^{Me}**.

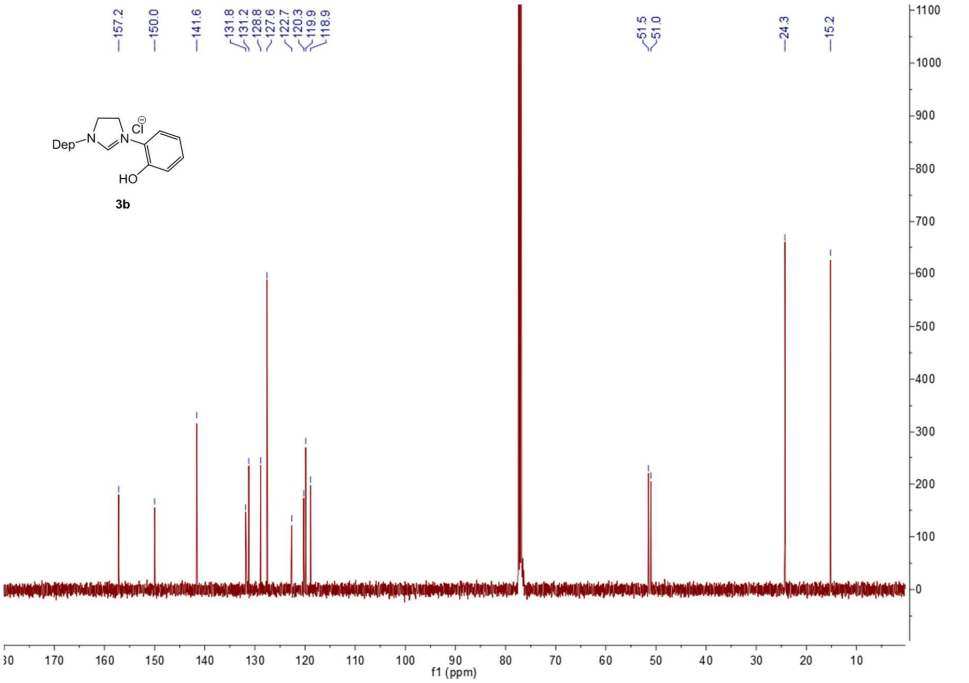

Figure S5. ^{13}C NMR spectrum of **3b**.

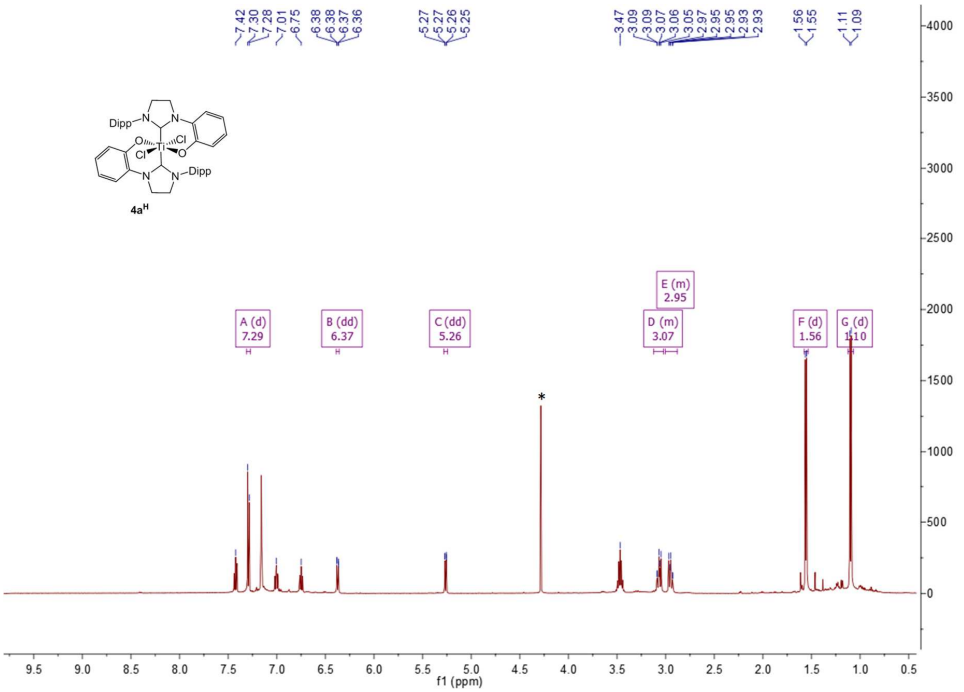

Figure S6. ^{1}H NMR spectrum of **4a^{H}**. (Residual solvent: * = CH_2Cl_2).

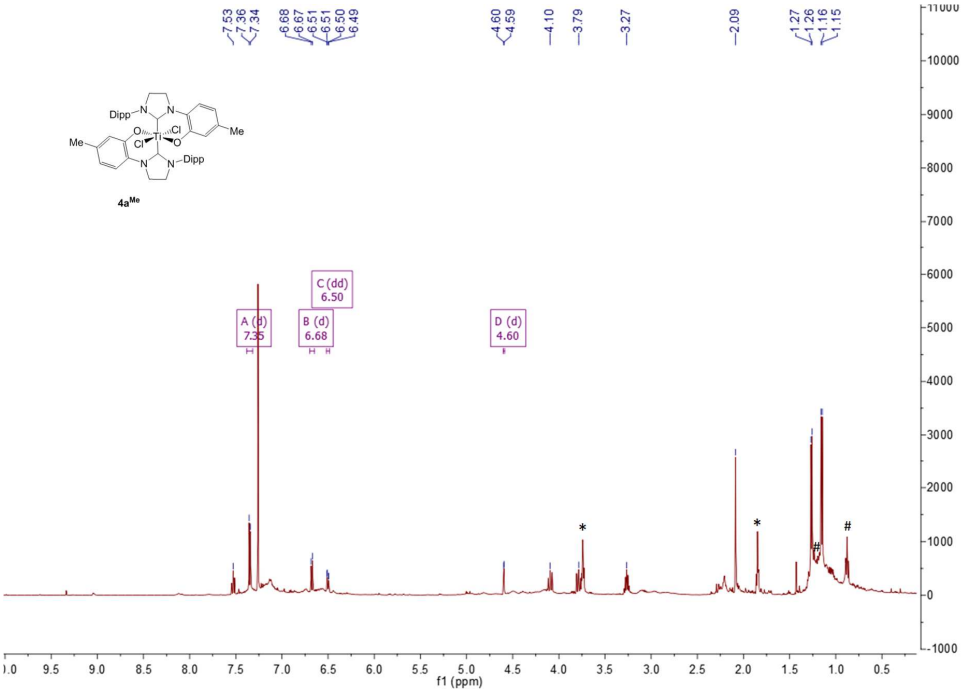

Figure S7. ^{1}H NMR spectrum of **4a^{Me}**. (Residual solvents: * = THF and # = hexane).

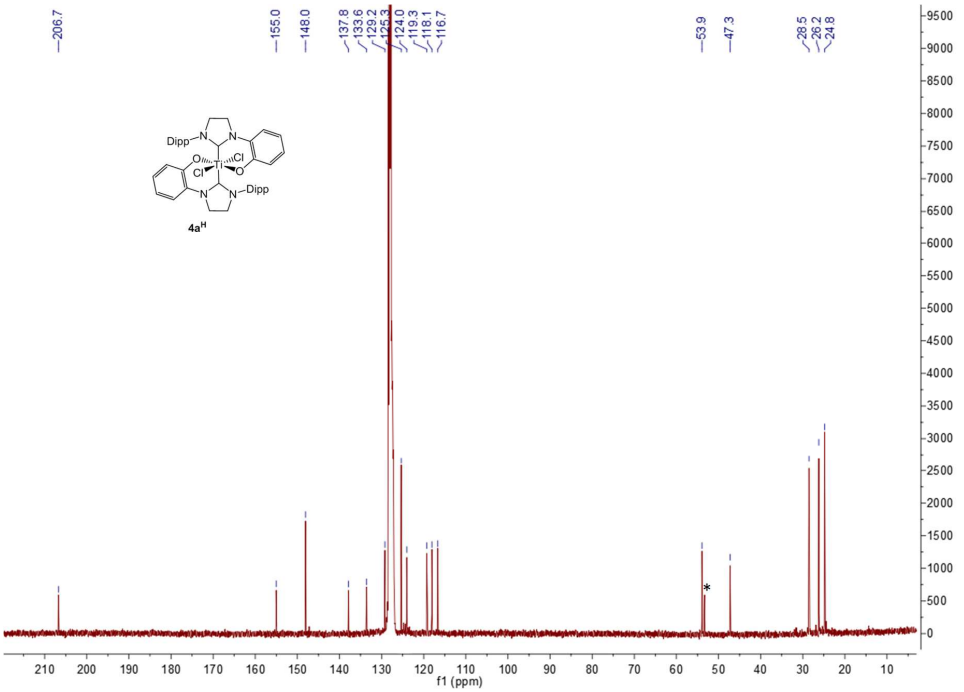

Figure S8. ^{13}C NMR spectrum of **4a^{H}**. (Residual solvent: * = CH_2Cl_2).

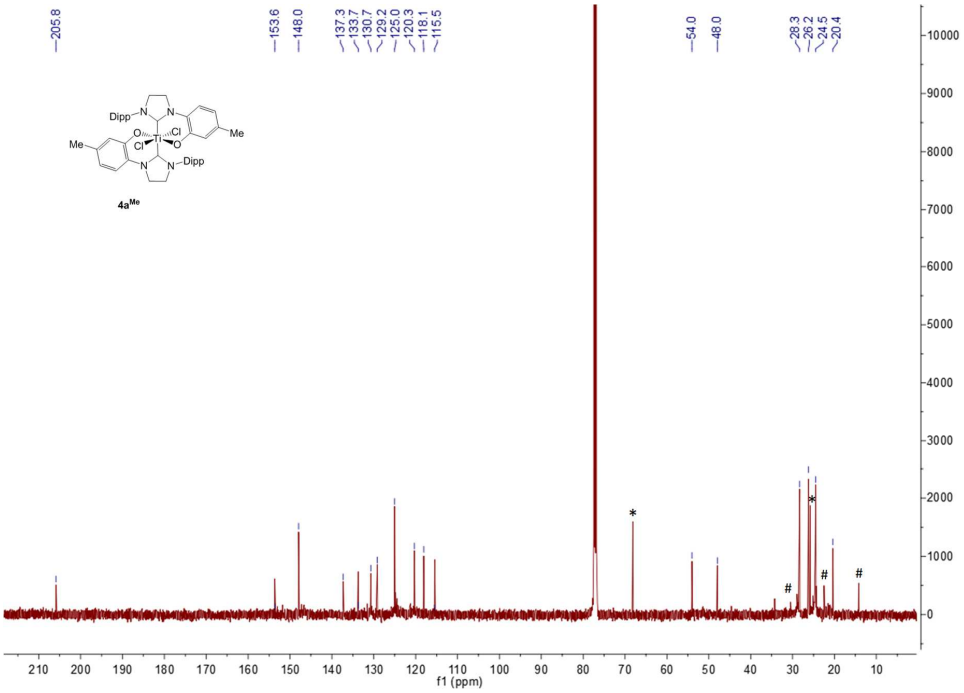

Figure S9. ^{13}C NMR spectrum of **4a^{Me}**.(Residual solvents: * = THF and # = hexane).

Table S4. Selected bond lengths [Å] and angles [°] for **4a^{H}**.

Ti(1)-O(1)#1	1.8578(12)	O(1)-Ti(1)-C(3)#1	97.60(6)
Ti(1)-O(1)	1.8579(12)	C(3)-Ti(1)-C(3)#1	180.00(8)
Ti(1)-C(3)	2.2597(18)	O(1)#1-Ti(1)-Cl(1)#1	89.29(4)
Ti(1)-C(3)#1	2.2597(18)	O(1)-Ti(1)-Cl(1)#1	90.71(4)
Ti(1)-Cl(1)#1	2.3269(5)	C(3)-Ti(1)-Cl(1)#1	95.27(4)
Ti(1)-Cl(1)	2.3269(5)	C(3)#1-Ti(1)-Cl(1)#1	84.73(4)
O(1)-C(1)	1.336(2)	O(1)#1-Ti(1)-Cl(1)	90.71(4)
N(1)-C(3)	1.353(2)	O(1)-Ti(1)-Cl(1)	89.29(4)
N(1)-C(2)	1.415(2)	C(3)-Ti(1)-Cl(1)	84.73(4)
N(1)-C(17)	1.480(2)	C(3)#1-Ti(1)-Cl(1)	95.27(4)
N(2)-C(3)	1.334(2)	Cl(1)#1-Ti(1)-Cl(1)	180.0
N(2)-C(4)	1.444(2)	C(1)-O(1)-Ti(1)	137.52(12)
N(2)-C(16)	1.476(2)	C(3)-N(1)-C(2)	128.42(15)
C(2)-C(1)	1.409(3)	C(1)-C(2)-N(1)	121.87(16)
		O(1)-C(1)-C(2)	119.94(16)
O(1)#1-Ti(1)-O(1)	180.0	N(2)-C(3)-N(1)	108.04(15)
O(1)#1-Ti(1)-C(3)	97.60(6)	N(2)-C(3)-Ti(1)	130.81(13)
O(1)-Ti(1)-C(3)	82.40(6)	N(1)-C(3)-Ti(1)	120.96(12)
O(1)#1-Ti(1)-C(3)#1	82.40(6)		

Symmetry transformations used to generate equivalent atoms: #1 -x+1,-y+1,-z+1

Table S5. Selected torsion angles [°] for **4a^{H}**.

C(3)-Ti(1)-O(1)-C(1)	36.52(18)	N(1)-C(2)-C(1)-O(1)	3.3(3)
C(3)#1-Ti(1)-O(1)-C(1)	-143.48(18)	N(1)-C(2)-C(1)-C(21)	-177.94(17)
Cl(1)#1-Ti(1)-O(1)-C(1)	131.74(17)	C(4)-N(2)-C(3)-N(1)	179.82(16)
Cl(1)-Ti(1)-O(1)-C(1)	-48.26(17)	C(4)-N(2)-C(3)-Ti(1)	-5.3(3)
C(3)-N(1)-C(2)-C(1)	9.9(3)	C(16)-N(2)-C(3)-Ti(1)	174.76(13)
C(17)-N(1)-C(2)-C(1)	-177.69(17)	C(2)-N(1)-C(3)-N(2)	176.37(16)
Ti(1)-O(1)-C(1)-C(2)	-36.0(3)	C(2)-N(1)-C(3)-Ti(1)	0.9(2)

Symmetry transformations used to generate equivalent atoms: #1 -x+1,-y+1,-z+1

APPENDIX D: Paper IV

"Di-μ-chlorido-bis{bis[*N*,*N*-bis(trimethylsilyl)amido]-titanium(III)}"

Coralie C. Quadri, Karl. W. Törnroos and Erwan Le Roux

IUCrData 2017, Vol 2, pp x171488-x171490

IUCrData

ISSN 2414-3146

Di-μ-chlorido-bis{bis[*N*,*N*-bis(trimethylsilyl)amido]-titanium(III)}

Coralie C. Quadri, Karl W. Törnroos and Erwan Le Roux*

Department of Chemistry, University of Bergen, Allégaten 41, N-5007 Bergen, Norway. *Correspondence e-mail: Erwan.LeRoux@uib.no

Received 9 September 2017
Accepted 13 October 2017

Edited by M. Weil, Vienna University of Technology, Austria

Keywords: crystal structure; titanium(III) silylamide complex; chloride-bridged dimer; binuclear complex.

CCDC reference: 1579885

Structural data: full structural data are available from iucrdata.iucr.org

The molecular structure of the title compound, $[Ti_2Cl_2(C_6H_{18}NSi_2)_4]$. shows a binuclear motif of Ti^{III} atoms, formulated as $[Ti(\mu\text{-}Cl)(N(SiMe_3)_2)_2]_2$, with two μ-Cl atoms bridging two $((Me_3Si)_2N)_2Ti$ moieties. The coordination environment of both central Ti^{III} atoms is distorted tetrahedral, with a nearly planar four-membered Ti_2Cl_2 core [Ti—Cl—Ti—Cl = 2.796 (15)°].

3D view

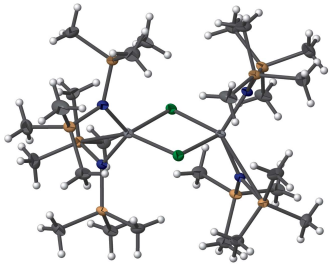

Chemical scheme

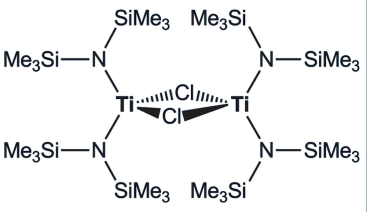

Structure description

Group 4 metal silylamide chlorides are versatile starting materials for many inorganic and organometallic compounds, and have been widely used as catalysts (Lappert *et al.*, 1980,2009) and as precursors in chemical vapor deposition (CVD) (Just & Rees, 2000; Carmalt *et al.*, 2005) and atomic layer deposition (ALD) of microelectronic films (Fix *et al.*, 1990,1991; Winter *et al.*, 1994). The use of halide ligands has been established to enhance the volatility of the group 4 silylamide precursors for CVD/ALD processes (Vaartstra *et al.*, 2006). Although analogous compounds such as $[Ti(Cl)_{4-x}(N(SiMe_3)_2)_x]$ (with x = 4, 3, 2 and 1) of titanium(IV) (Alcock *et al.*, 1976; Planalp *et al.*, 1983; Airoldi & Bradley, 1975; Airoldi *et al.*, 1980), $[Ti(N(SiMe_3)_2)_3]$ (Bradley & Copperthwaite, 1971; Alyea *et al.*, 1972; Bradley *et al.*, 1978; Minhas *et al.*, 1992) and $[Ti(Cl)_2(N(SiMe_3)_2)(THF)_2]$ (Putzer *et al.*, 1996) of titanium(III) have been synthesized, there is so far no other report of titanium(III) silylamide chloride compounds.

The title compound crystallizes as a chloride-bridged dimer $[Ti(\mu\text{-}Cl)(N(SiMe_3)_2)_2]_2$ with two four-coordinate titanium(III) atoms. It is isostructural with the molecular compounds $[M(\mu\text{-}Cl)(N(SiMe_3)_2)_2]_2$ with M = Yb (Niemeyer, 2002) and In (Yamashita *et al.*, 2014). The titanium(III) atoms occupy a pseudo-tetrahedral environment with two bonded $\{(Me_3Si)_2N\}$ moieties and two bridging chloride atoms bonded to each titanium(III) atom resulting in the formation of a characteristic edge-sharing ditetrahedral configuration (Fig. 1). The four-membered Ti_2Cl_2 core is nearly planar [torsion

Table 1
Selected geometric parameters (Å, °).

Ti1—N1	1.9371 (13)	Ti2—N3	1.9459 (13)
Ti1—N4	1.9379 (14)	Ti2—N2	1.9534 (13)
Ti1—Cl1	2.4226 (5)	Ti2—Cl2	2.4094 (5)
Ti1—Cl2	2.4227 (5)	Ti2—Cl1	2.4190 (5)
N1—Ti1—N4	118.42 (6)	N3—Ti2—Cl2	114.38 (4)
N1—Ti1—Cl1	121.02 (4)	N2—Ti2—Cl2	102.71 (4)
N4—Ti1—Cl1	102.91 (4)	N3—Ti2—Cl1	103.24 (4)
N1—Ti1—Cl2	100.57 (4)	N2—Ti2—Cl1	115.13 (4)
N4—Ti1—Cl2	123.75 (4)	Cl2—Ti2—Cl1	87.938 (16)
Cl1—Ti1—Cl2	87.550 (16)	Ti2—Cl1—Ti1	92.070 (16)
N3—Ti2—N2	126.91 (6)	Ti2—Cl2—Ti1	92.306 (16)

angle Ti1—Cl1—Ti2—Cl2 = 2.796 (15)°] with the four nitrogen atoms in a trigonal–planar coordination geometry [deviation from the $N_{(silylamide)}$-centroid (Si—Ti—Si) ring ranges from 0.077 to 0.116 Å], suggesting a possible π-overlap between the N lone pair and the vacant Ti orbitals. The Ti—Cl bond lengths (Table 1) are shorter than those observed in the Ti^{III},Ti^{III}-chloride bridged dimers $[Ti(\mu\text{-Cl})(\eta\text{-}C_5H_5)_2]_2$ (Jungst *et al.*, 1977), $[Ti(\mu\text{-Cl})(\eta\text{-}C_5H_4Me)_2]_2$ (Bradley & Copperthwaite, 1971; Alyea *et al.*, 1972; Bradley *et al.*, 1978; Minhas *et al.*, 1992), $[Ti(\mu\text{-Cl})\{(\eta^5\text{-}C_5H_4NSiMe_3)_2Fe\}]_2^{2+}$ (Shafir & Arnold, 2001), $[Ti(\mu\text{-Cl})\{(Me_3SiNCH_2CH_2)_2\text{-}NSiMe_3\}]_2$ (Love *et al.*, 1999) ranging from 2.566 (2)–2.4414 (10) Å. This is most probably the result of a better rearrangement between the less-bulky silylamide ligands bonded to each titanium(III) atom with torsion angles, N3—Ti1—Ti2—N1 and N2—Ti1—Ti2—N4, of −24.05 (7) and −26.50 (8)°, respectively, which deviates from perfect alignment following the non-crystallographic plane perpendicular to the four-membered Ti_2Cl_2 plane and through the pseudo-C_2 axis Ti1—Ti2. The Ti—N bond lengths (Table 1) are similar to those found in other Ti^{III} silylamide complexes ($d_{avg} \simeq 1.94$ Å) (Alcock *et al.*, 1976; Planalp *et al.*, 1983; Airoldi & Bradley, 1975; Airoldi *et al.*, 1980).

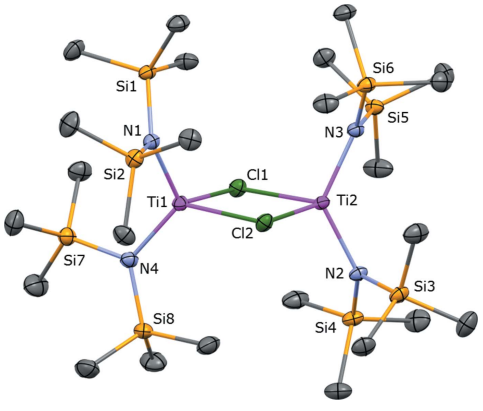

Figure 1
The molecular structure of the title compound with anisotropic displacement parameters set at the 50% probability level. Hydrogen atoms are omitted for clarity.

Table 2
Experimental details.

Crystal data	
Chemical formula	$[Ti_2Cl_2(C_6H_{18}NSi_2)_4]$
M_r	808.27
Crystal system, space group	Triclinic, $P\overline{1}$
Temperature (K)	103
a, b, c (Å)	8.8550 (5), 11.7359 (7), 24.0066 (14)
α, β, γ (°)	93.199 (1), 97.370 (1), 111.684 (1)
V (Å^3)	2284.6 (2)
Z	2
Radiation type	Mo $K\alpha$
μ (mm^{-1})	0.70
Crystal size (mm)	0.45 × 0.20 × 0.02
Data collection	
Diffractometer	Bruker TXS Rotating anode, Pt^{135} CCD
Absorption correction	Numerical (*SADABS*; Bruker, 2013)
T_{min}, T_{max}	0.820, 0.986
No. of measured, independent and observed [$I > 2\sigma(I)$] reflections	39360, 13897, 11154
R_{int}	0.051
(sin $\theta/\lambda)_{max}$ (Å^{-1})	0.714
Refinement	
$R[F^2 > 2\sigma(F^2)]$, $wR(F^2)$, S	0.040, 0.112, 1.04
No. of reflections	13897
No. of parameters	385
H-atom treatment	H-atom parameters constrained
$\Delta\rho_{max}$, $\Delta\rho_{min}$ (e Å^{-3})	0.87, −0.36

Computer programs: *APEX2* (Bruker, 2014), *SAINT* (Bruker, 2013), *SHELXT* (Sheldrick, 2015*a*), *SHELXL2017* (Sheldrick, 2015*b*) and *Mercury* (Macrae *et al.*, 2006).

The packing of the molecules in the title compound is displayed in Fig. 2.

Synthesis and crystallization

In an argon-filled glove-box, to a solution of 1*M* titanium tetrachloride in toluene (1 mmol) in 5 ml of toluene at 243 K

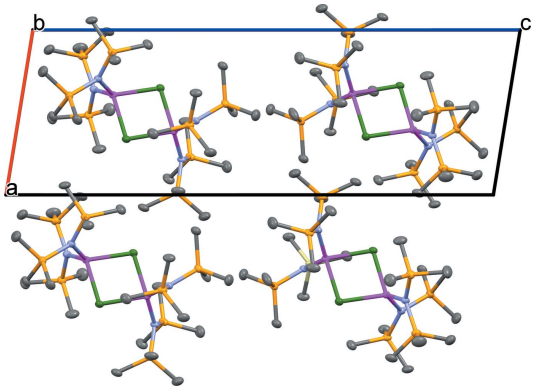

Figure 2
The crystal packing of the title compound seen down the *b* axis, showing four molecules, three of which are related to the unique one *via* inversion centres at $(\frac{1}{2}, \frac{1}{2}, \frac{1}{2})$ and $(0, \frac{1}{2}, \frac{1}{2})$. The packing is essentially based on van der Waals interactions only.

was added a pre-cooled solution at 243 K of lithium bis(trimethylsilyl)amide (334.6 mg, 2 mmol) in pentane (5 ml). The mixture was warmed to room temperature and stirred at that temperature overnight. The green solution was then centrifuged, filtered and dried under vacuum. Single crystals were obtained by preparing a concentrated solution of the reaction mixture in dichloromethane and cooling it for two days at 243 K.

Refinement

Crystal data, data collection and structure refinement details are summarized in Table 2.

Funding information

Funding for this research was provided by: Norges Forskningsråd (contract No. FRINATEK 240333 to E. Le Roux); Universitetet i Bergen (grant to E. Le Roux, C. C. Quadri); L. Meltzers Høyskolefond (bursary to K. W. Törnroos).

References

Airoldi, C. & Bradley, D. C. (1975). *Inorg. Nucl. Chem. Lett.* **11**, 155.
Airoldi, C., Bradley, D. C., Chudzynska, H., Hursthouse, M. B., Malik, K. M. A. & Raithby, P. R. J. (1980). *J. Chem. Soc. Dalton Trans.* pp. 2010.
Alcock, N. W., Pierce-Butler, M. & Willey, G. R. (1976). *J. Chem. Soc. Dalton Trans.* pp. 707–713.
Alyea, E. C., Bradley, D. C. & Copperthwaite, R. G. (1972). *J. Chem. Soc. Dalton Trans.* pp. 1580.
Bradley, D. C. & Copperthwaite, R. G. (1971). *J. Chem. Soc. D*, pp. 764.
Bradley, D. C., Copperthwaite, R. G., Extine, M. W., Reichert, W. W. & Chisholm, M. H. (1978). *Inorg. Synth.* **18**, 112–120.
Bruker (2013). *SAINT* and *SADABS*. Bruker AXS, Madison, Wisconsin, USA.
Bruker (2014). *APEX2*. Bruker AXS, Madison, Wisconsin, USA.
Carmalt, C. J., Newport, A. C., O'Neill, S. A., Parkin, I. P., White, A. J. P. & Williams, D. J. (2005). *Inorg. Chem.* **44**, 615–619.
Fix, R. M., Gordon, R. G. & Hoffman, D. M. (1990). *Chem. Mater.* **2**, 235–241.
Fix, R. M., Gordon, R. G. & Hoffman, D. M. (1991). *Chem. Mater.* **3**, 1138–1148.
Jungst, R., Sekutowski, D., Davis, J., Luly, M. & Stucky, J. (1977). *Inorg. Chem.* **16**, 1645–1655.
Just, O. & Rees, W. S. Jr (2000). *Adv. Mater. Opt. Electron.* **10**, 213–221.
Lappert, M. F., Power, P. P., Protchenko, A. V. & Seeber, A. (2009). In *Metal Amide Chemistry.* Chichester: John Wiley & Sons Ltd.
Lappert, M. F., Power, P. P., Sanger, A. R. & Srivastava, R. C. (1980). In *Metal and Metalloid Amide, Synthesis, Structures, and Physical and Chemical Properties.* New York: John Wiley & Sons Ltd.
Love, J. B., Clark, H. C. S., Cloke, F. G. N., Green, J. C. & Hitchcock, P. B. (1999). *J. Am. Chem. Soc.* **121**, 6843–6849.
Macrae, C. F., Edgington, P. R., McCabe, P., Pidcock, E., Shields, G. P., Taylor, R., Towler, M. & van de Streek, J. (2006). *J. Appl. Cryst.* **39**, 453–457.
Minhas, R., Duchateau, R., Gambarotta, S. & Bensimon, C. (1992). *Inorg. Chem.* **31**, 4933–4938.
Niemeyer, M. (2002). *Z. Anorg. Allg. Chem.* **628**, 647–657.
Planalp, R. P., Andersen, R. A. & Zalkin, A. (1983). *Organometallics*, **2**, 16–20.
Putzer, M. A., Magull, J., Goesmann, H., Neumüller, B. & Dehnicke, K. (1996). *Chem. Ber.* **129**, 1401–1405.
Shafir, A. & Arnold, J. (2001). *J. Am. Chem. Soc.* **123**, 9212–9213.
Sheldrick, G. M. (2015*a*). *Acta Cryst.* A**71**, 3–8.
Sheldrick, G. M. (2015*b*). *Acta Cryst.* C**71**, 3–8.
Vaartstra, B. A., Westmoreland, D., Marsh, E. P. & Uhlenbrock, S. (2006). US Patent 2006046521.
Winter, C. H., Proscia, J. W., Rheingold, A. L. & Lewkebandara, T. S. (1994). *Inorg. Chem.* **33**, 1227–1229.
Yamashita, Y., Saito, Y., Imaizumi, T. & Kobayashi, S. (2014). *Chem. Sci.* **5**, 3958–3962.

full crystallographic data

IUCrData (2017). **2**, x171488 [https://doi.org/10.1107/S2414314617014882]

Di-μ-chlorido-bis{bis[*N*,*N*-bis(trimethylsilyl)amido]titanium(III)}

Coralie C. Quadri, Karl W. Törnroos and Erwan Le Roux

Di-μ-chlorido-bis{bis[*N*,*N*-bis(trimethylsilyl)amido]titanium(III)}

Crystal data

$[Ti_2Cl_2(C_6H_{18}NSi_2)_4]$
M_r = 808.27
Triclinic, $P\overline{1}$
a = 8.8550 (5) Å
b = 11.7359 (7) Å
c = 24.0066 (14) Å
α = 93.199 (1)°
β = 97.370 (1)°
γ = 111.684 (1)°
V = 2284.6 (2) Å^3
Z = 2
$F(000)$ = 868
D_x = 1.175 Mg m^{-3}
Mo $K\alpha$ radiation, λ = 0.71073 Å
Cell parameters from 9927 reflections
θ = 2.4–30.4°
μ = 0.70 mm^{-1}
T = 103 K
Thin plate, blue
0.45 × 0.20 × 0.02 mm

Data collection

Bruker TXS Rotating anode, Pt^{135} CCD diffractometer
Radiation source: Bruker TXS Rotating anode
ω scans
Absorption correction: numerical (*SADABS*; Bruker, 2013)
T_{min} = 0.820, T_{max} = 0.986
39360 measured reflections
13897 independent reflections
11154 reflections with $I > 2\sigma(I)$
R_{int} = 0.051
θ_{max} = 30.5°, θ_{min} = 1.9°
h = −12→12
k = −16→16
l = −34→34

Refinement

Refinement on F^2
Least-squares matrix: full
$R[F^2 > 2\sigma(F^2)]$ = 0.040
$wR(F^2)$ = 0.112
S = 1.04
13897 reflections
385 parameters
0 restraints
Hydrogen site location: inferred from neighbouring sites
H-atom parameters constrained
$w = 1/[\sigma^2(F_o^2) + (0.0605P)^2 + 0.0514P]$ where $P = (F_o^2 + 2F_c^2)/3$
$(\Delta/\sigma)_{max}$ = 0.001
$\Delta\rho_{max}$ = 0.87 e Å^{-3}
$\Delta\rho_{min}$ = −0.36 e Å^{-3}

Special details

Geometry. All esds (except the esd in the dihedral angle between two l.s. planes) are estimated using the full covariance matrix. The cell esds are taken into account individually in the estimation of esds in distances, angles and torsion angles; correlations between esds in cell parameters are only used when they are defined by crystal symmetry. An approximate (isotropic) treatment of cell esds is used for estimating esds involving l.s. planes.

Fractional atomic coordinates and isotropic or equivalent isotropic displacement parameters (Å²)

	x	*y*	*z*	U_{iso}*/U_{eq}
Ti1	0.39441 (3)	0.30081 (2)	0.18633 (2)	0.01492 (7)
Ti2	0.61439 (3)	0.34925 (2)	0.32250 (2)	0.01526 (7)
Cl1	0.35239 (5)	0.35207 (4)	0.28076 (2)	0.01844 (8)
Cl2	0.66257 (5)	0.30888 (4)	0.22823 (2)	0.01891 (8)
Si1	0.13473 (5)	0.01105 (4)	0.17059 (2)	0.01756 (9)
Si2	0.39903 (6)	0.10306 (4)	0.09651 (2)	0.01876 (10)
Si3	0.98553 (5)	0.51034 (4)	0.35013 (2)	0.01995 (10)
Si4	0.76984 (6)	0.65233 (4)	0.36573 (2)	0.01897 (10)
Si5	0.44682 (6)	0.22235 (4)	0.41948 (2)	0.01771 (9)
Si6	0.57789 (5)	0.06572 (4)	0.35238 (2)	0.01837 (10)
Si7	0.15997 (6)	0.39762 (4)	0.11156 (2)	0.02084 (10)
Si8	0.51671 (6)	0.57332 (4)	0.14338 (2)	0.01976 (10)
N1	0.29662 (16)	0.13254 (12)	0.15026 (6)	0.0158 (2)
N2	0.78674 (16)	0.51130 (12)	0.34860 (6)	0.0160 (3)
N3	0.55174 (16)	0.20568 (12)	0.36416 (6)	0.0156 (2)
N4	0.36078 (16)	0.42951 (12)	0.14546 (6)	0.0176 (3)
C1	−0.0578 (2)	−0.03685 (18)	0.11736 (8)	0.0283 (4)
H1A	−0.072271	0.036697	0.104347	0.042*
H1B	−0.152591	−0.084398	0.134768	0.042*
H1C	−0.049311	−0.087897	0.085113	0.042*
C2	0.0888 (2)	0.05425 (16)	0.24066 (8)	0.0258 (4)
H2A	0.187690	0.077064	0.269187	0.039*
H2B	0.000081	−0.016058	0.251365	0.039*
H2C	0.054419	0.124437	0.238195	0.039*
C3	0.1844 (2)	−0.12943 (16)	0.17834 (9)	0.0268 (4)
H3A	0.199665	−0.160639	0.141633	0.040*
H3B	0.093680	−0.193105	0.191919	0.040*
H3C	0.285746	−0.108184	0.205533	0.040*
C4	0.2520 (3)	0.00131 (19)	0.03467 (8)	0.0324 (4)
H4A	0.192094	−0.079915	0.046220	0.049*
H4B	0.312970	−0.007854	0.004563	0.049*
H4C	0.173595	0.038278	0.020768	0.049*
C5	0.5248 (2)	0.25066 (17)	0.07026 (8)	0.0258 (4)
H5A	0.452511	0.291751	0.055247	0.039*
H5B	0.580772	0.232561	0.040296	0.039*
H5C	0.606841	0.304826	0.101507	0.039*
C6	0.5450 (2)	0.02861 (17)	0.12106 (8)	0.0252 (4)
H6A	0.626317	0.081499	0.152805	0.038*
H6B	0.601530	0.016854	0.090005	0.038*
H6C	0.483962	−0.051629	0.133274	0.038*
C7	1.1301 (2)	0.6014 (2)	0.41457 (9)	0.0341 (4)
H7A	1.147275	0.688685	0.414021	0.051*
H7B	1.235718	0.591854	0.415281	0.051*
H7C	1.083416	0.571434	0.448297	0.051*
C8	1.0782 (2)	0.56924 (17)	0.28657 (8)	0.0266 (4)

H8A	0.997837	0.529646	0.252337	0.040*
H8B	1.176512	0.550135	0.285205	0.040*
H8C	1.108706	0.658789	0.288864	0.040*
C9	0.9760 (2)	0.34943 (17)	0.35218 (10)	0.0315 (4)
H9A	0.926157	0.315209	0.384758	0.047*
H9B	1.087588	0.349647	0.355531	0.047*
H9C	0.909278	0.298778	0.317337	0.047*
C10	0.9034 (2)	0.77735 (16)	0.32842 (9)	0.0294 (4)
H10A	1.019229	0.791738	0.341220	0.044*
H10B	0.884908	0.853369	0.336899	0.044*
H10C	0.876107	0.752524	0.287566	0.044*
C11	0.8290 (3)	0.70627 (18)	0.44330 (8)	0.0328 (4)
H11A	0.772775	0.638676	0.464706	0.049*
H11B	0.796714	0.775988	0.451647	0.049*
H11C	0.948386	0.732344	0.454096	0.049*
C12	0.5572 (2)	0.64757 (17)	0.34511 (10)	0.0314 (4)
H12A	0.520119	0.618943	0.304744	0.047*
H12B	0.556877	0.730410	0.352646	0.047*
H12C	0.482788	0.590862	0.367111	0.047*
C13	0.6293 (2)	0.04081 (17)	0.28093 (8)	0.0278 (4)
H13A	0.546336	0.049009	0.252003	0.042*
H13B	0.630805	−0.042073	0.275139	0.042*
H13C	0.737924	0.102421	0.278092	0.042*
C14	0.3826 (2)	−0.06827 (15)	0.35585 (9)	0.0257 (4)
H14A	0.357593	−0.067546	0.394443	0.038*
H14B	0.395844	−0.145440	0.345160	0.038*
H14C	0.292099	−0.061890	0.329758	0.038*
C15	0.7441 (2)	0.05277 (18)	0.40522 (9)	0.0287 (4)
H15A	0.851801	0.107772	0.397738	0.043*
H15B	0.737788	−0.032546	0.402178	0.043*
H15C	0.729713	0.076308	0.443402	0.043*
C16	0.5171 (3)	0.16823 (19)	0.48585 (8)	0.0312 (4)
H16A	0.480331	0.078108	0.480814	0.047*
H16B	0.470349	0.193116	0.516997	0.047*
H16C	0.637568	0.205033	0.494593	0.047*
C17	0.4886 (3)	0.38942 (17)	0.43672 (9)	0.0327 (4)
H17A	0.607722	0.435963	0.445805	0.049*
H17B	0.436739	0.399920	0.469278	0.049*
H17C	0.443294	0.420061	0.404112	0.049*
C18	0.2185 (2)	0.14155 (17)	0.40172 (8)	0.0250 (4)
H18A	0.179303	0.165442	0.365918	0.037*
H18B	0.166814	0.164665	0.431820	0.037*
H18C	0.189658	0.052111	0.398103	0.037*
C19	0.0103 (2)	0.30239 (18)	0.15467 (9)	0.0289 (4)
H19A	0.027150	0.225319	0.159410	0.043*
H19B	−0.102140	0.283538	0.135463	0.043*
H19C	0.026947	0.348153	0.191834	0.043*
C20	0.1197 (2)	0.3118 (2)	0.03996 (8)	0.0342 (4)

H20A	0.199961	0.360063	0.017228	0.051*
H20B	0.008229	0.298365	0.021457	0.051*
H20C	0.129617	0.232056	0.043589	0.051*
C21	0.1100 (3)	0.53780 (19)	0.10321 (11)	0.0381 (5)
H21A	0.122658	0.581663	0.140532	0.057*
H21B	−0.003813	0.512985	0.084098	0.057*
H21C	0.184923	0.592248	0.080617	0.057*
C22	0.7226 (2)	0.57858 (17)	0.17584 (10)	0.0329 (4)
H22A	0.721610	0.564799	0.215698	0.049*
H22B	0.806864	0.659555	0.173027	0.049*
H22C	0.747460	0.514162	0.155825	0.049*
C23	0.4826 (3)	0.70071 (17)	0.18345 (9)	0.0341 (4)
H23A	0.404100	0.725609	0.159716	0.051*
H23B	0.587397	0.771397	0.193897	0.051*
H23C	0.438453	0.671851	0.217725	0.051*
C24	0.5339 (3)	0.60785 (19)	0.06891 (8)	0.0363 (5)
H24A	0.563521	0.545918	0.048974	0.054*
H24B	0.619079	0.689924	0.068835	0.054*
H24C	0.428075	0.605825	0.049832	0.054*

Atomic displacement parameters (Å²)

	U^{11}	U^{22}	U^{33}	U^{12}	U^{13}	U^{23}
Ti1	0.01427 (13)	0.01257 (13)	0.01745 (13)	0.00477 (10)	0.00199 (10)	0.00148 (10)
Ti2	0.01249 (13)	0.01240 (12)	0.01828 (14)	0.00156 (10)	0.00260 (10)	0.00260 (10)
Cl1	0.01564 (17)	0.02084 (18)	0.01963 (18)	0.00765 (14)	0.00376 (13)	0.00135 (14)
Cl2	0.01367 (16)	0.02160 (18)	0.02062 (18)	0.00591 (14)	0.00325 (13)	0.00018 (14)
Si1	0.0133 (2)	0.01390 (19)	0.0234 (2)	0.00310 (16)	0.00236 (16)	0.00136 (17)
Si2	0.0189 (2)	0.0202 (2)	0.0177 (2)	0.00803 (18)	0.00401 (17)	−0.00034 (17)
Si3	0.01163 (19)	0.0191 (2)	0.0268 (2)	0.00370 (17)	0.00232 (17)	0.00030 (18)
Si4	0.0164 (2)	0.0135 (2)	0.0258 (2)	0.00352 (16)	0.00683 (18)	0.00027 (17)
Si5	0.0183 (2)	0.0160 (2)	0.0182 (2)	0.00470 (17)	0.00558 (16)	0.00310 (16)
Si6	0.0145 (2)	0.0140 (2)	0.0268 (2)	0.00547 (16)	0.00364 (17)	0.00304 (17)
Si7	0.0166 (2)	0.0204 (2)	0.0267 (2)	0.00833 (18)	0.00247 (18)	0.00567 (18)
Si8	0.0204 (2)	0.0152 (2)	0.0218 (2)	0.00422 (17)	0.00358 (18)	0.00435 (17)
N1	0.0142 (6)	0.0142 (6)	0.0187 (6)	0.0052 (5)	0.0025 (5)	0.0012 (5)
N2	0.0118 (6)	0.0143 (6)	0.0210 (6)	0.0036 (5)	0.0038 (5)	0.0007 (5)
N3	0.0130 (6)	0.0135 (6)	0.0197 (6)	0.0042 (5)	0.0032 (5)	0.0023 (5)
N4	0.0150 (6)	0.0163 (6)	0.0214 (7)	0.0051 (5)	0.0043 (5)	0.0041 (5)
C1	0.0157 (8)	0.0279 (9)	0.0363 (10)	0.0048 (7)	−0.0013 (7)	−0.0009 (8)
C2	0.0265 (9)	0.0202 (8)	0.0293 (9)	0.0046 (7)	0.0110 (7)	0.0051 (7)
C3	0.0226 (8)	0.0164 (8)	0.0402 (10)	0.0062 (7)	0.0037 (8)	0.0036 (7)
C4	0.0326 (10)	0.0362 (11)	0.0239 (9)	0.0112 (9)	−0.0005 (8)	−0.0086 (8)
C5	0.0279 (9)	0.0300 (9)	0.0240 (8)	0.0130 (8)	0.0119 (7)	0.0078 (7)
C6	0.0253 (9)	0.0266 (9)	0.0290 (9)	0.0146 (7)	0.0095 (7)	0.0024 (7)
C7	0.0209 (9)	0.0390 (11)	0.0354 (11)	0.0069 (8)	−0.0024 (8)	−0.0049 (9)
C8	0.0173 (8)	0.0269 (9)	0.0351 (10)	0.0061 (7)	0.0100 (7)	0.0031 (7)
C9	0.0182 (8)	0.0250 (9)	0.0532 (13)	0.0098 (7)	0.0061 (8)	0.0067 (8)

C10	0.0298 (10)	0.0175 (8)	0.0394 (11)	0.0043 (7)	0.0143 (8)	0.0049 (7)
C11	0.0400 (11)	0.0269 (9)	0.0297 (10)	0.0101 (8)	0.0105 (8)	−0.0053 (8)
C12	0.0227 (9)	0.0180 (8)	0.0555 (13)	0.0095 (7)	0.0074 (9)	0.0057 (8)
C13	0.0304 (9)	0.0197 (8)	0.0352 (10)	0.0104 (7)	0.0106 (8)	−0.0007 (7)
C14	0.0186 (8)	0.0152 (7)	0.0409 (10)	0.0040 (6)	0.0044 (7)	0.0040 (7)
C15	0.0202 (8)	0.0271 (9)	0.0411 (11)	0.0114 (7)	0.0036 (8)	0.0097 (8)
C16	0.0342 (10)	0.0356 (10)	0.0218 (9)	0.0110 (8)	0.0024 (8)	0.0071 (8)
C17	0.0447 (12)	0.0203 (8)	0.0332 (10)	0.0078 (8)	0.0220 (9)	0.0007 (7)
C18	0.0200 (8)	0.0272 (9)	0.0279 (9)	0.0079 (7)	0.0081 (7)	0.0020 (7)
C19	0.0190 (8)	0.0291 (9)	0.0415 (11)	0.0105 (7)	0.0094 (8)	0.0086 (8)
C20	0.0266 (10)	0.0432 (12)	0.0284 (10)	0.0112 (9)	−0.0030 (8)	−0.0007 (8)
C21	0.0296 (10)	0.0298 (10)	0.0588 (14)	0.0162 (8)	0.0022 (10)	0.0139 (10)
C22	0.0208 (9)	0.0218 (9)	0.0494 (12)	0.0024 (7)	−0.0011 (8)	0.0051 (8)
C23	0.0440 (12)	0.0191 (8)	0.0398 (11)	0.0126 (8)	0.0078 (9)	0.0025 (8)
C24	0.0405 (12)	0.0307 (10)	0.0279 (10)	0.0003 (9)	0.0093 (8)	0.0096 (8)

Geometric parameters (Å, º)

Ti1—N1	1.9371 (13)	C6—H6A	0.9800
Ti1—N4	1.9379 (14)	C6—H6B	0.9800
Ti1—Cl1	2.4226 (5)	C6—H6C	0.9800
Ti1—Cl2	2.4227 (5)	C7—H7A	0.9800
Ti1—Si2	3.0937 (5)	C7—H7B	0.9800
Ti2—N3	1.9459 (13)	C7—H7C	0.9800
Ti2—N2	1.9534 (13)	C8—H8A	0.9800
Ti2—Cl2	2.4094 (5)	C8—H8B	0.9800
Ti2—Cl1	2.4190 (5)	C8—H8C	0.9800
Ti2—Si5	3.0790 (5)	C9—H9A	0.9800
Ti2—Si3	3.0861 (5)	C9—H9B	0.9800
Si1—N1	1.7530 (14)	C9—H9C	0.9800
Si1—C2	1.8668 (19)	C10—H10A	0.9800
Si1—C3	1.8693 (18)	C10—H10B	0.9800
Si1—C1	1.8731 (18)	C10—H10C	0.9800
Si2—N1	1.7576 (14)	C11—H11A	0.9800
Si2—C6	1.8652 (18)	C11—H11B	0.9800
Si2—C4	1.8661 (19)	C11—H11C	0.9800
Si2—C5	1.8746 (19)	C12—H12A	0.9800
Si3—N2	1.7601 (14)	C12—H12B	0.9800
Si3—C9	1.8627 (19)	C12—H12C	0.9800
Si3—C7	1.863 (2)	C13—H13A	0.9800
Si3—C8	1.8705 (19)	C13—H13B	0.9800
Si4—N2	1.7474 (14)	C13—H13C	0.9800
Si4—C12	1.8638 (19)	C14—H14A	0.9800
Si4—C10	1.8681 (19)	C14—H14B	0.9800
Si4—C11	1.875 (2)	C14—H14C	0.9800
Si5—N3	1.7570 (14)	C15—H15A	0.9800
Si5—C16	1.8656 (19)	C15—H15B	0.9800
Si5—C18	1.8666 (18)	C15—H15C	0.9800

Si5—C17	1.8672 (19)	C16—H16A	0.9800
Si6—N3	1.7544 (14)	C16—H16B	0.9800
Si6—C13	1.8651 (19)	C16—H16C	0.9800
Si6—C15	1.8725 (19)	C17—H17A	0.9800
Si6—C14	1.8743 (18)	C17—H17B	0.9800
Si7—N4	1.7513 (14)	C17—H17C	0.9800
Si7—C19	1.8610 (19)	C18—H18A	0.9800
Si7—C20	1.865 (2)	C18—H18B	0.9800
Si7—C21	1.869 (2)	C18—H18C	0.9800
Si8—N4	1.7499 (14)	C19—H19A	0.9800
Si8—C22	1.866 (2)	C19—H19B	0.9800
Si8—C24	1.868 (2)	C19—H19C	0.9800
Si8—C23	1.871 (2)	C20—H20A	0.9800
C1—H1A	0.9800	C20—H20B	0.9800
C1—H1B	0.9800	C20—H20C	0.9800
C1—H1C	0.9800	C21—H21A	0.9800
C2—H2A	0.9800	C21—H21B	0.9800
C2—H2B	0.9800	C21—H21C	0.9800
C2—H2C	0.9800	C22—H22A	0.9800
C3—H3A	0.9800	C22—H22B	0.9800
C3—H3B	0.9800	C22—H22C	0.9800
C3—H3C	0.9800	C23—H23A	0.9800
C4—H4A	0.9800	C23—H23B	0.9800
C4—H4B	0.9800	C23—H23C	0.9800
C4—H4C	0.9800	C24—H24A	0.9800
C5—H5A	0.9800	C24—H24B	0.9800
C5—H5B	0.9800	C24—H24C	0.9800
C5—H5C	0.9800		

N1—Ti1—N4	118.42 (6)	Si2—C5—H5A	109.5
N1—Ti1—Cl1	121.02 (4)	Si2—C5—H5B	109.5
N4—Ti1—Cl1	102.91 (4)	H5A—C5—H5B	109.5
N1—Ti1—Cl2	100.57 (4)	Si2—C5—H5C	109.5
N4—Ti1—Cl2	123.75 (4)	H5A—C5—H5C	109.5
Cl1—Ti1—Cl2	87.550 (16)	H5B—C5—H5C	109.5
N1—Ti1—Si2	31.37 (4)	Si2—C6—H6A	109.5
N4—Ti1—Si2	106.50 (4)	Si2—C6—H6B	109.5
Cl1—Ti1—Si2	148.298 (17)	H6A—C6—H6B	109.5
Cl2—Ti1—Si2	85.901 (15)	Si2—C6—H6C	109.5
N3—Ti2—N2	126.91 (6)	H6A—C6—H6C	109.5
N3—Ti2—Cl2	114.38 (4)	H6B—C6—H6C	109.5
N2—Ti2—Cl2	102.71 (4)	Si3—C7—H7A	109.5
N3—Ti2—Cl1	103.24 (4)	Si3—C7—H7B	109.5
N2—Ti2—Cl1	115.13 (4)	H7A—C7—H7B	109.5
Cl2—Ti2—Cl1	87.938 (16)	Si3—C7—H7C	109.5
N3—Ti2—Si5	31.84 (4)	H7A—C7—H7C	109.5
N2—Ti2—Si5	112.35 (4)	H7B—C7—H7C	109.5
Cl2—Ti2—Si5	142.757 (17)	Si3—C8—H8A	109.5

Cl1—Ti2—Si5	88.334 (15)	Si3—C8—H8B	109.5
N3—Ti2—Si3	112.82 (4)	H8A—C8—H8B	109.5
N2—Ti2—Si3	31.85 (4)	Si3—C8—H8C	109.5
Cl2—Ti2—Si3	86.479 (15)	H8A—C8—H8C	109.5
Cl1—Ti2—Si3	142.490 (17)	H8B—C8—H8C	109.5
Si5—Ti2—Si3	117.236 (16)	Si3—C9—H9A	109.5
Ti2—Cl1—Ti1	92.070 (16)	Si3—C9—H9B	109.5
Ti2—Cl2—Ti1	92.306 (16)	H9A—C9—H9B	109.5
N1—Si1—C2	111.33 (7)	Si3—C9—H9C	109.5
N1—Si1—C3	112.16 (7)	H9A—C9—H9C	109.5
C2—Si1—C3	106.10 (9)	H9B—C9—H9C	109.5
N1—Si1—C1	111.65 (8)	Si4—C10—H10A	109.5
C2—Si1—C1	108.60 (9)	Si4—C10—H10B	109.5
C3—Si1—C1	106.71 (9)	H10A—C10—H10B	109.5
N1—Si2—C6	112.71 (7)	Si4—C10—H10C	109.5
N1—Si2—C4	111.91 (8)	H10A—C10—H10C	109.5
C6—Si2—C4	107.62 (9)	H10B—C10—H10C	109.5
N1—Si2—C5	110.54 (7)	Si4—C11—H11A	109.5
C6—Si2—C5	106.29 (8)	Si4—C11—H11B	109.5
C4—Si2—C5	107.47 (9)	H11A—C11—H11B	109.5
C6—Si2—Ti1	113.02 (6)	Si4—C11—H11C	109.5
C4—Si2—Ti1	135.70 (7)	H11A—C11—H11C	109.5
C5—Si2—Ti1	77.57 (6)	H11B—C11—H11C	109.5
N2—Si3—C9	109.52 (8)	Si4—C12—H12A	109.5
N2—Si3—C7	112.45 (8)	Si4—C12—H12B	109.5
C9—Si3—C7	105.95 (10)	H12A—C12—H12B	109.5
N2—Si3—C8	112.74 (8)	Si4—C12—H12C	109.5
C9—Si3—C8	107.37 (9)	H12A—C12—H12C	109.5
C7—Si3—C8	108.46 (9)	H12B—C12—H12C	109.5
C9—Si3—Ti2	75.79 (6)	Si6—C13—H13A	109.5
C7—Si3—Ti2	135.46 (7)	Si6—C13—H13B	109.5
C8—Si3—Ti2	113.34 (6)	H13A—C13—H13B	109.5
N2—Si4—C12	112.97 (7)	Si6—C13—H13C	109.5
N2—Si4—C10	111.77 (8)	H13A—C13—H13C	109.5
C12—Si4—C10	105.39 (9)	H13B—C13—H13C	109.5
N2—Si4—C11	112.83 (8)	Si6—C14—H14A	109.5
C12—Si4—C11	106.38 (10)	Si6—C14—H14B	109.5
C10—Si4—C11	106.99 (9)	H14A—C14—H14B	109.5
N3—Si5—C16	112.68 (8)	Si6—C14—H14C	109.5
N3—Si5—C18	113.65 (7)	H14A—C14—H14C	109.5
C16—Si5—C18	107.98 (9)	H14B—C14—H14C	109.5
N3—Si5—C17	109.08 (8)	Si6—C15—H15A	109.5
C16—Si5—C17	106.48 (10)	Si6—C15—H15B	109.5
C18—Si5—C17	106.56 (9)	H15A—C15—H15B	109.5
C16—Si5—Ti2	134.95 (7)	Si6—C15—H15C	109.5
C18—Si5—Ti2	114.66 (6)	H15A—C15—H15C	109.5
C17—Si5—Ti2	75.09 (6)	H15B—C15—H15C	109.5
N3—Si6—C13	112.98 (8)	Si5—C16—H16A	109.5

N3—Si6—C15	112.70 (8)	Si5—C16—H16B	109.5
C13—Si6—C15	106.99 (9)	H16A—C16—H16B	109.5
N3—Si6—C14	110.68 (7)	Si5—C16—H16C	109.5
C13—Si6—C14	105.39 (9)	H16A—C16—H16C	109.5
C15—Si6—C14	107.67 (9)	H16B—C16—H16C	109.5
N4—Si7—C19	109.43 (8)	Si5—C17—H17A	109.5
N4—Si7—C20	111.34 (8)	Si5—C17—H17B	109.5
C19—Si7—C20	108.73 (10)	H17A—C17—H17B	109.5
N4—Si7—C21	114.02 (8)	Si5—C17—H17C	109.5
C19—Si7—C21	105.32 (10)	H17A—C17—H17C	109.5
C20—Si7—C21	107.72 (10)	H17B—C17—H17C	109.5
N4—Si8—C22	111.84 (8)	Si5—C18—H18A	109.5
N4—Si8—C24	110.95 (8)	Si5—C18—H18B	109.5
C22—Si8—C24	106.25 (10)	H18A—C18—H18B	109.5
N4—Si8—C23	111.98 (9)	Si5—C18—H18C	109.5
C22—Si8—C23	106.17 (10)	H18A—C18—H18C	109.5
C24—Si8—C23	109.37 (10)	H18B—C18—H18C	109.5
Si1—N1—Si2	119.76 (8)	Si7—C19—H19A	109.5
Si1—N1—Ti1	126.34 (8)	Si7—C19—H19B	109.5
Si2—N1—Ti1	113.63 (7)	H19A—C19—H19B	109.5
Si4—N2—Si3	117.90 (7)	Si7—C19—H19C	109.5
Si4—N2—Ti2	129.66 (7)	H19A—C19—H19C	109.5
Si3—N2—Ti2	112.31 (7)	H19B—C19—H19C	109.5
Si6—N3—Si5	117.87 (8)	Si7—C20—H20A	109.5
Si6—N3—Ti2	129.67 (8)	Si7—C20—H20B	109.5
Si5—N3—Ti2	112.41 (7)	H20A—C20—H20B	109.5
Si8—N4—Si7	120.13 (8)	Si7—C20—H20C	109.5
Si8—N4—Ti1	123.47 (8)	H20A—C20—H20C	109.5
Si7—N4—Ti1	116.36 (7)	H20B—C20—H20C	109.5
Si1—C1—H1A	109.5	Si7—C21—H21A	109.5
Si1—C1—H1B	109.5	Si7—C21—H21B	109.5
H1A—C1—H1B	109.5	H21A—C21—H21B	109.5
Si1—C1—H1C	109.5	Si7—C21—H21C	109.5
H1A—C1—H1C	109.5	H21A—C21—H21C	109.5
H1B—C1—H1C	109.5	H21B—C21—H21C	109.5
Si1—C2—H2A	109.5	Si8—C22—H22A	109.5
Si1—C2—H2B	109.5	Si8—C22—H22B	109.5
H2A—C2—H2B	109.5	H22A—C22—H22B	109.5
Si1—C2—H2C	109.5	Si8—C22—H22C	109.5
H2A—C2—H2C	109.5	H22A—C22—H22C	109.5
H2B—C2—H2C	109.5	H22B—C22—H22C	109.5
Si1—C3—H3A	109.5	Si8—C23—H23A	109.5
Si1—C3—H3B	109.5	Si8—C23—H23B	109.5
H3A—C3—H3B	109.5	H23A—C23—H23B	109.5
Si1—C3—H3C	109.5	Si8—C23—H23C	109.5
H3A—C3—H3C	109.5	H23A—C23—H23C	109.5
H3B—C3—H3C	109.5	H23B—C23—H23C	109.5
Si2—C4—H4A	109.5	Si8—C24—H24A	109.5

Si2—C4—H4B	109.5	Si8—C24—H24B	109.5
H4A—C4—H4B	109.5	H24A—C24—H24B	109.5
Si2—C4—H4C	109.5	Si8—C24—H24C	109.5
H4A—C4—H4C	109.5	H24A—C24—H24C	109.5
H4B—C4—H4C	109.5	H24B—C24—H24C	109.5
C2—Si1—N1—Si2	163.08 (9)	C13—Si6—N3—Si5	161.93 (9)
C3—Si1—N1—Si2	44.37 (12)	C15—Si6—N3—Si5	−76.63 (11)
C1—Si1—N1—Si2	−75.35 (11)	C14—Si6—N3—Si5	44.01 (11)
C2—Si1—N1—Ti1	−10.50 (12)	C13—Si6—N3—Ti2	−15.17 (13)
C3—Si1—N1—Ti1	−129.22 (10)	C15—Si6—N3—Ti2	106.27 (11)
C1—Si1—N1—Ti1	111.07 (10)	C14—Si6—N3—Ti2	−133.09 (10)
C6—Si2—N1—Si1	−76.23 (11)	C16—Si5—N3—Si6	45.52 (11)
C4—Si2—N1—Si1	45.24 (12)	C18—Si5—N3—Si6	−77.73 (10)
C5—Si2—N1—Si1	164.99 (9)	C17—Si5—N3—Si6	163.54 (10)
Ti1—Si2—N1—Si1	−174.36 (14)	Ti2—Si5—N3—Si6	−177.58 (13)
C6—Si2—N1—Ti1	98.13 (9)	C16—Si5—N3—Ti2	−136.90 (9)
C4—Si2—N1—Ti1	−140.40 (9)	C18—Si5—N3—Ti2	99.86 (9)
C5—Si2—N1—Ti1	−20.65 (10)	C17—Si5—N3—Ti2	−18.88 (11)
C12—Si4—N2—Si3	165.48 (10)	C22—Si8—N4—Si7	−173.96 (10)
C10—Si4—N2—Si3	46.82 (12)	C24—Si8—N4—Si7	−55.51 (12)
C11—Si4—N2—Si3	−73.81 (11)	C23—Si8—N4—Si7	67.00 (12)
C12—Si4—N2—Ti2	−10.18 (14)	C22—Si8—N4—Ti1	8.39 (13)
C10—Si4—N2—Ti2	−128.84 (11)	C24—Si8—N4—Ti1	126.83 (11)
C11—Si4—N2—Ti2	110.54 (11)	C23—Si8—N4—Ti1	−110.65 (11)
C9—Si3—N2—Si4	162.97 (10)	C19—Si7—N4—Si8	−142.94 (10)
C7—Si3—N2—Si4	45.45 (12)	C20—Si7—N4—Si8	96.82 (11)
C8—Si3—N2—Si4	−77.55 (11)	C21—Si7—N4—Si8	−25.30 (13)
Ti2—Si3—N2—Si4	−176.38 (14)	C19—Si7—N4—Ti1	34.87 (11)
C9—Si3—N2—Ti2	−20.65 (11)	C20—Si7—N4—Ti1	−85.36 (11)
C7—Si3—N2—Ti2	−138.16 (9)	C21—Si7—N4—Ti1	152.52 (10)
C8—Si3—N2—Ti2	98.83 (9)		

Graphic design: Communication Division, UiB / Print: Skipnes Kommunikasjon AS

uib.no

ISBN: 978-82-308-3779-5